X-ray Imaging

Ian McNulty

Center for Nanoscale Materials

16 August 2012

14th National School on Neutron and X-ray Scattering

Argonne National Laboratory

Outline

Part I

1. Fundamentals

- resolution
- contrast
- x-ray sources
- x-ray optics

2. Direct methods

- projection
- full-field
- scanning

Part II

3. Indirect methods

- microdiffraction
- coherent diffraction
- holography

1. Fundamentals

- **Resolution**
- **Contrast**
- **X-ray sources**
- **X-ray optics**

References:

1. M. Howells, "Soft-x-ray microscopes," Physics Today 38, 22 (Aug. 1985).
2. J. Kirz and H. Rarback, "Soft xray microscopes," Rev. Sci. Instrum. 56, 1 (1985).
3. J. Als-Nielsen and D. McMorrow, *Elements of Modern X-ray Physics* (Wiley, New York, 2000).
4. D. Attwood, *Soft X-Rays and Extreme Ultraviolet Radiation: Principles and Applications* (Cambridge, 2007).
5. J. Goodman, *Introduction to Fourier Optics*, 3rd ed. (Roberts and Company, 2005).

Imaging

image ['ɪmɪdʒ]

Noun:
The optical counterpart of an object produced by an optical device (as a lens or mirror) or an electronic device

Verb:
Make a visual representation of (something) by scanning it with a detector or electromagnetic beam.

- *Merriam-Webster Dictionary*

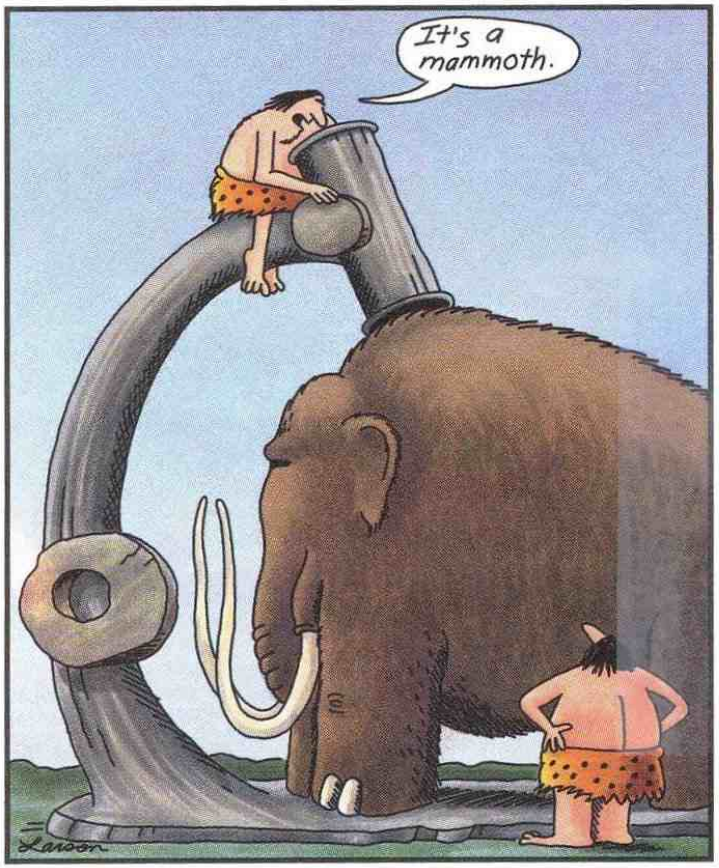

Early microscope

Image formation as a scattering process

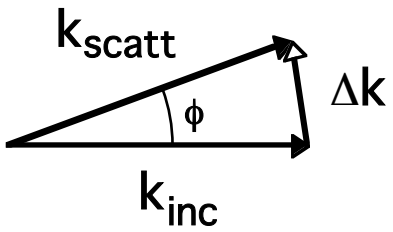

Incident waves with initial momentum k_{inc} are elastically scattered into new direction k_{scatt} with momentum transfer Δk.

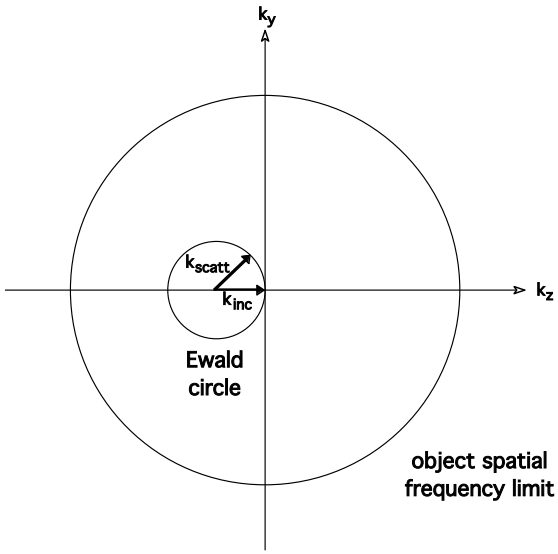

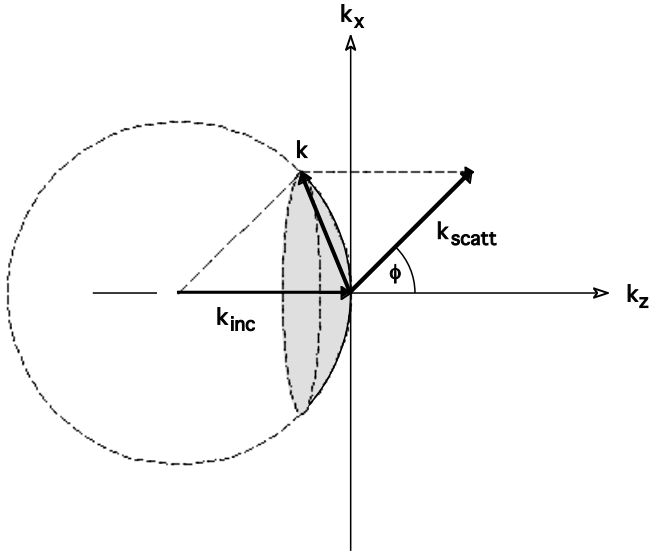

Ewald sphere is defined by conservation of momentum. Only spatial frequencies on the Ewald sphere are accessible to the imaging process, limiting attainable resolution.

Diffraction limits to resolution

Point-spread function

$$P(x,y) = \frac{\sin x}{x}\,\frac{\sin y}{y}$$

with $x = \frac{kax}{z}$, $y = \frac{kay}{z}$

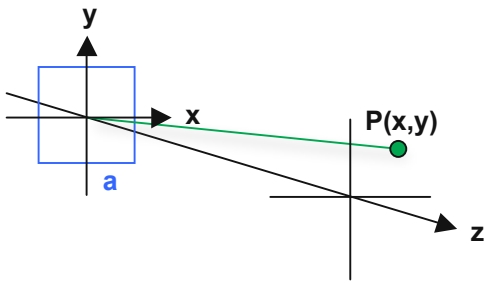

Transverse $R = 0.5\frac{\lambda}{NA}$

where $NA \sim \frac{a}{z}$

$k = \frac{2\pi}{\lambda}$

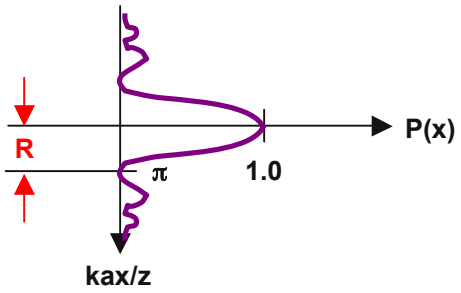

What do we mean by "resolution"?

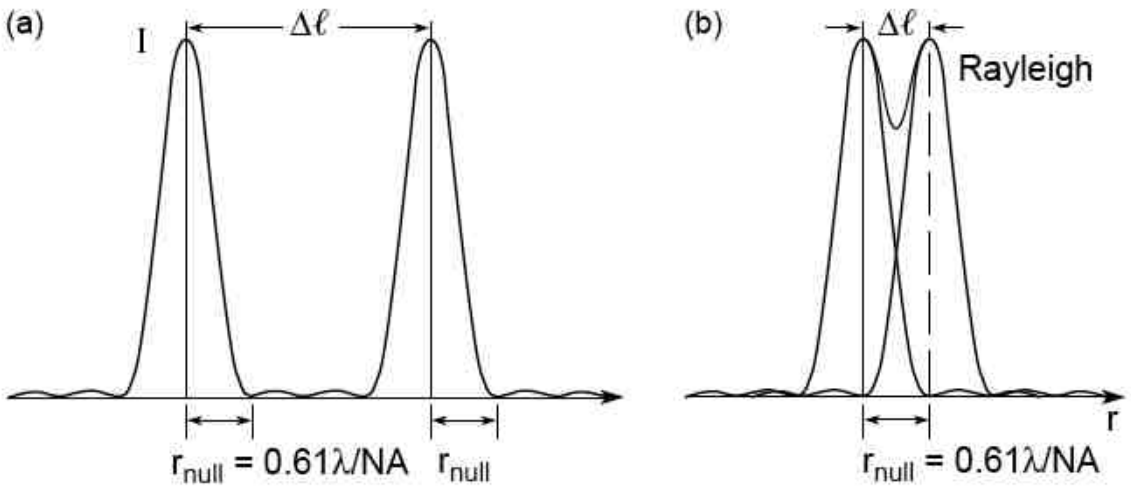

- Point sources are spatially coherent
- Mutually incoherent
- Intensities add
- Rayleigh criterion (26.5% dip)

Conclusion: With spatially coherent illumination, objects are "just resolvable" when

$$\text{Res}|_{\text{coh}} = \frac{0.61\,\lambda}{\text{NA}} = 1.22\,\Delta r$$

Diffraction limits to resolution

Point-spread function

$$P(x,y) = \frac{\sin x}{x}\,\frac{\sin y}{y}$$

with $x = \frac{kax}{z}$, $y = \frac{kay}{z}$

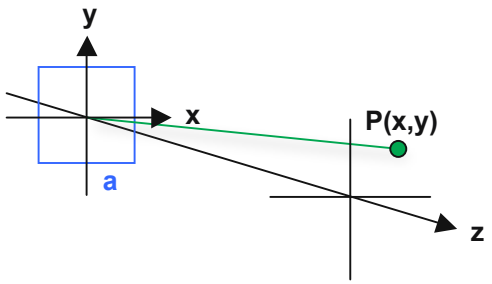

Transverse $R = 0.5\frac{\lambda}{NA}$

where $NA \sim \frac{a}{z}$

$k = \frac{2\pi}{\lambda}$

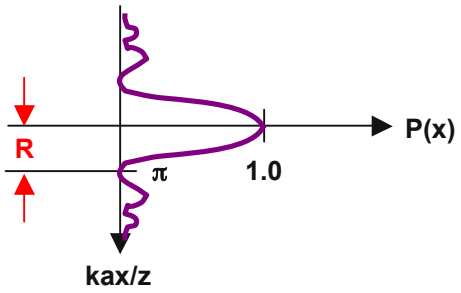

Coherence

longitudinal coherence

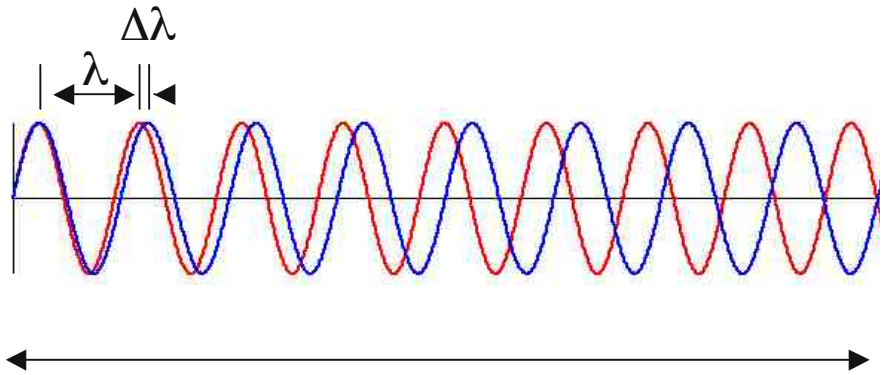

$$l_c \sim \frac{\lambda^2}{\Delta\lambda}$$

$$\tau_c \sim \frac{\lambda^2}{c\Delta\lambda}$$

transverse coherence

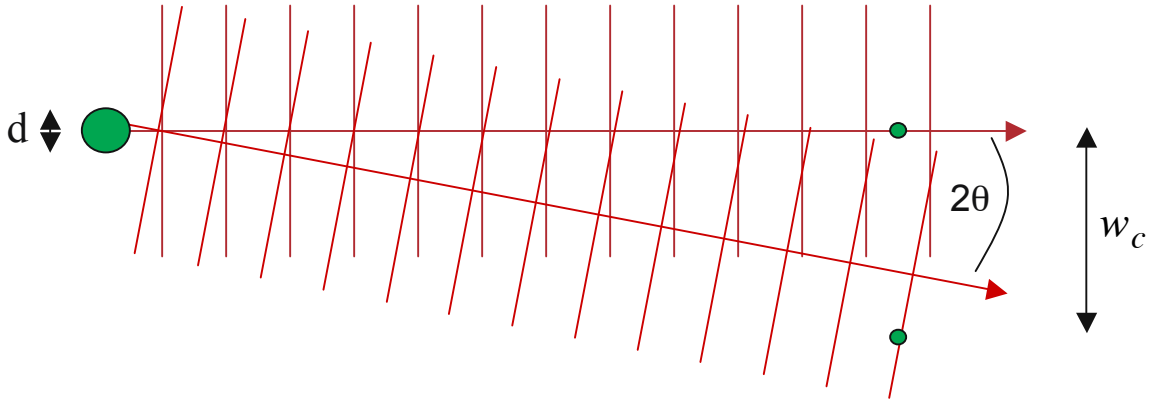

$$w_c \sim \frac{\lambda z}{d}$$

$$d \cdot \theta = \lambda / 2\pi$$

$$\Delta x \, \Delta p \geq \hbar / 2$$

Coherent vs. incoherent

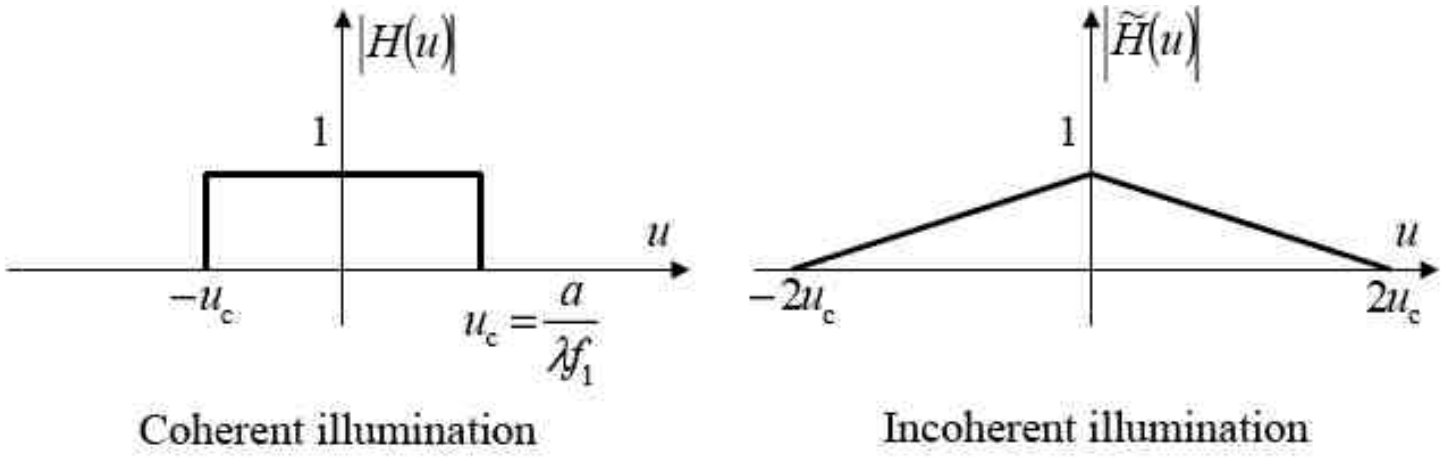

Scanning and full-field microscopy are *incoherent* methods

- Transfer function is linear in the field *intensities*
- Characterized by sloping function down to 2NA

Diffraction and holographic microscopy are *coherent* methods

- Transfer function is linear in the field *amplitudes*
- Characterized by flat top, sharp cutoff at limiting NA

X-ray microscopy: early history

- 1946 - 1971: Engstrom develops quantitative elemental imaging, Kirkpatrick and Baez develop crossed-mirror system for focusing x-rays, Cosslett and Nixon develop point-projection microscopy methods. Baez suggests use of zone plate lenses.

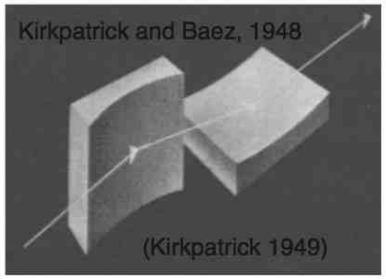

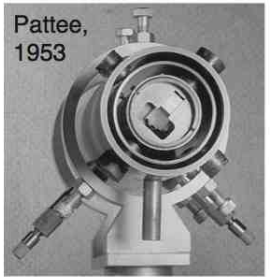

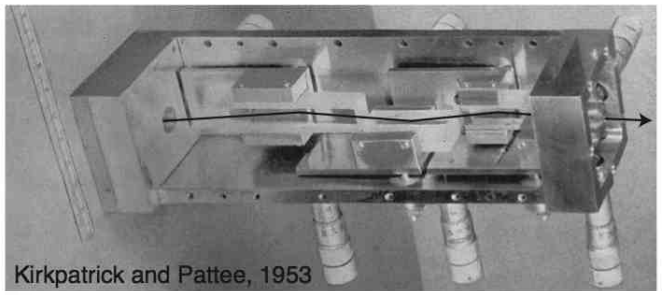

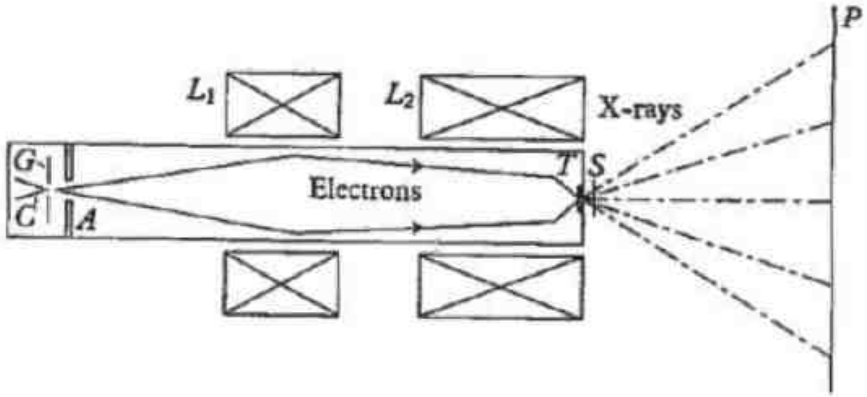

Fig. 1.3. Projection X-ray microscopy. The electron lenses $L_1 L_2$ form a reduced image at T of the cathode C; the X-rays emitted from T project an image of a specimen S on to the screen (or plate) P.

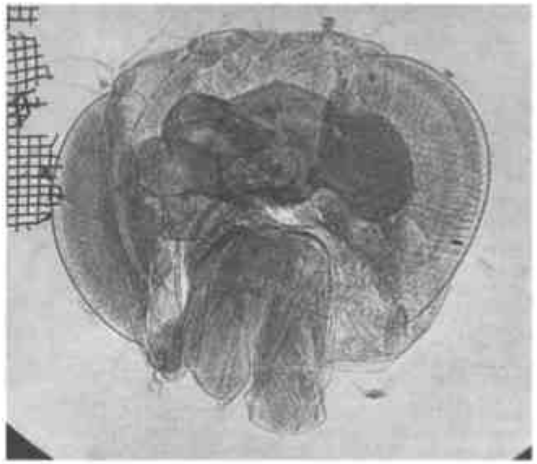

Fig. 3. Head of *Drosophila melanogaster*, freeze-dried, with 1,500 mesh reference grid.

J. Kirz and C. Jacobsen, *J. Phys. Conf. Ser.* 186, 102001 (2009)

SCIENTIFIC AMERICAN

Established 1845

CONTENTS FOR MARCH 1949 VOLUME 180, NUMBER 3

THE X-RAY MICROSCOPE

by Paul Kirkpatrick

It would be a useful complement to microscopes using light or electrons, for X-rays combine short wavelengths, giving fine resolution, and penetration. The main problems standing in the way have now been solved. 44

X-ray microscopy: early history

- 1972 - 1993: Horowitz & Howell build first scanning microscope at Cambridge Electron Accelerator, Aoki and Kikuta perform x-ray holography experiments, Schmahl builds first transmission x-ray microscope at DESY and ACO, Rarback & Kirz advance scanning microscopy with zone plates at NSLS. Schmahl & Rudolph develop Zernike phase contrast microscopy.

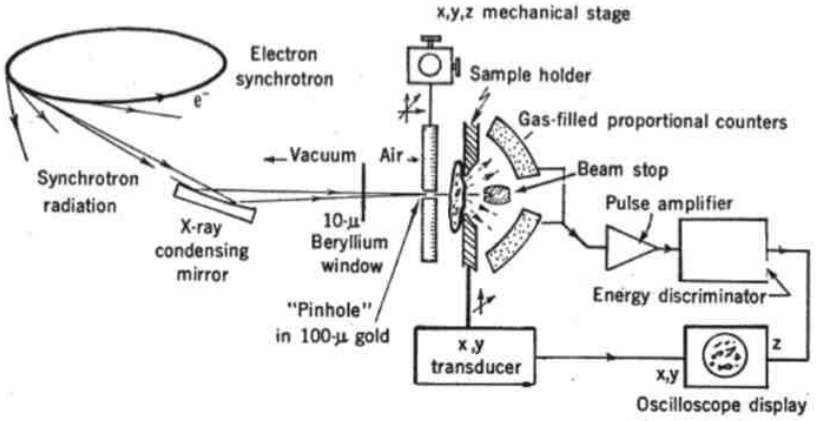

Fig. 1. Diagram of the microscope. The beam stop just behind the specimen absorbs the transmitted beam, reducing the elastically scattered background.

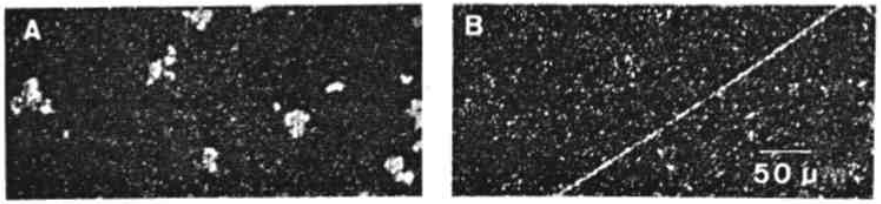

Fig. 4. A sample consisting of sulfur dust and a 2-μ silicon whisker viewed: (A) in sulfur K fluorescence and (B) in silicon K fluorescence.

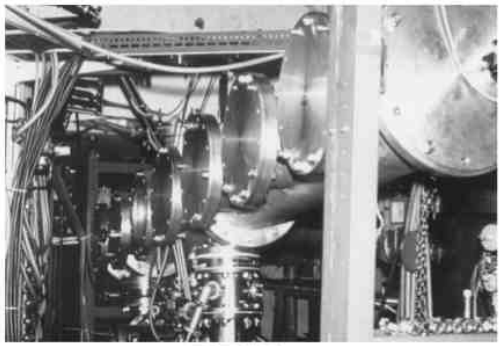

DESY, 1976

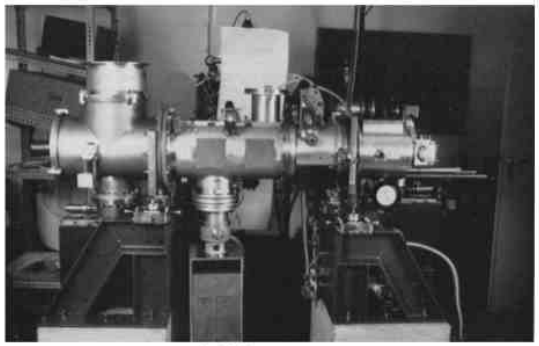

ACO, 1983

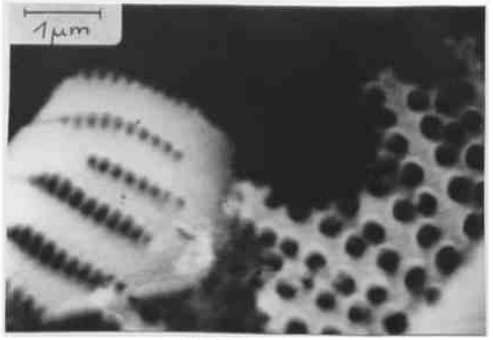

ACO, 1983

X-ray microscopy: recent history

- 1994 - 2002: Scanning and transmission x-ray microscopes proliferate at facilities wordwide including ALS, ESRF, ELETTRA, NSRRC, APS, and SPring8.
  - 3D imaging via tomography and cryo-tomography take off.
  - Coherent diffraction imaging first demostrated by Sayre & Miao.

- 2003 - present: X-ray microscopes become commercially available and that use laboratory sources. Applications expand to include environmental, geological/cosmo-chemistry, polymers, biology, magnetism, materials, and energy science, among others.

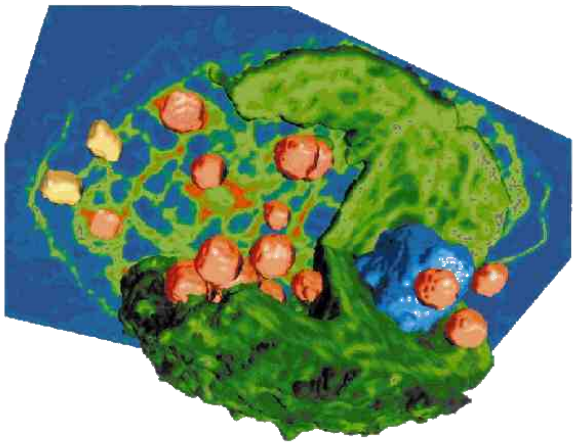

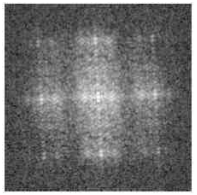

Why x-ray microscopy?

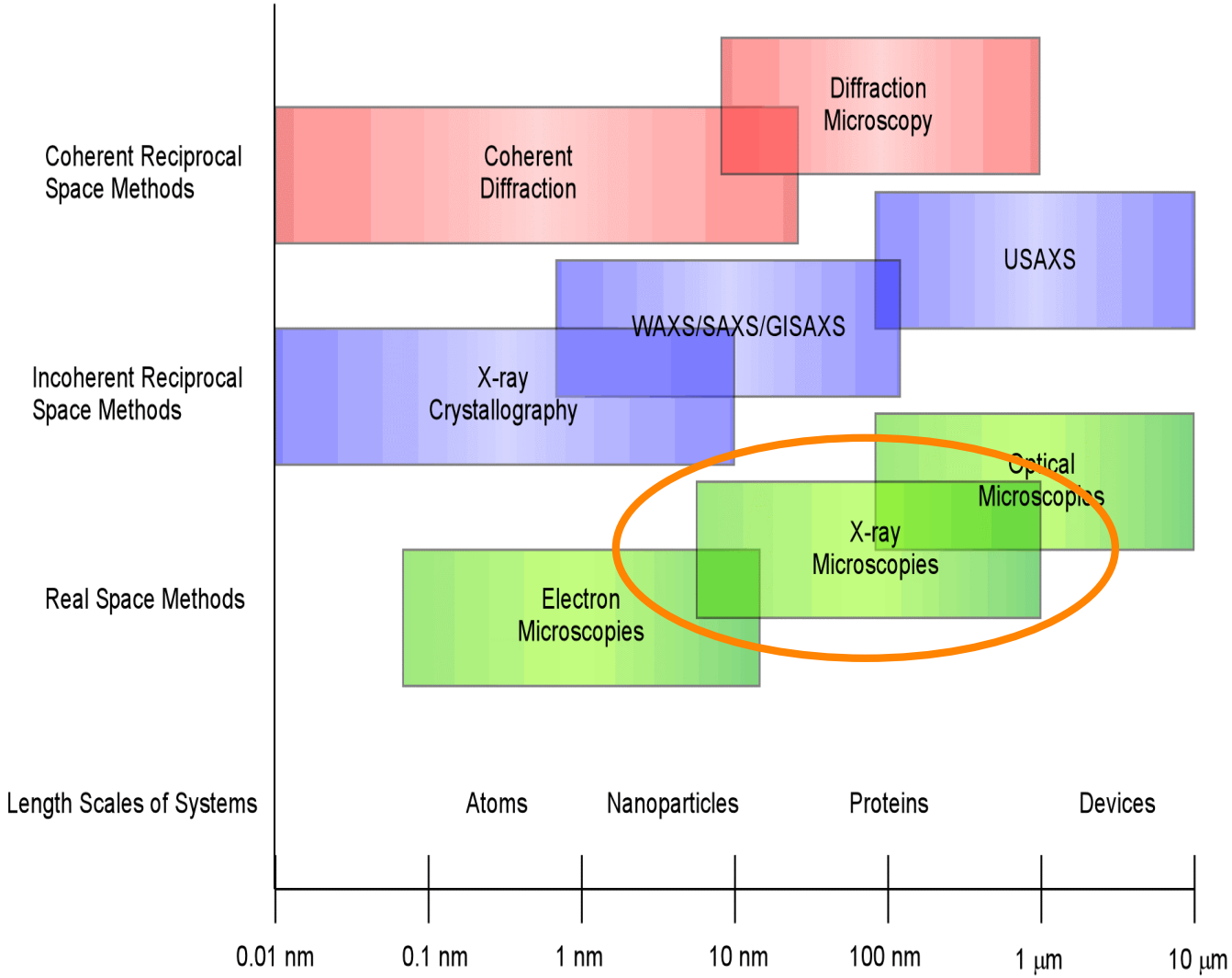

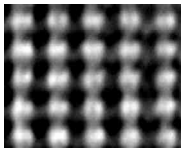
Si atoms - 0.078 nm spacing


DNA - 2.5 nm

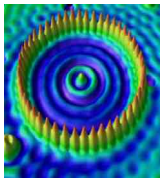
Fe quantum corral - 14 nm

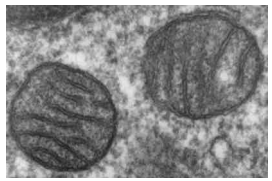
Mitochondria - 500 nm


Red blood cell - 8 μm

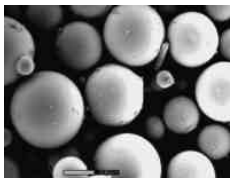
Fly ash 10-20 μm

X-rays offer:

- Short wavelengths, so high spatial resolution
- Short pulses, so high time resolution is possible
- Weakly interacting, high penetration
- Coupling to core-level electrons: “clean” measurement of electronic and chemical states
- Coupling to electronic spin via polarization: probe magnetic and orbital states

But: ionizing radiation, so repeated high-resolution imaging of radiation-sensitive samples (e.g. live cells) is not possible

Contrast mechanisms in x-ray imaging

Access a wealth of information

- Absorption — measure electron density
- Phase — measure real part of refractive index
- Fluorescence — measure elemental distribution
- Spectroscopy — extract chemical state, spin state
- Diffraction — reveal lattice structure and strain

- Natural sample contrast is possible; staining not required
- Image structure of thick samples, sectioning not required
- More penetrating, less damage, less charging than with electrons

Refractive index and contrast in the x-ray region

$$n = 1 - \delta - i\beta = 1 - \frac{r_e}{2\pi}\lambda^2 \sum_i n_i f_i(0)$$

$$A = A_0 \exp(-inkt)$$

$$k = 2\pi / \lambda$$

- Absorption contrast:

  sensitive to *Im(n)*

  $\sim 4\pi\beta(x,y)t/\lambda$

- Phase contrast:

  sensitive to *Re(n)*

  $\sim 2\pi\delta(x,y)t/\lambda$

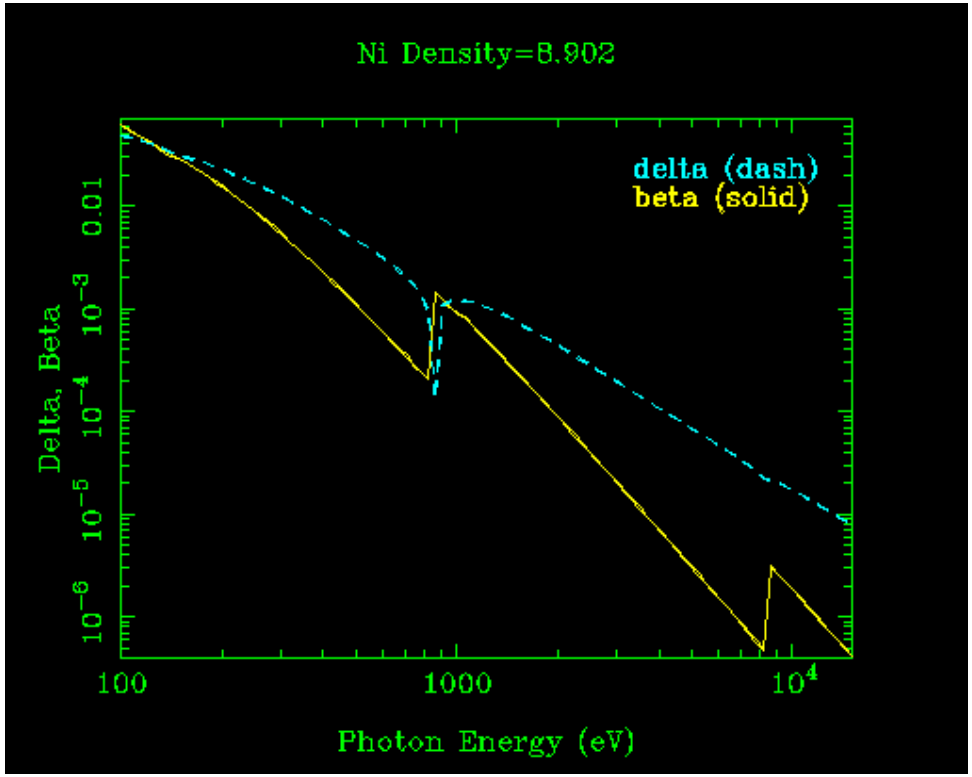

Absorption edges provide elemental and chemical *specificity*

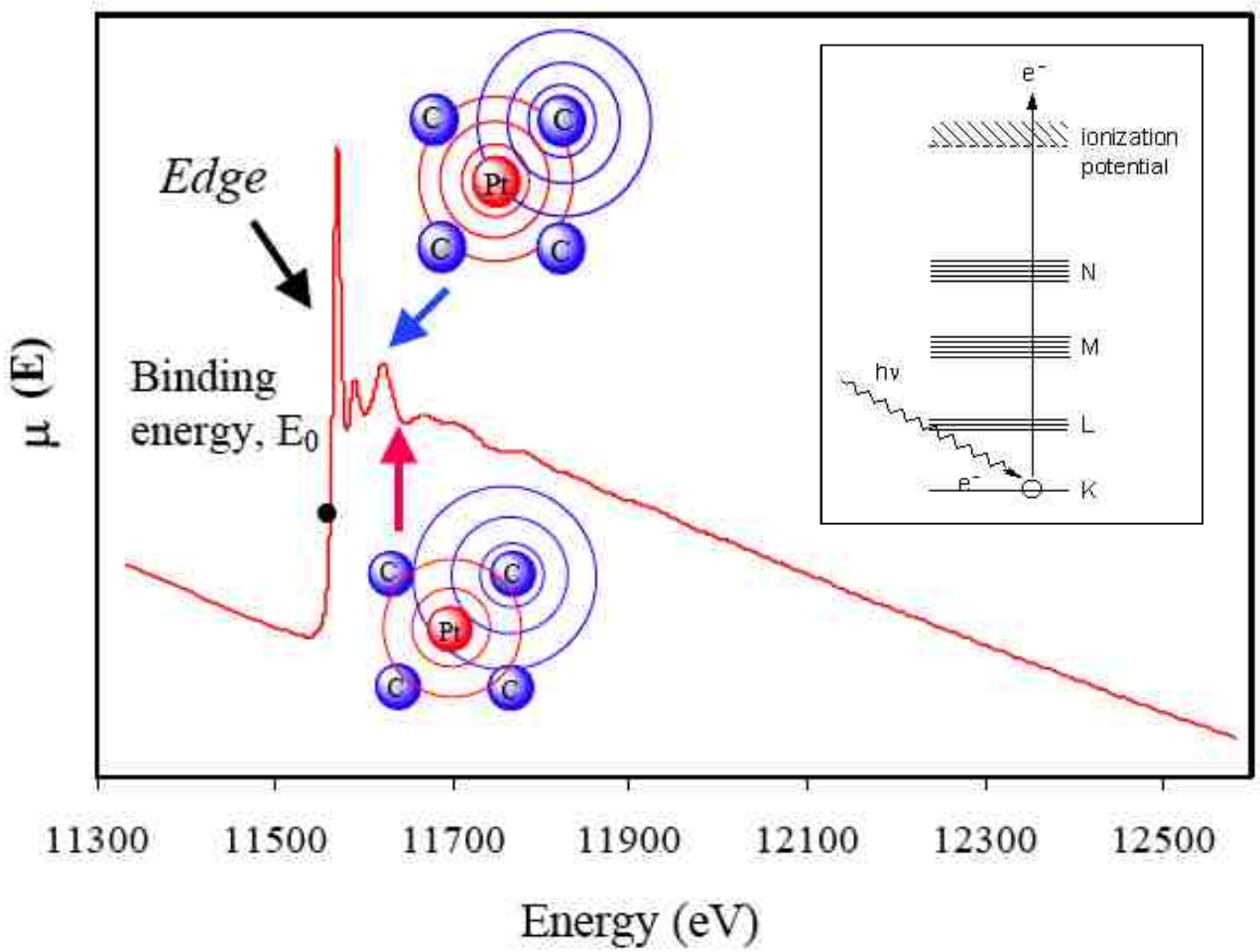

Details of edge spectra tell us about chemical state

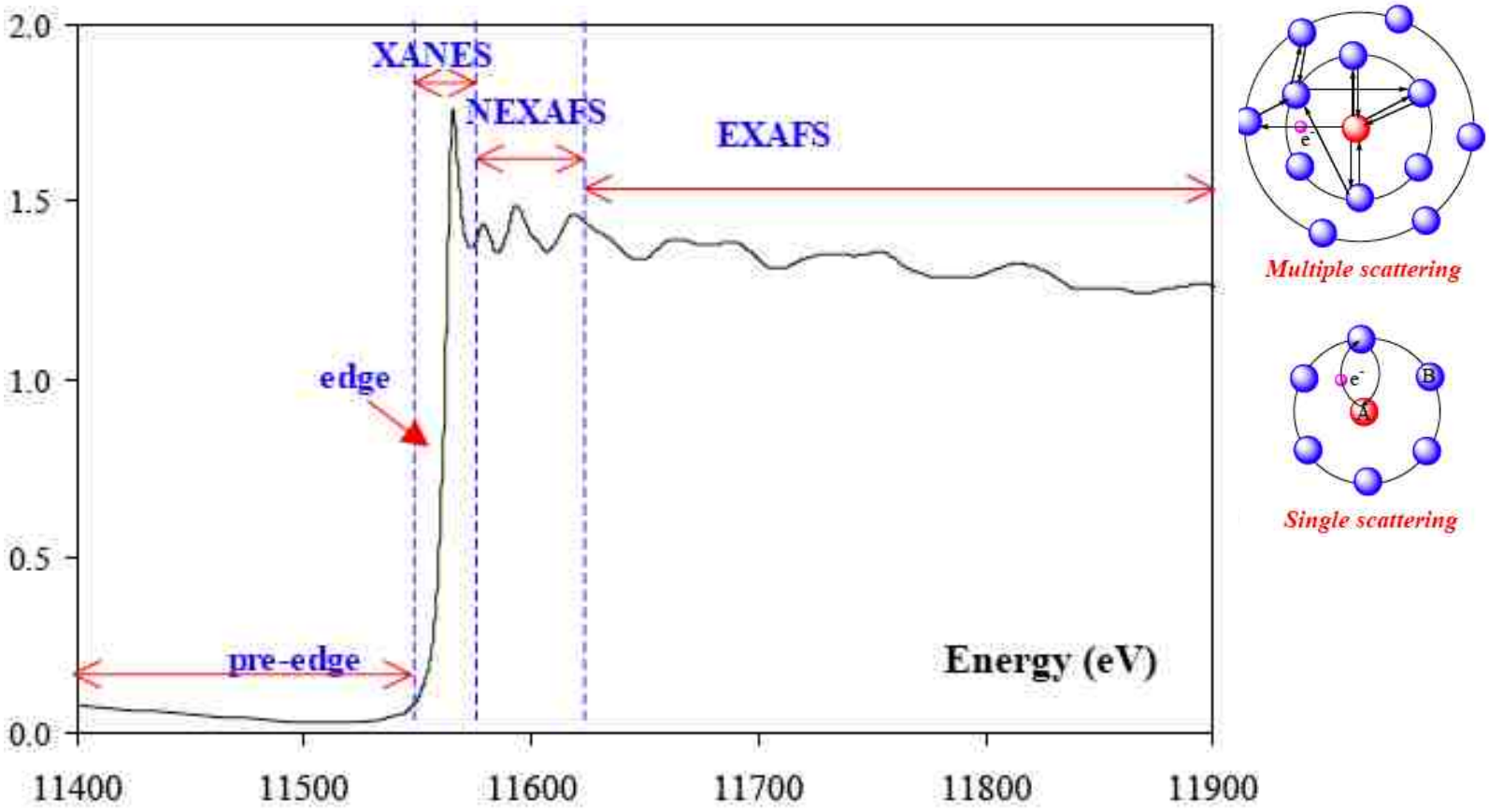

The "water window"

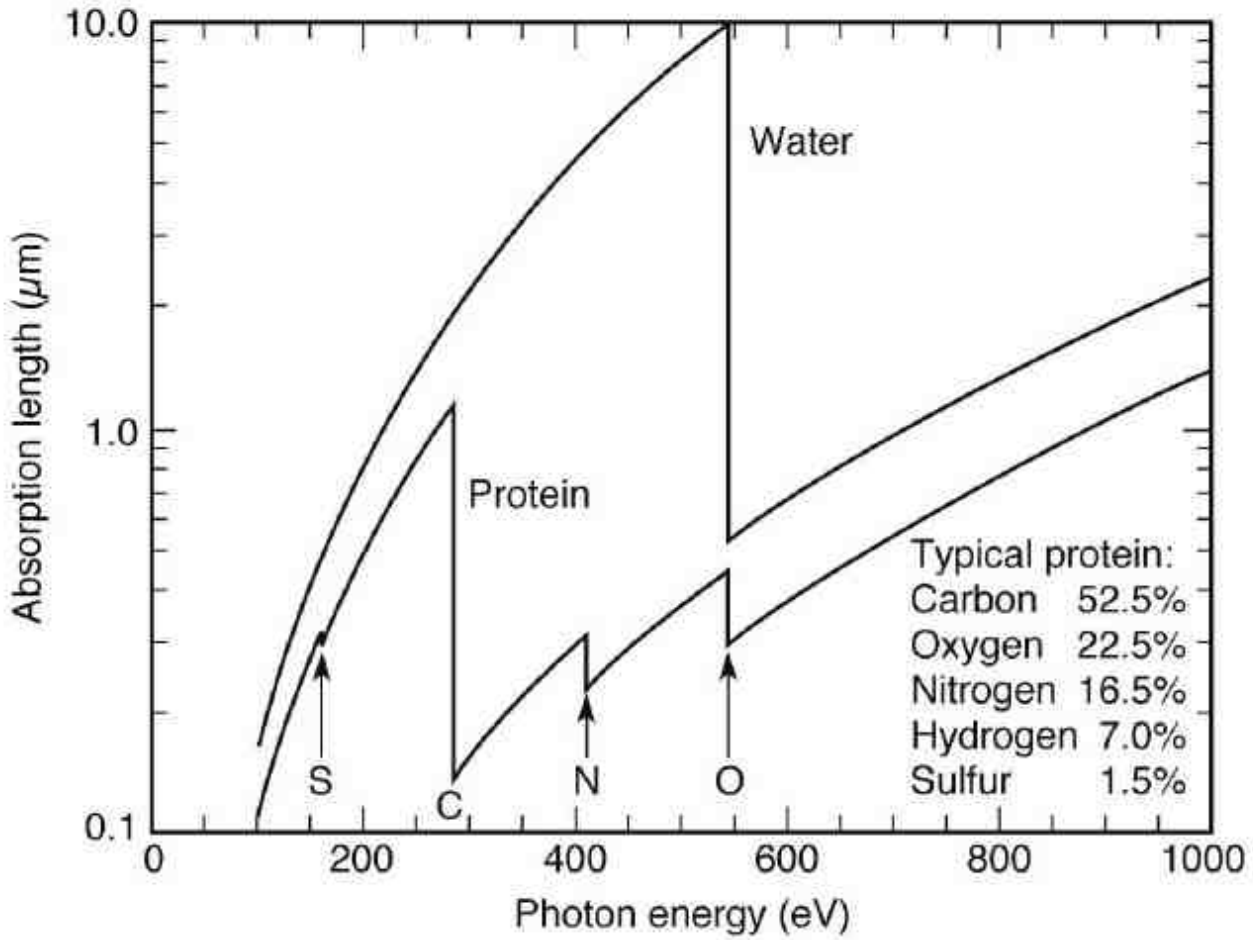

Fluorescence spectroscopy

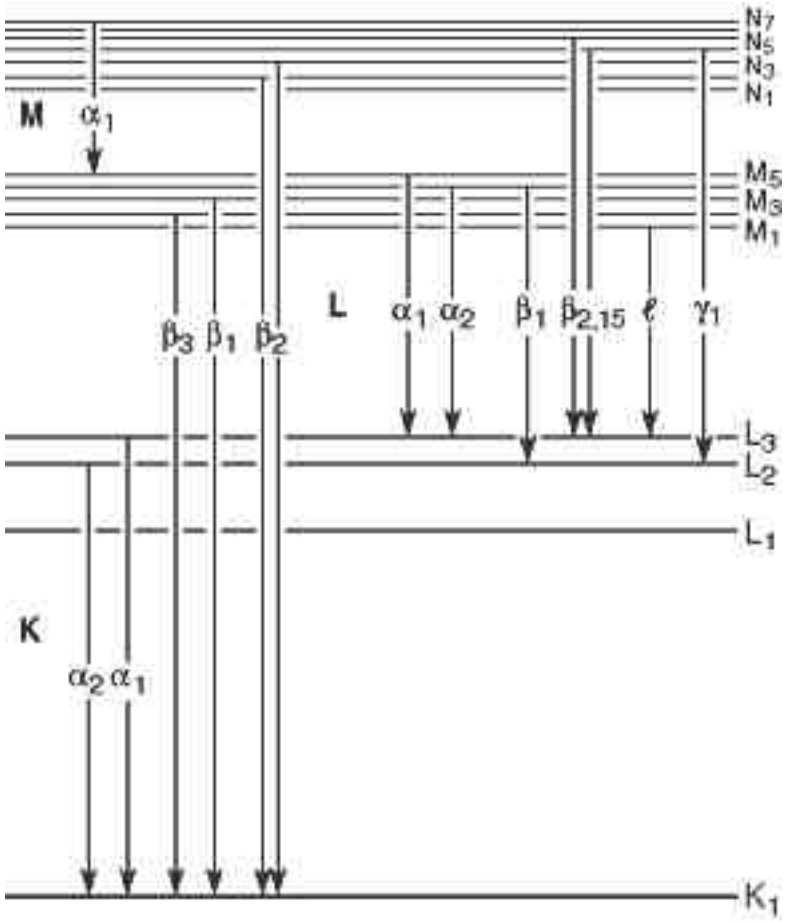

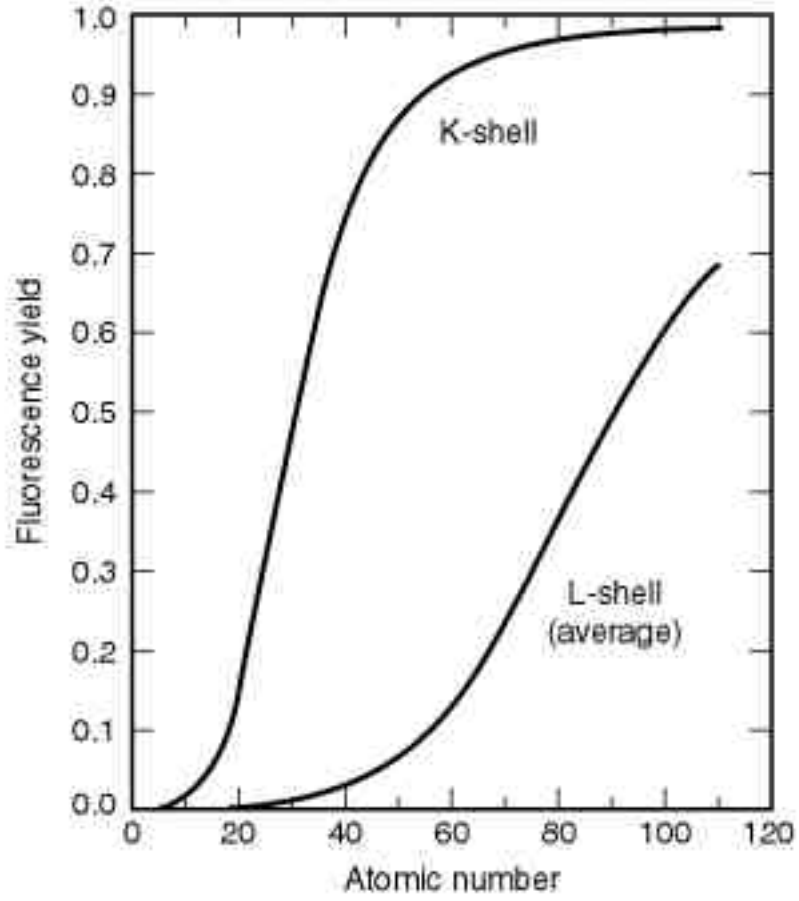

Why use synchrotron radiation?

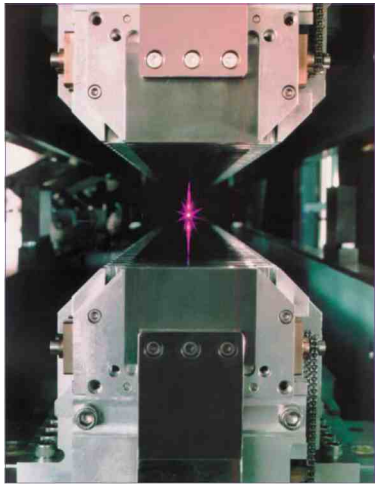

Synchrotron sources offer:

- Brilliance (small source, collimated)
- Tunability (IR to hard x-rays)
- Polarization (linear, circular)
- Time structure (short pulses)

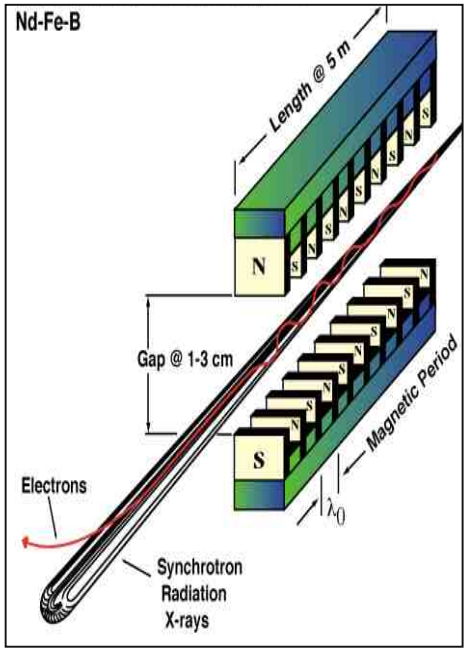

➢ Source brilliance is a key figure of merit for an x-ray microscope

B = photons/source area, divergence, bandwidth

$F_c \sim \lambda^2 B$

Undulator radiation

- SR sources (except FEL) are incoherent, but highly forward directed due to relativistic effects $\theta \sim 1/\gamma$

- Spatial and temporal filtering (pinholes, monochromators) are needed to select the coherent flux $F_c \sim \lambda^2 B$

- Only the coherent flux can be focused into a diffraction-limited spot or be used to form interference fringes

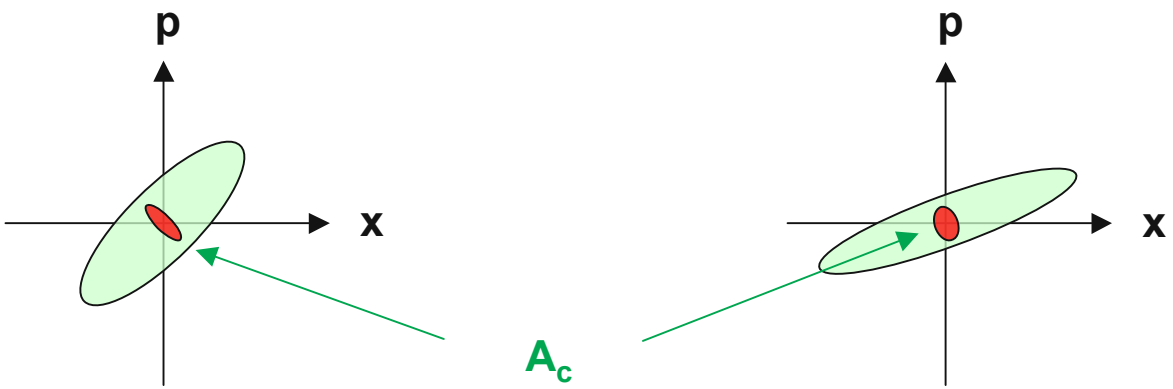

Focusing optics for x-rays

Achieving high NA is challenging because x-rays interact weakly

$n = 1 - \delta - i\beta$ $\quad \delta,\beta \sim 10^{-3}$ to 10^{-6} $\quad \Rightarrow \quad |n| \approx 1$

Refractive (compound refractive lenses) ~ 50 nm

Low efficiency, highly chromatic, aberrations

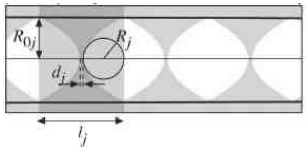

Reflective (Kirkpatrick-Baez mirrors) ~ 40 nm

High efficiency, achromatic, limited to ~10 nm

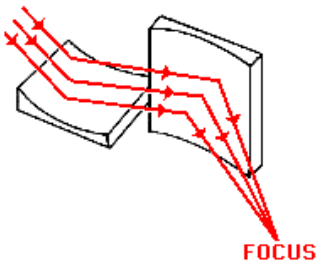

Diffractive (Fresnel zone plates, MLLs) ~ 15 nm

Moderate efficiency, limited to ~10 nm except MLL

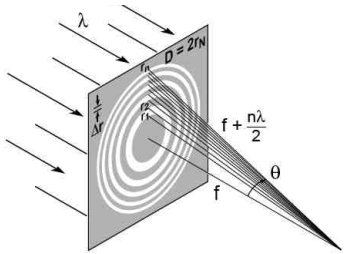

Waveguides ~ 10 nm

Low efficiency, 2D is challenging

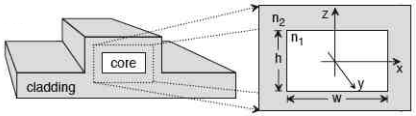

Fresnel zone plate

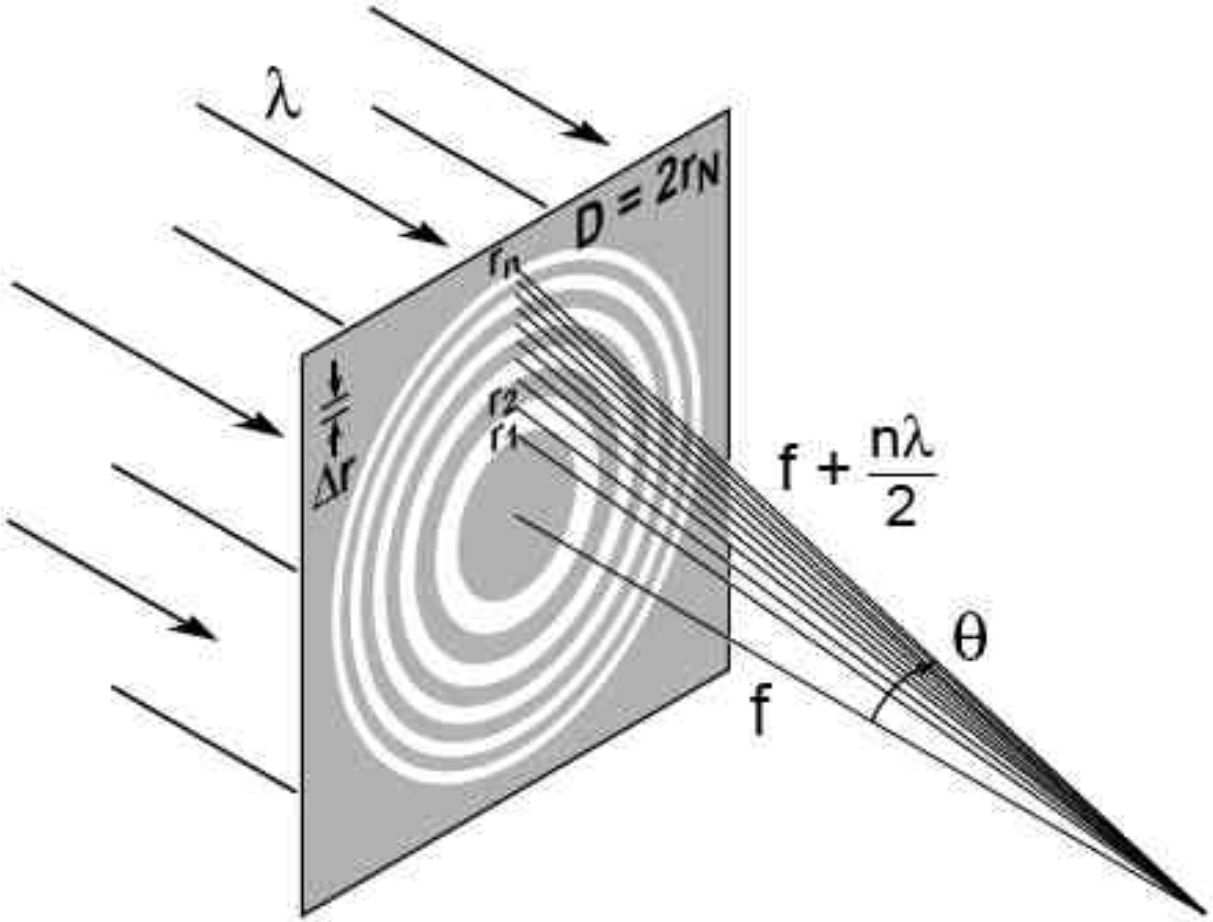

$$f^2 + r_n^2 = \left(f + \frac{n\lambda}{2}\right)^2$$

$$r_n^2 = nf\lambda + \frac{n^2\lambda^2}{4}$$

$$r_n \approx \sqrt{nf\lambda}$$

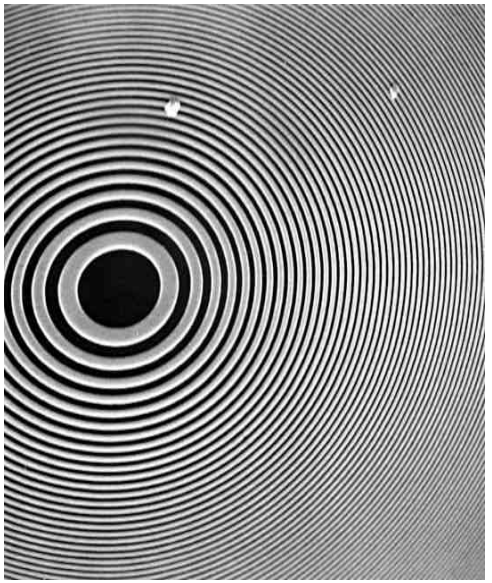

J.L. Soret. Arch. Sci. Phys. Nat. 52. 320 (1875).
R.W. Wood, Physical Optics, (Macmillan, New York, 1934), p. 37.
J. Kirz, J. Opt. Soc. Am. 64, 301 (1974).

Resolution of a zone plate

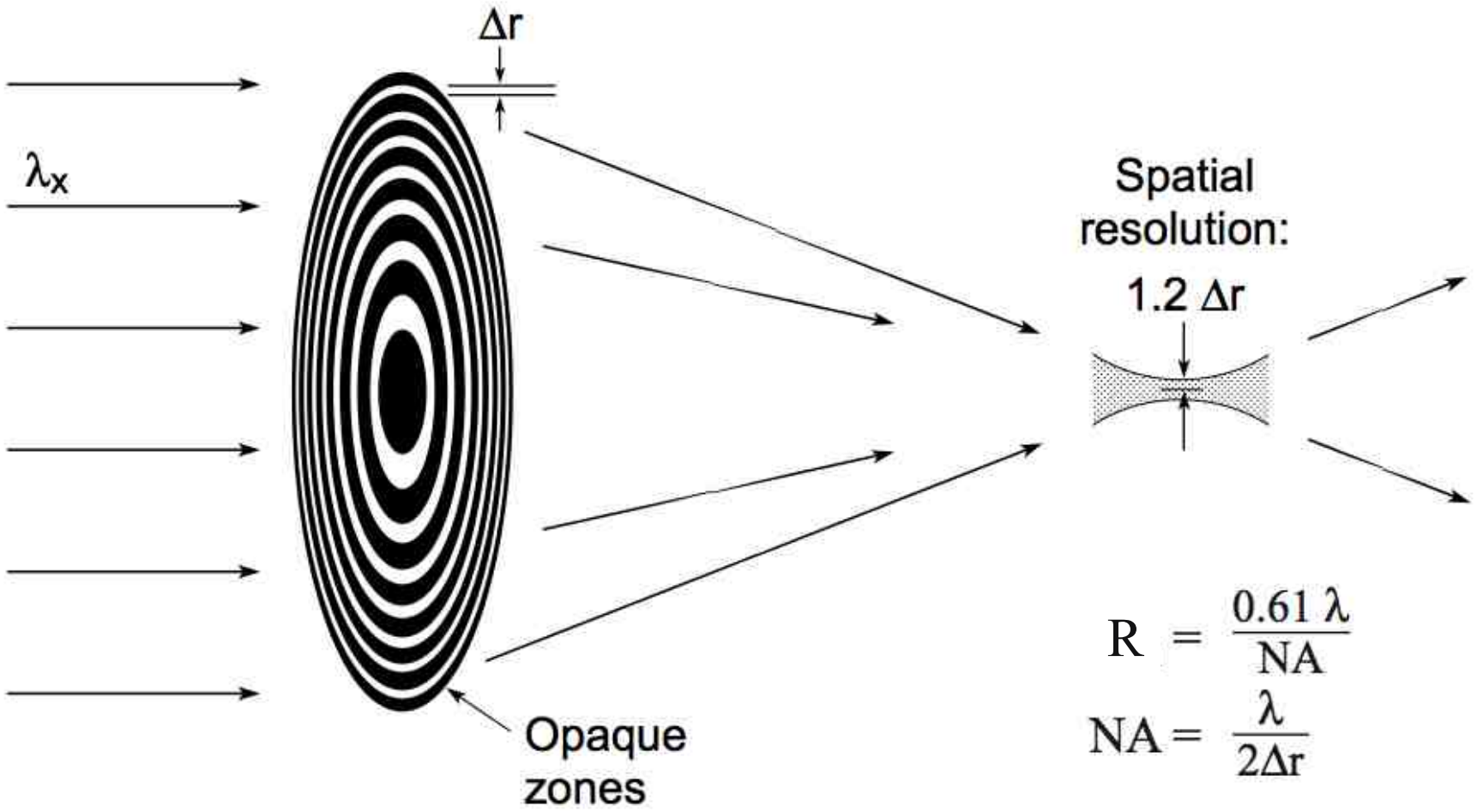

$$R = \frac{0.61\,\lambda}{NA}$$

$$NA = \frac{\lambda}{2\Delta r}$$

A zone plates forms an image like a thin lens

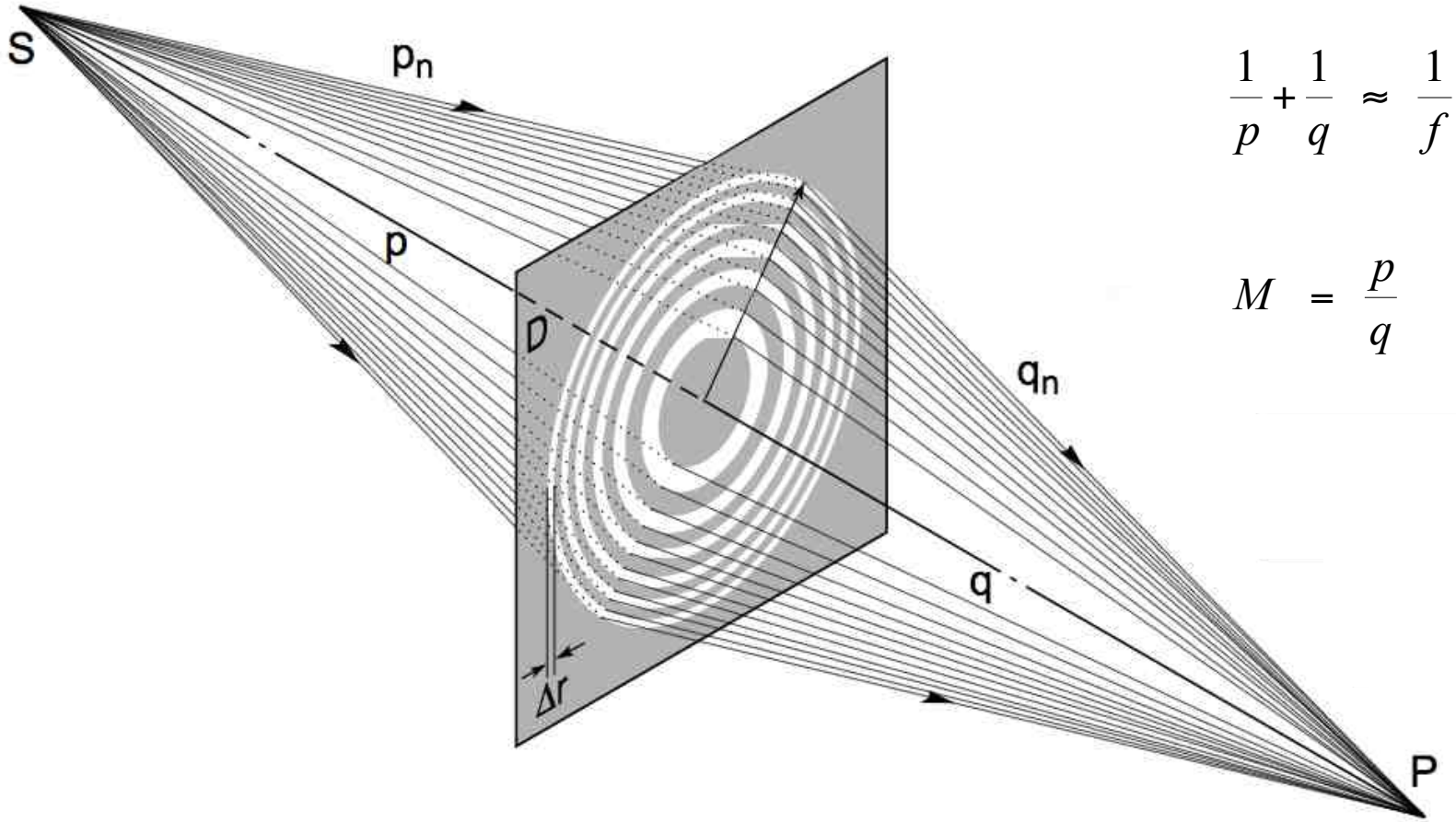

$$\frac{1}{p}+\frac{1}{q} \approx \frac{1}{f}$$

$$M = \frac{p}{q}$$

Efficiency of a gold zone plate

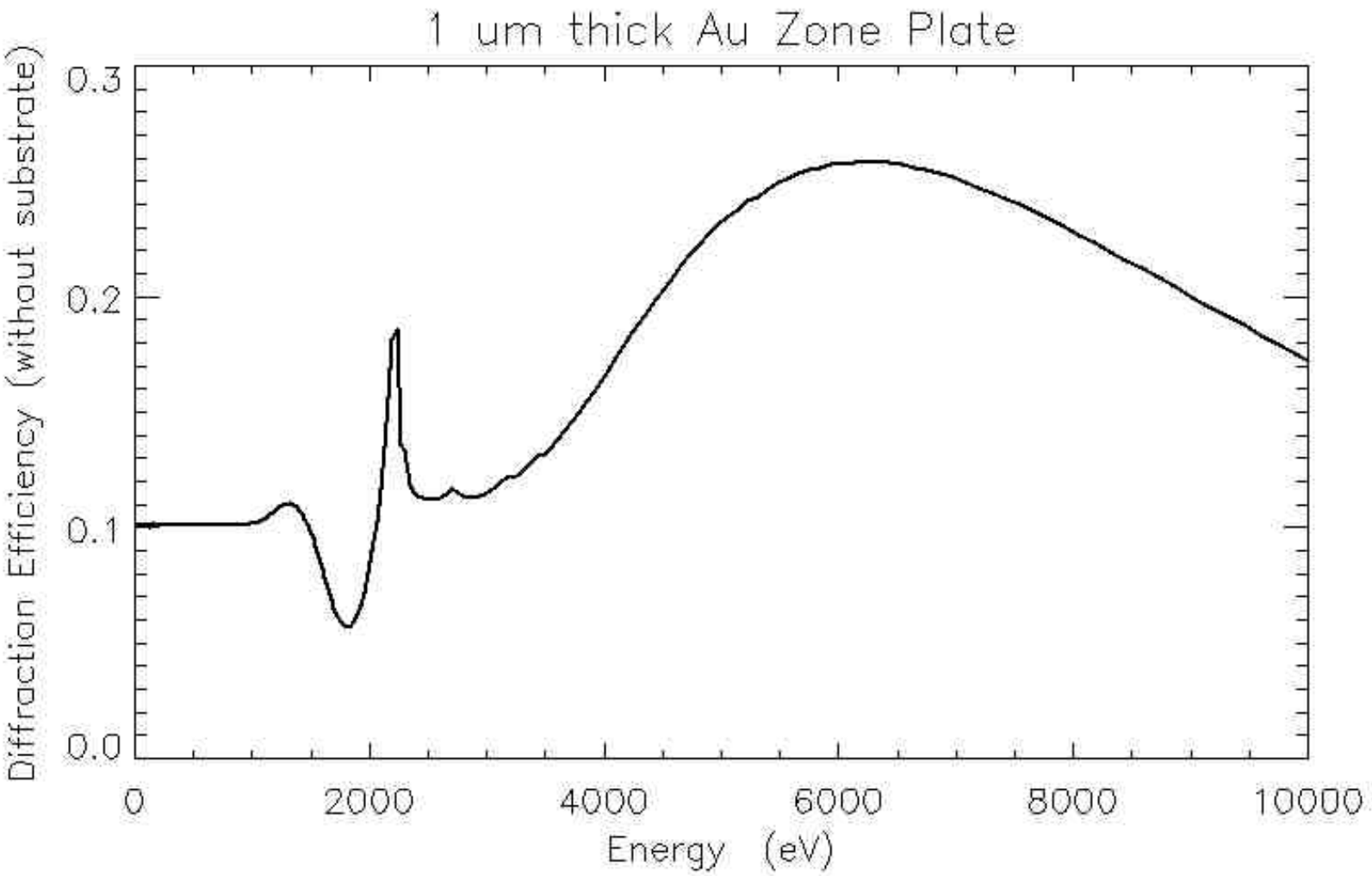

Performance of best zone plates to date

25 nm zone plate

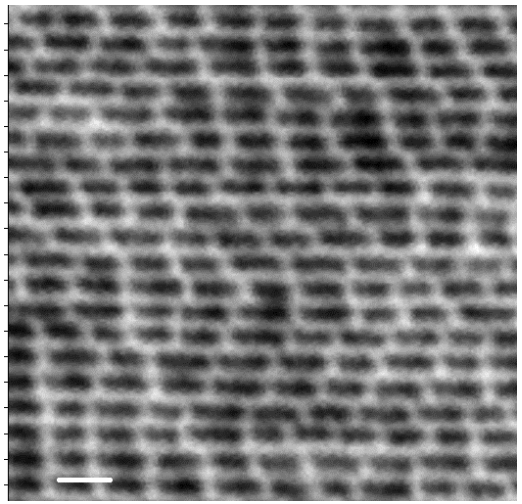

20 nm (vertical) Au lines

20 nm zone plate

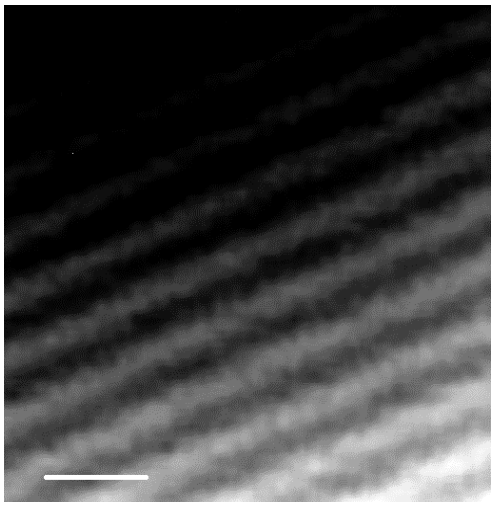

12 nm lines Si/Mo

17 nm zone plate

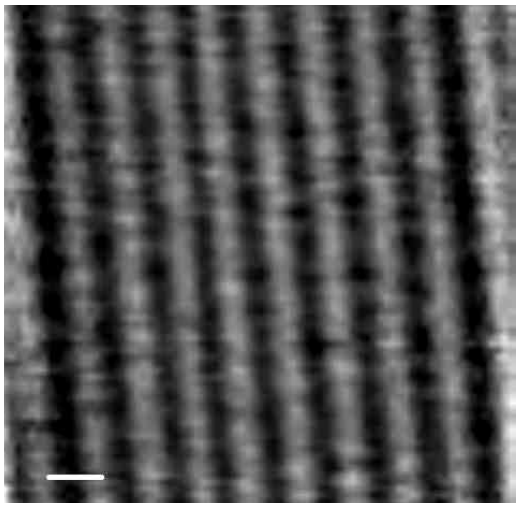

10 nm lines Si/Mo

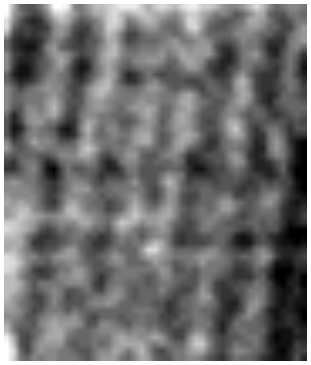

9 nm lines Si/Mo

Imaged by 17 nm zone plate

All images taken at 700 eV

Structures have equal line/space nominal dimensions

Dimensions of half periods are quoted

Achieved resolution close to the theoretical limits

W. Chao, *Opt. Expr.* 20, 9778 (2012)

2. Direct methods

- **Projection imaging**
- **Full-field imaging**
- **Scanning methods**

References:
1. M. Howells, "Soft-x-ray microscopes," Physics Today 38, 22 (Aug. 1985).
2. J. Kirz, "Soft X-ray microscopes and their biological applications," Q. Rev. Biophys. 28, 1 (1995).

Direct imaging methods

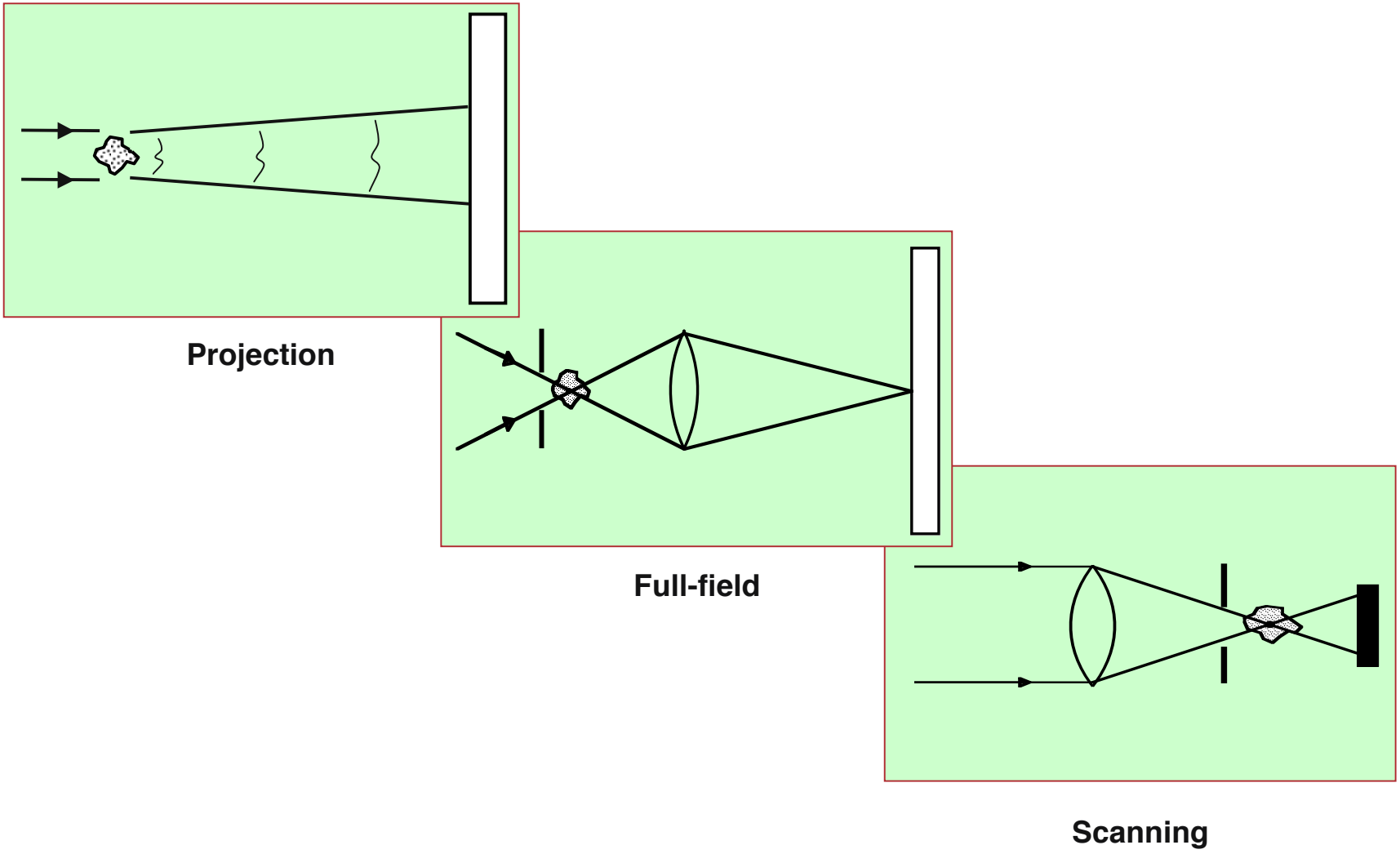

Different regimes for x-ray imaging

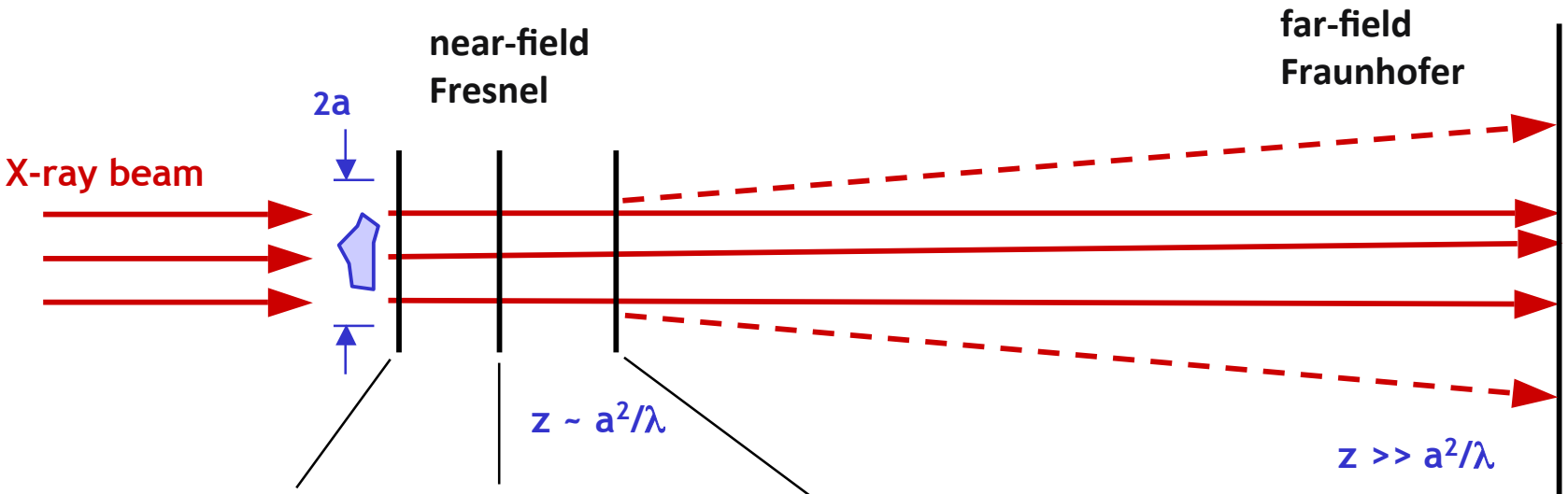

absorption radiograph

phase contrast

Kagoshima (1999)

in-line holography

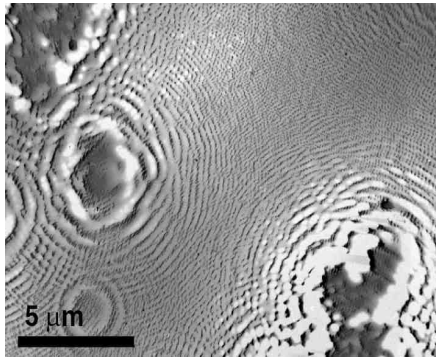

Jacobsen (1990)

coherent diffraction

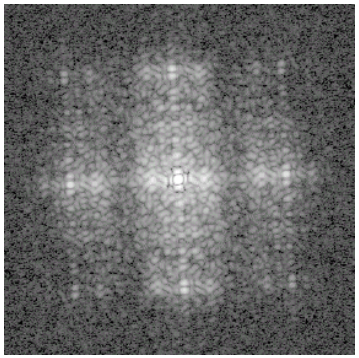

Miao (1999)

Phase contrast: tool of choice for low absorption samples

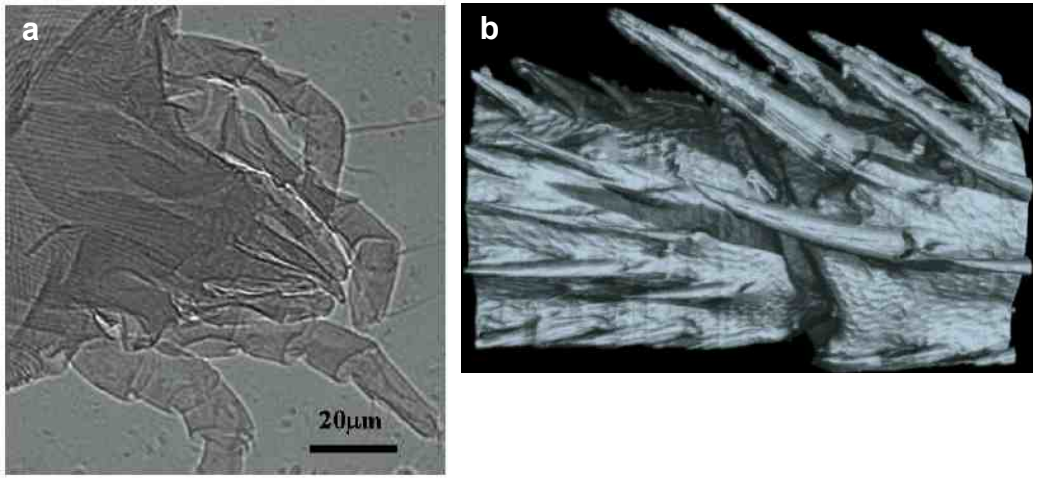

(a) Dust mite and (b) tomographically reconstructed fly leg joint, recorded with ~8 keV x-rays and propagation phase contrast.

S. Mayo, Opt. Express 11, 2289 (2003)

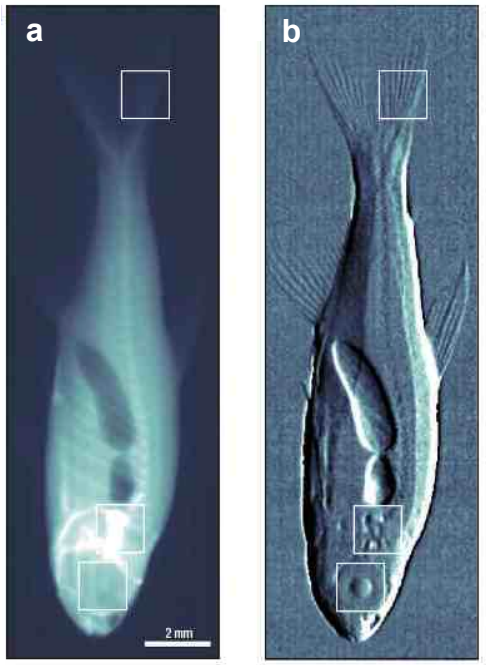

Small fish, recorded with three-grating method and standard x-ray tube (40 kV/25 mA). (a) Transmission. (b) Differential phase.

F. Pfeiffer, Nature Phys. 2, 258 (2006)

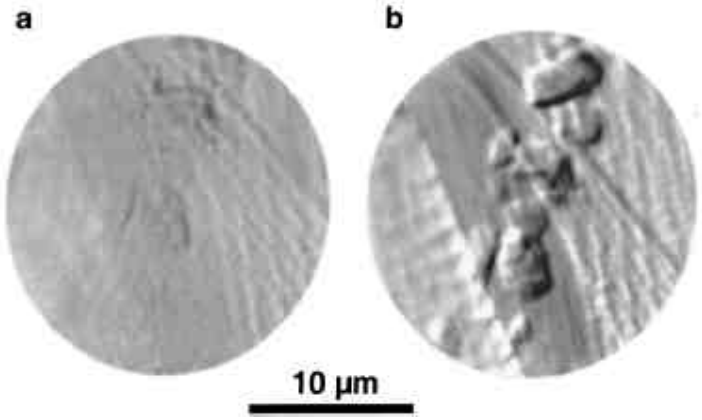

Moth wing, recorded with 4 keV x-rays.
(a) Bright-field. (b) Differential interference contrast.

B. Kaulich, T. Wilhein, JOSA A19, 797 (2002)

Utilizing the time structure of the source

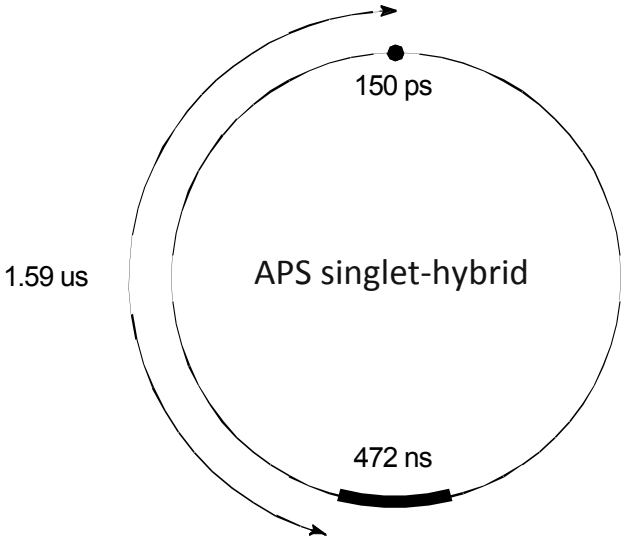

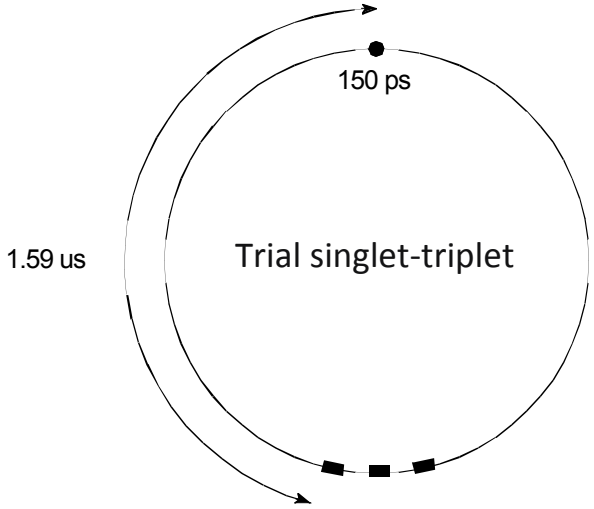

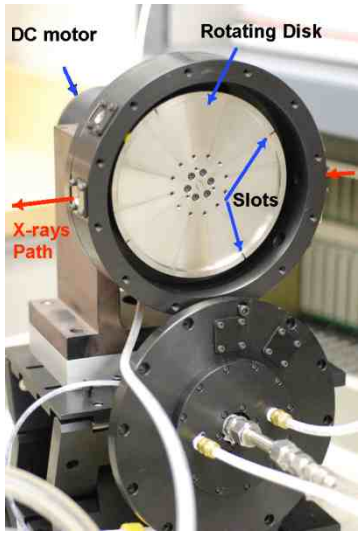

Mechanical shutters

Sample stages and HS detector

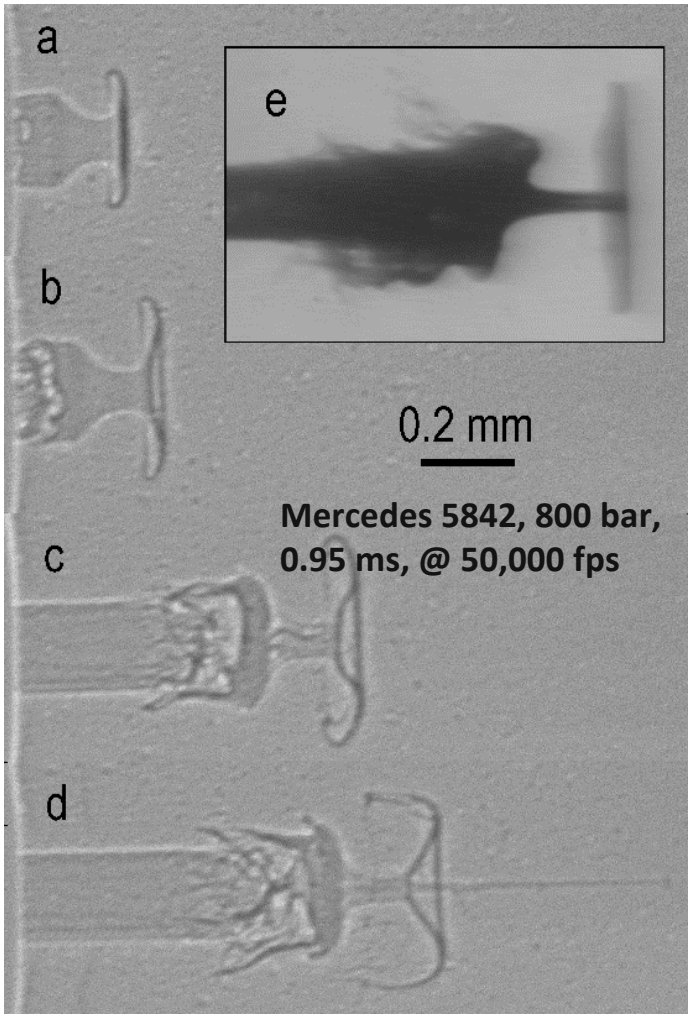

Transportation technology: spray breakup from a fuel injector

C. Powell, Proc. ASME ICEF 2009

High-speed imaging of jets and droplet coalescence

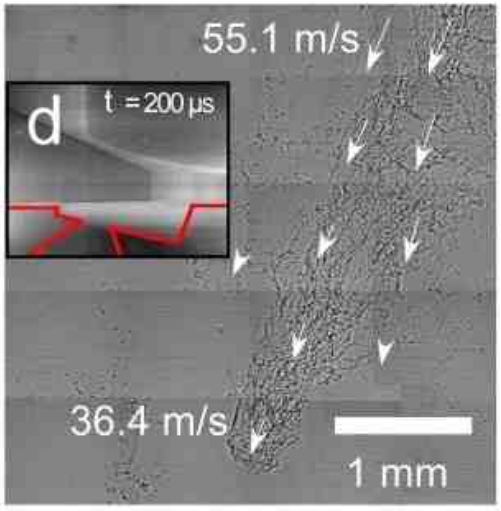

"Study of dense liquid jet flow dynamics using structure tracking velocimetry,"

Y. Wang, Nature Physics 4, 305 (2008)

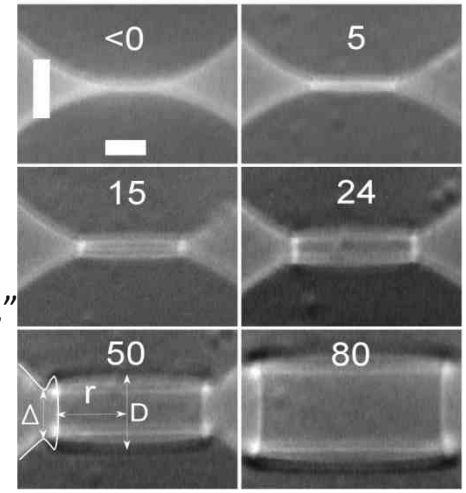

"Coalescence Singularity of Two Water Droplets,"

K. Fezzaa, Phys. Rev. Lett. 100, 104501 (2008)

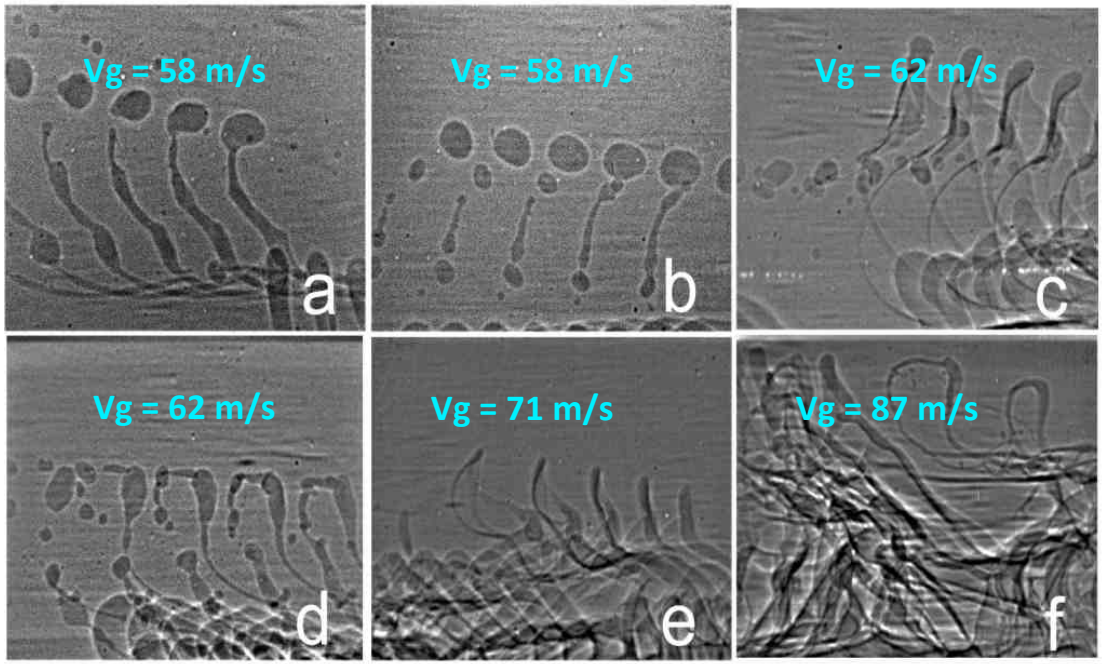

Full-field x-ray microscope

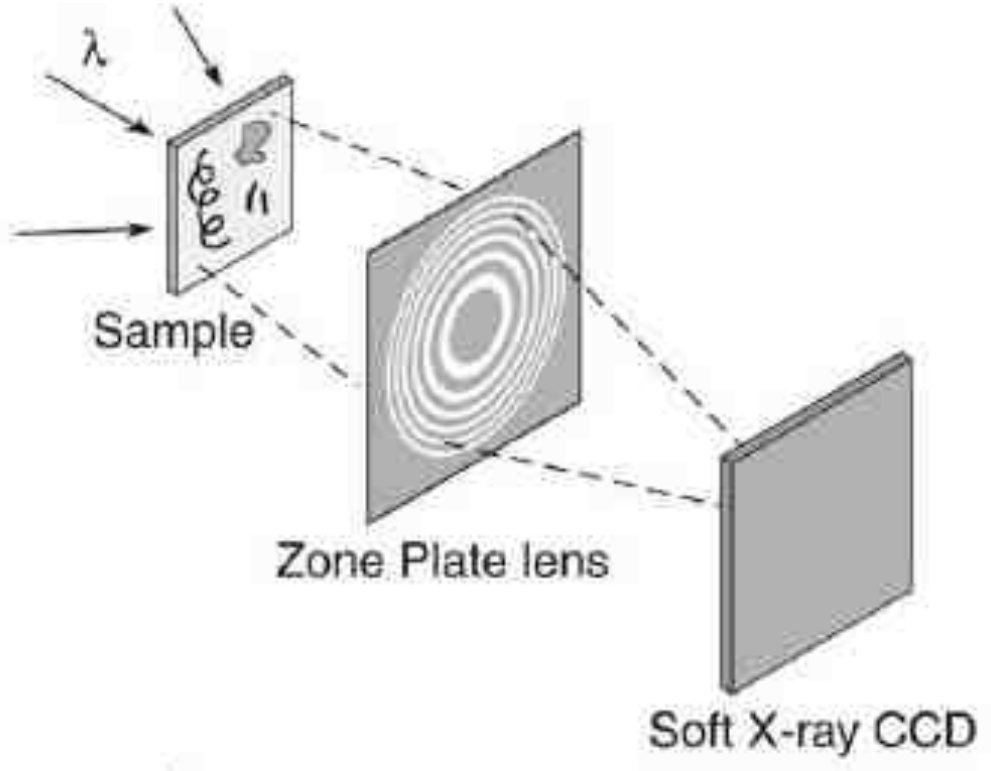

0. Rudolph and G. Schmahl, Ann. N. Y. Acad. Sci. 342, 94 (1980)

XM-1 microscope at the ALS

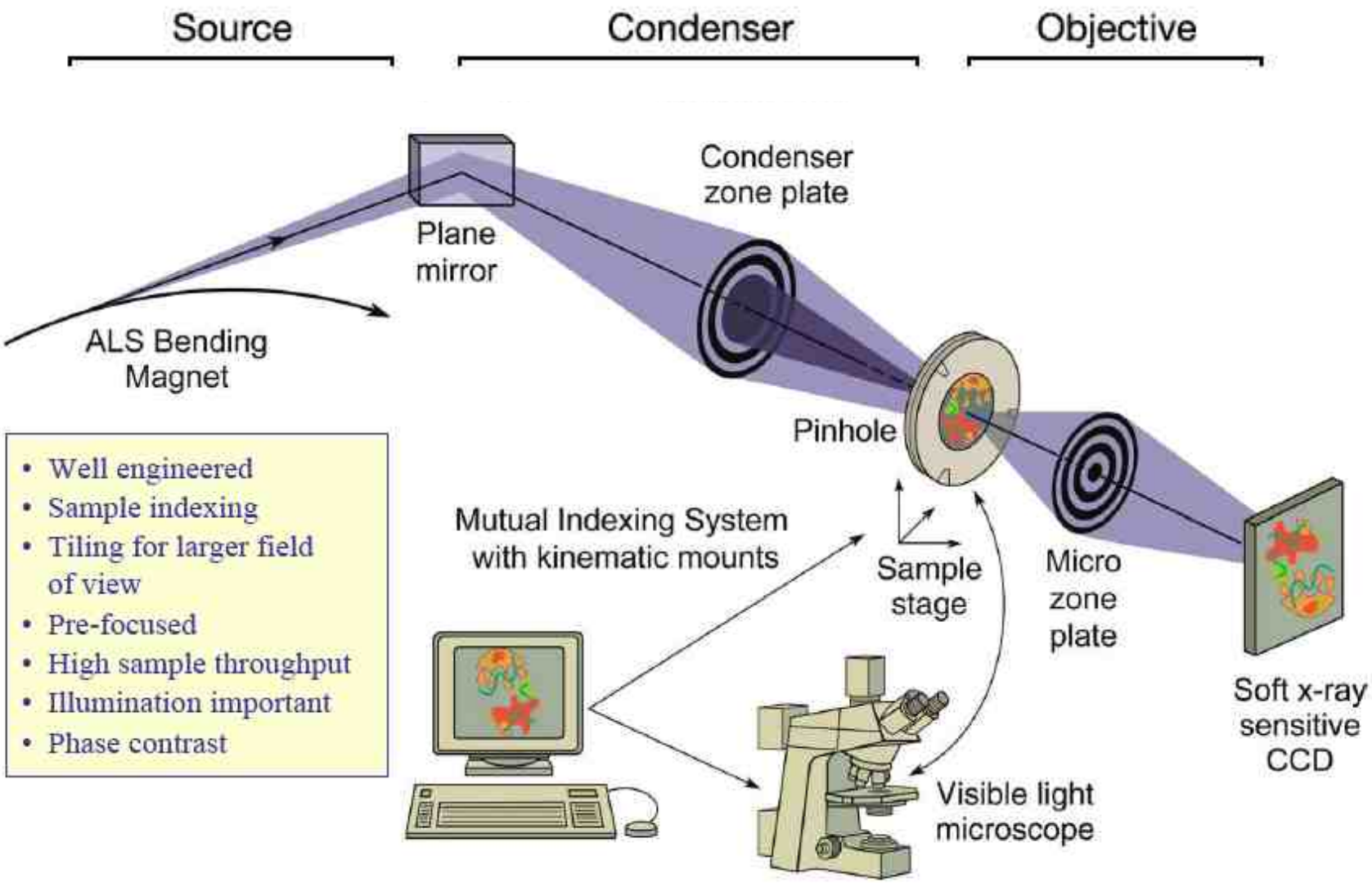

Wet specimens can be studied up to damage limits

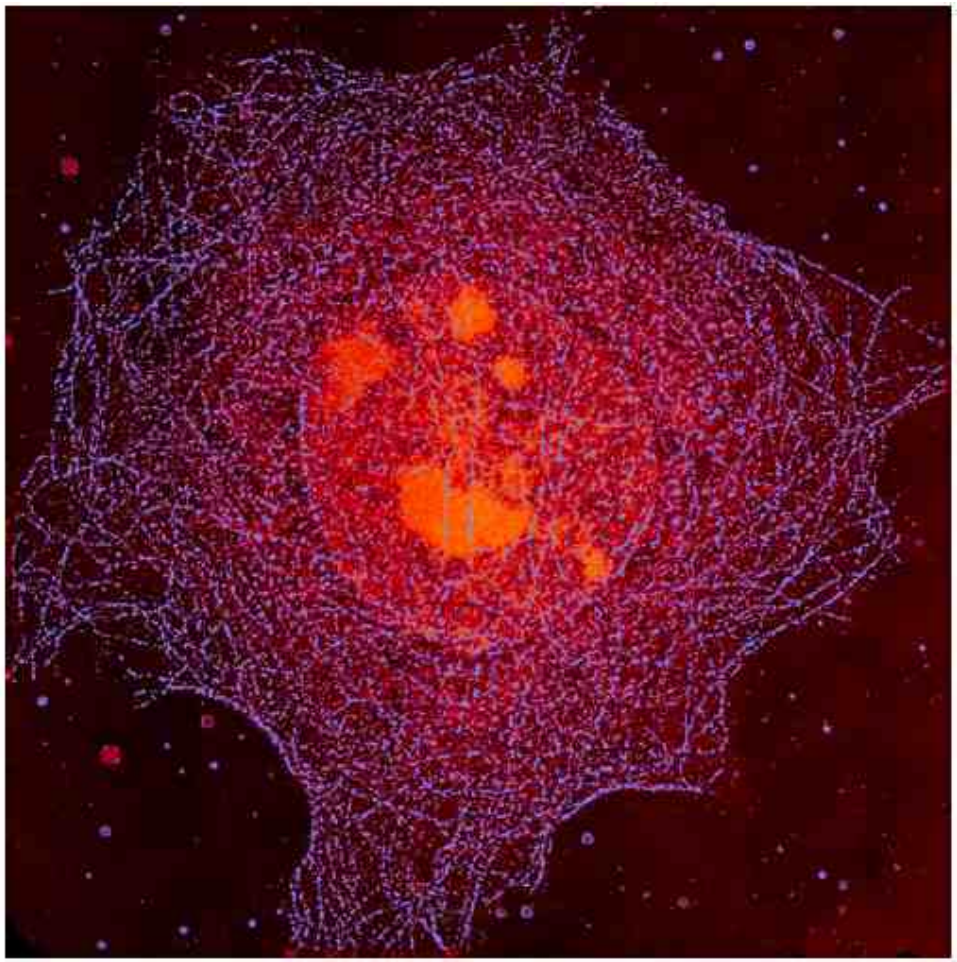

$\hbar w = 520$ eV

32 μm x 32 μm

Ag enhanced Au labeling of the microtubule network, color coded blue.

Cell nucleus and nucleoli, moderately absorbing, coded orange.

Less absorbing aqueous regions coded black.

W. Meyer-Ilse et al.
J. Microsc. 201, 395 (2001)

Whole, hydrated mouse epithelial cell

Cryo-preparation of sample mitigates radiation damage

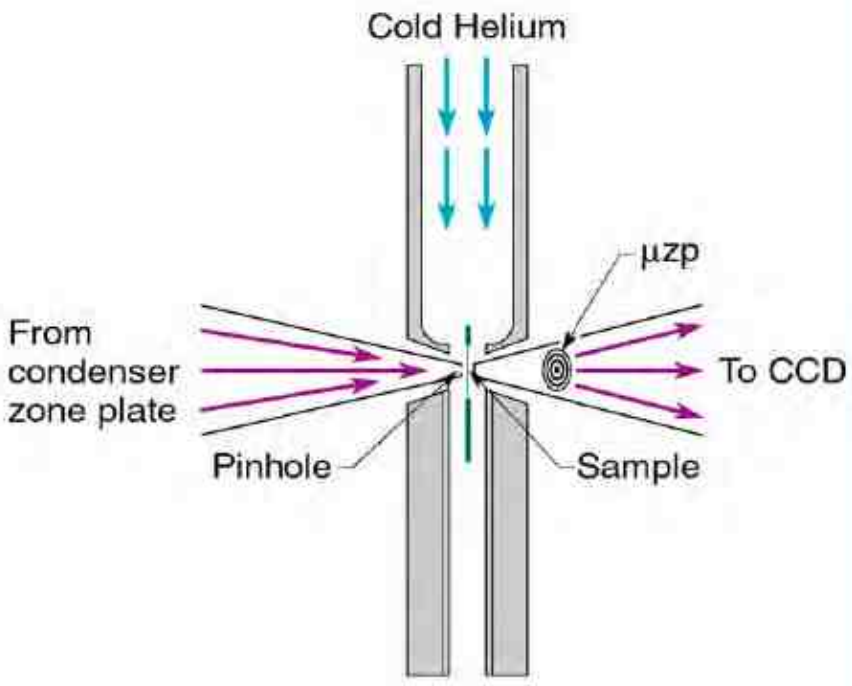

Helium passes through LN, is cooled,
and directed onto sample windows

Fast Freeze

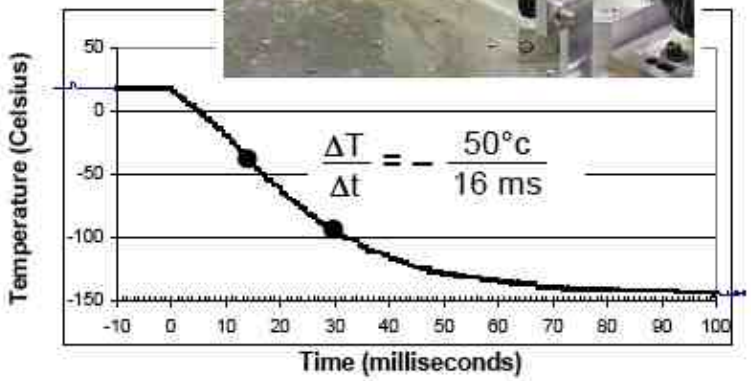

Interconnects in chips are more "hardy"

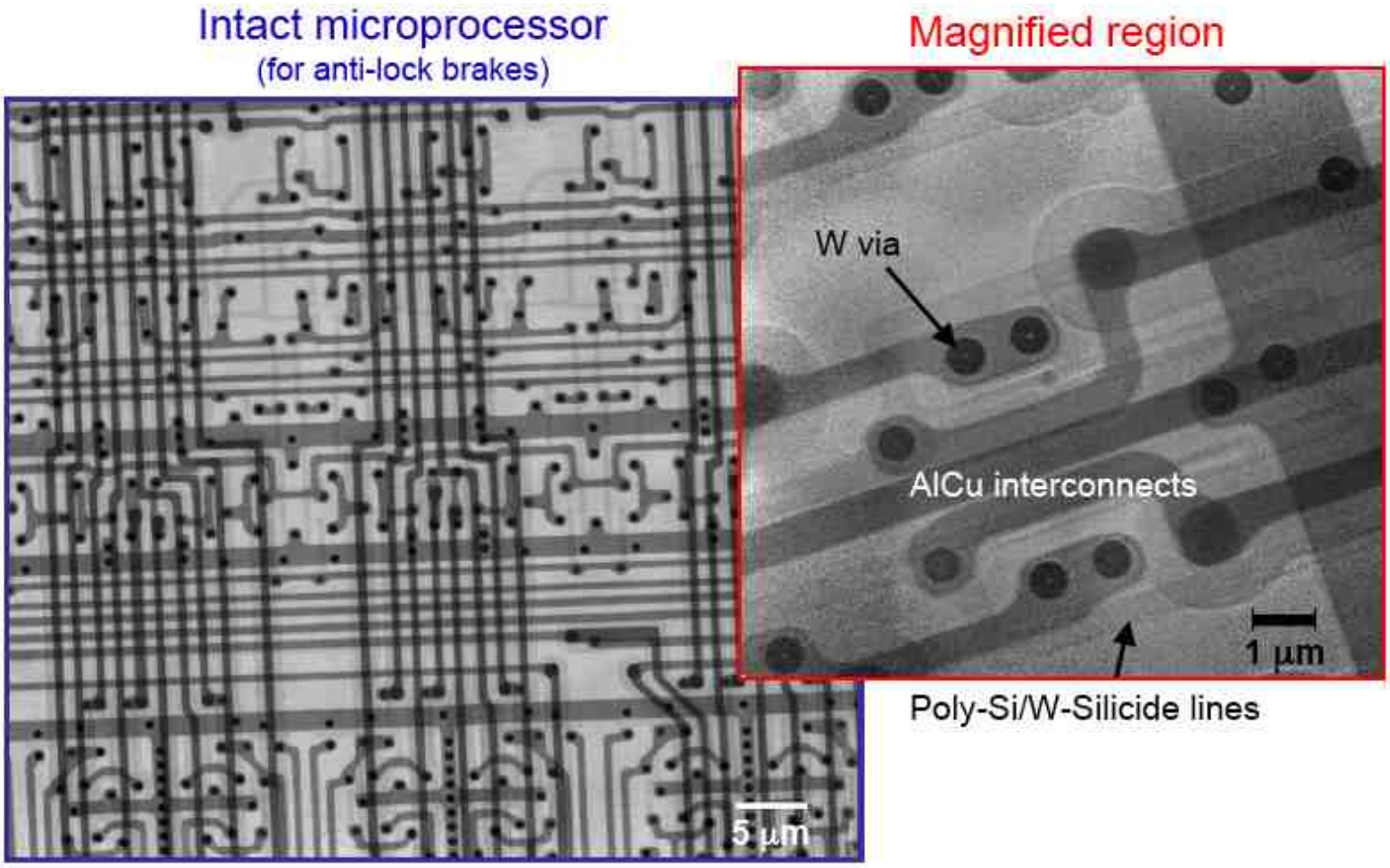

Another example: nanoporous metals

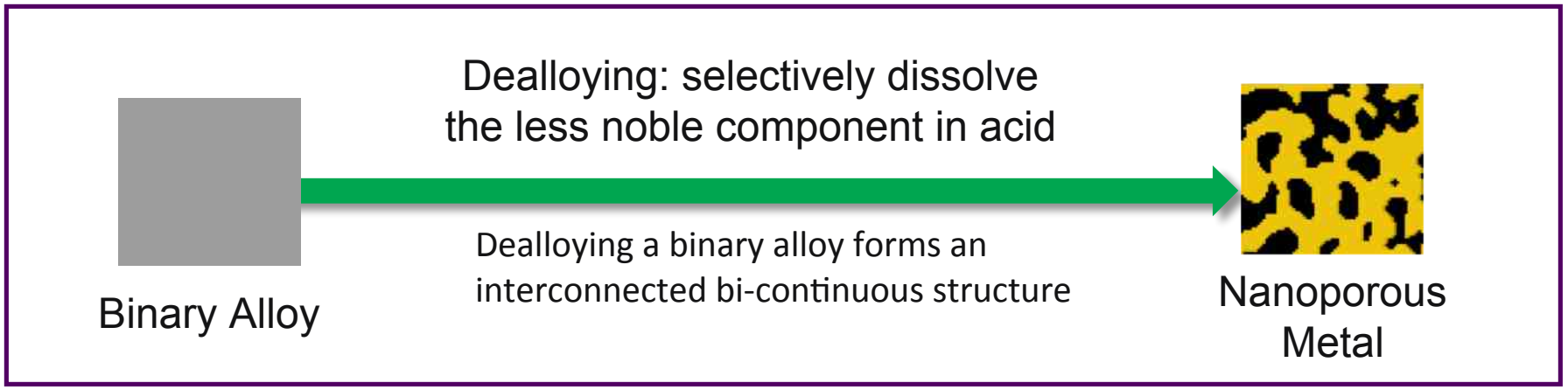

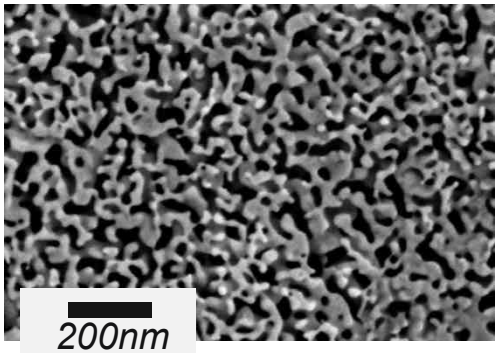

Nanoporous Au
from AgAu

The large surface/volume ratio and confined internal structure of nanoporous metals drives their properties

Applications:

Physical: surface enhanced Raman, super-capacitors
Chemical: surface chemistry driven actuation, catalysis
Biological: immobilization of enzyme and bio-sensors
Mechanical: tunable properties (eg. ductility)

J. Weissmüller, Science 300, 312 (2003)

How does the dealloying process proceed?

APS 32-ID hard x-ray TXM

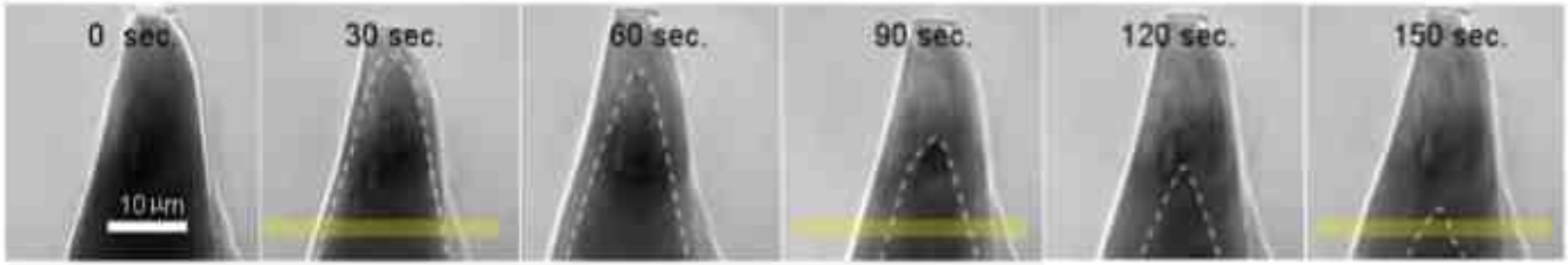

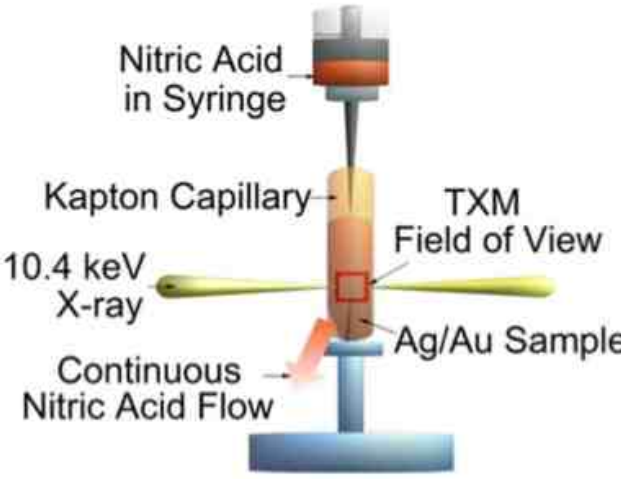

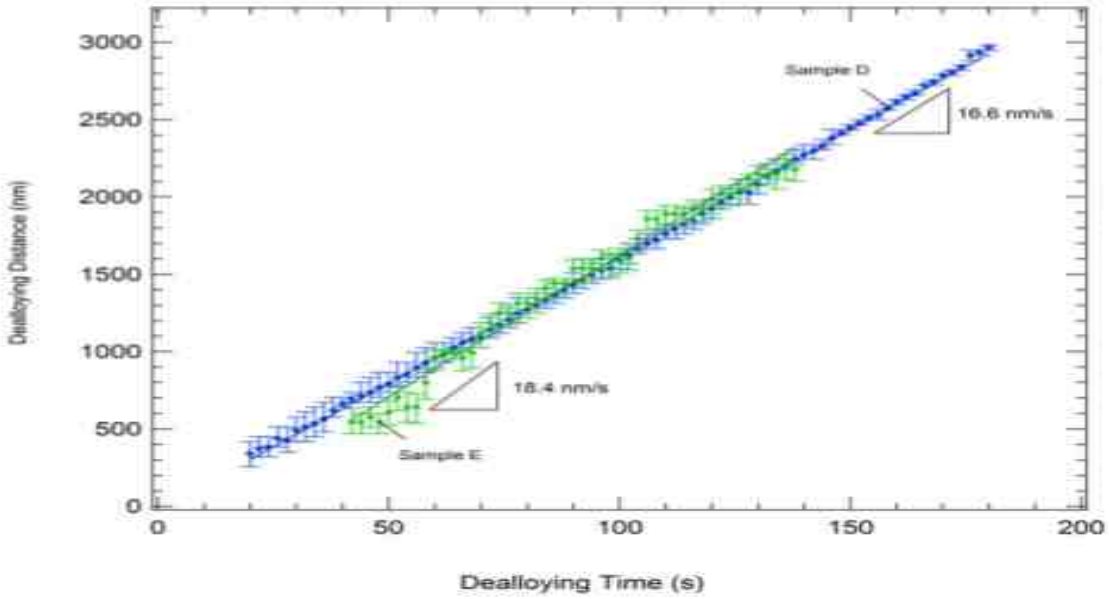

Linear relationship indicates that the dealloying rate is independent of the depth of the front, acid concentration, and temperature.

Y.-C. Chen, et al., Acta Mater. 60, 4972 (2012)

Following coarsening during annealing at 600° C

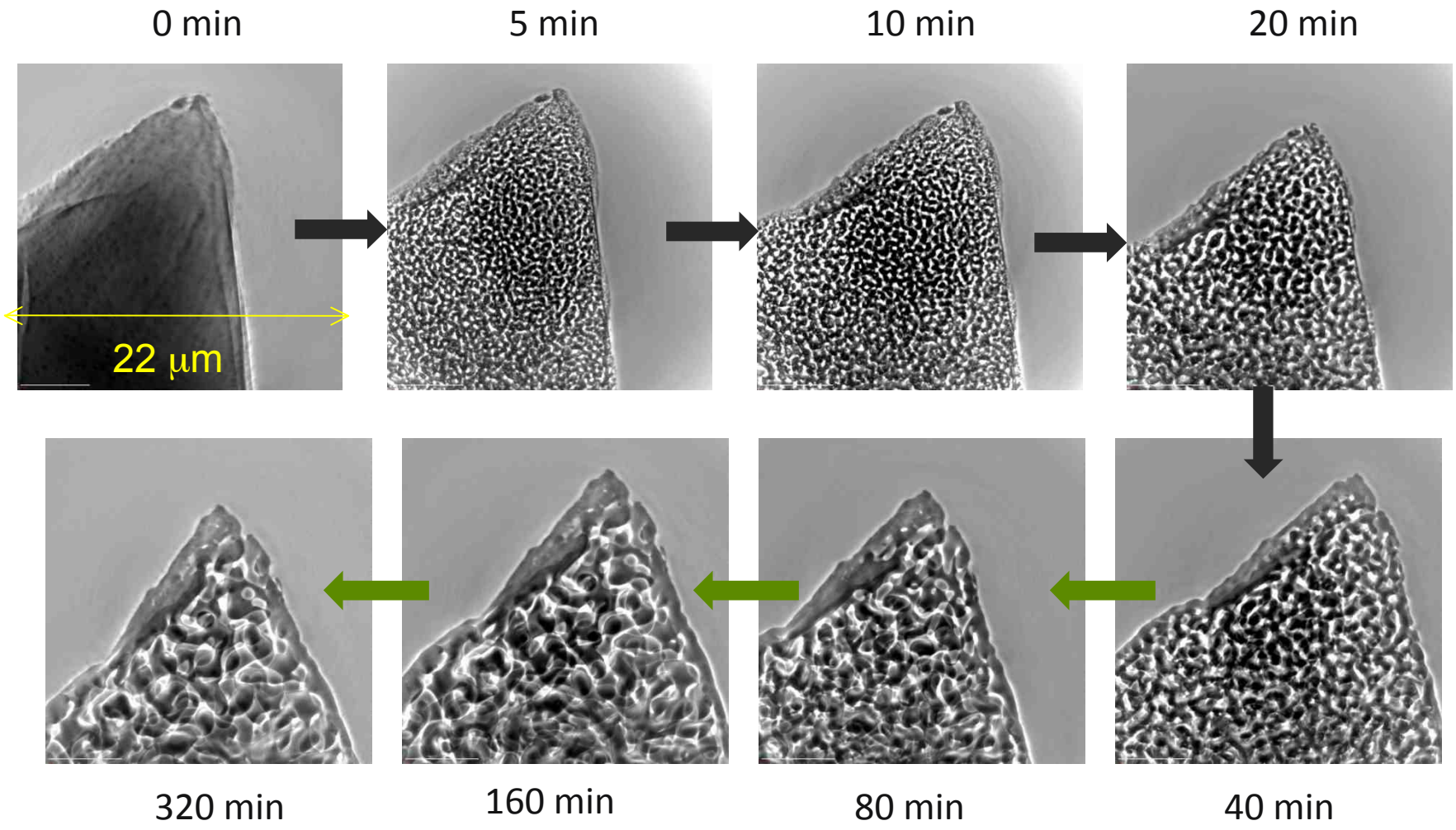

Interfacial surface distribution indicates coarsening does not proceed by bulk diffusion

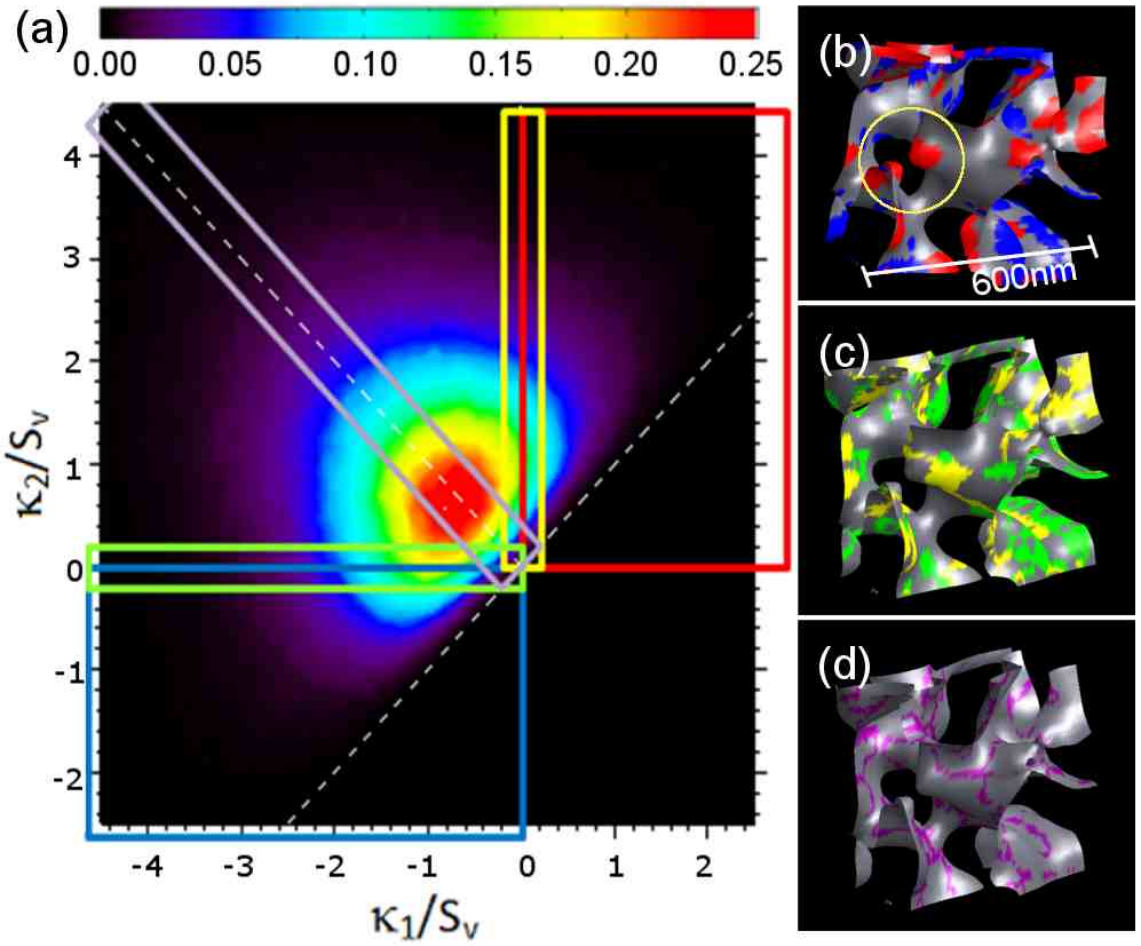

A local (e.g. surface) diffusion mechanism, similar to but different than evaporation/ condensation, most likely occurred during the coarsening process

Y.-C. Chen, APL 96, 043122 (2010)

Polarized x-rays give sensitivity to electron spin

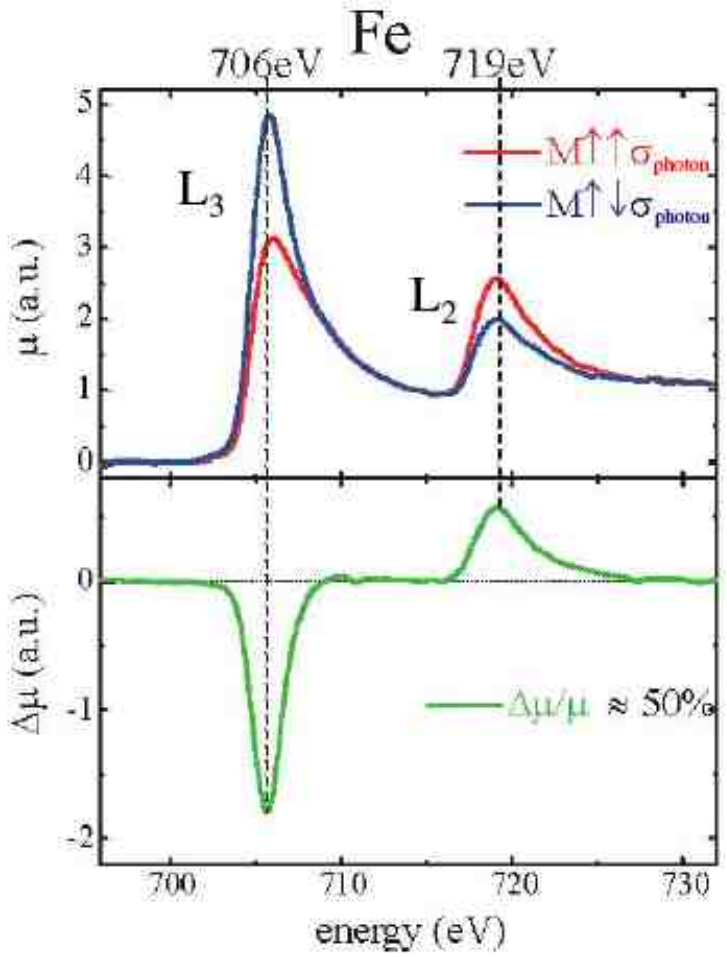

Magnetic x-ray microscopy

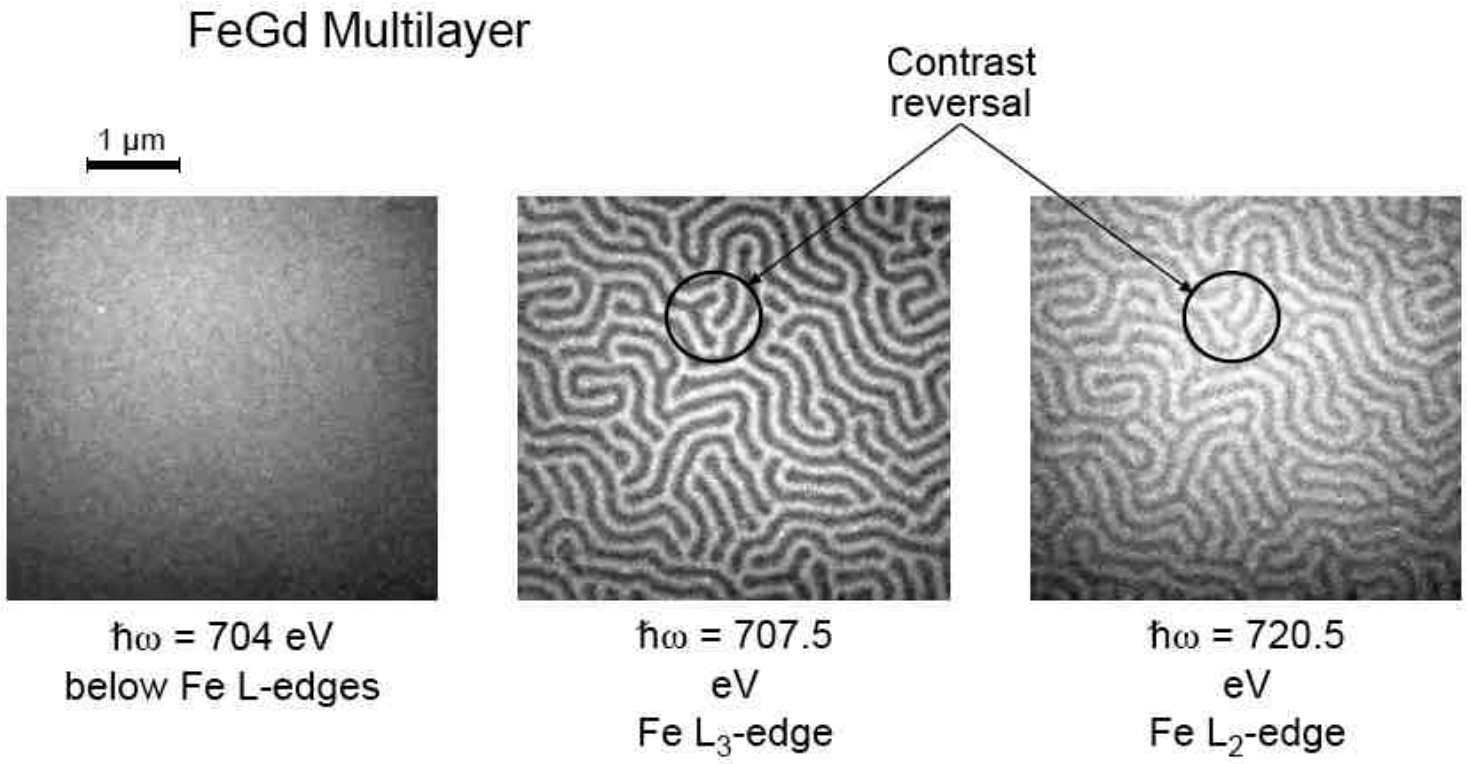

Magnetic recording materials:
FeTbCo multilayer with Al cap layer

P. Fischer et al. (LBL)

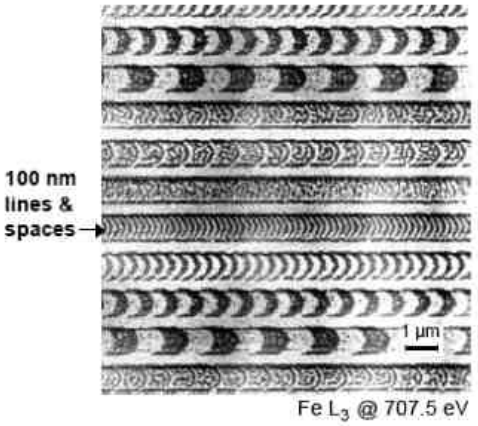

Spin current induced domain wall motion

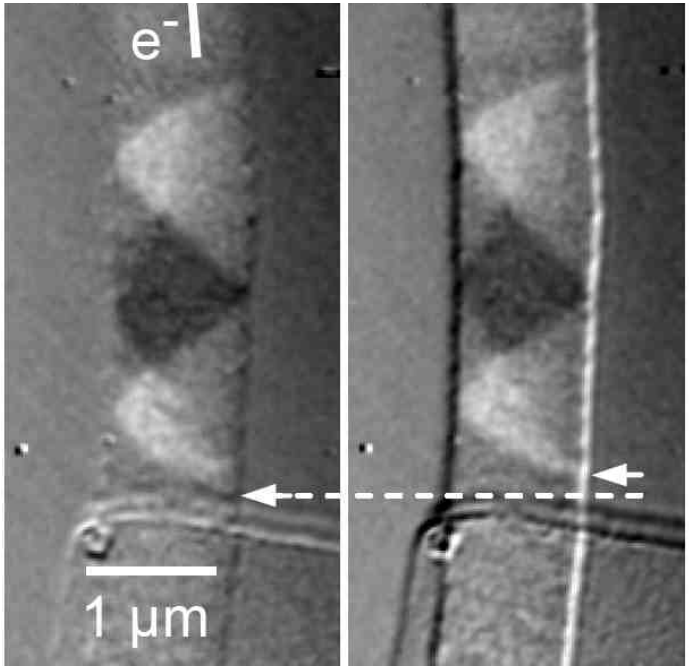

before after

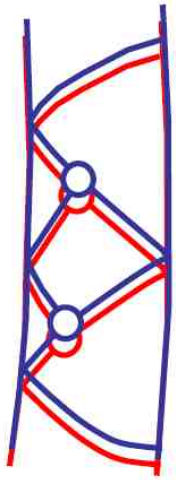

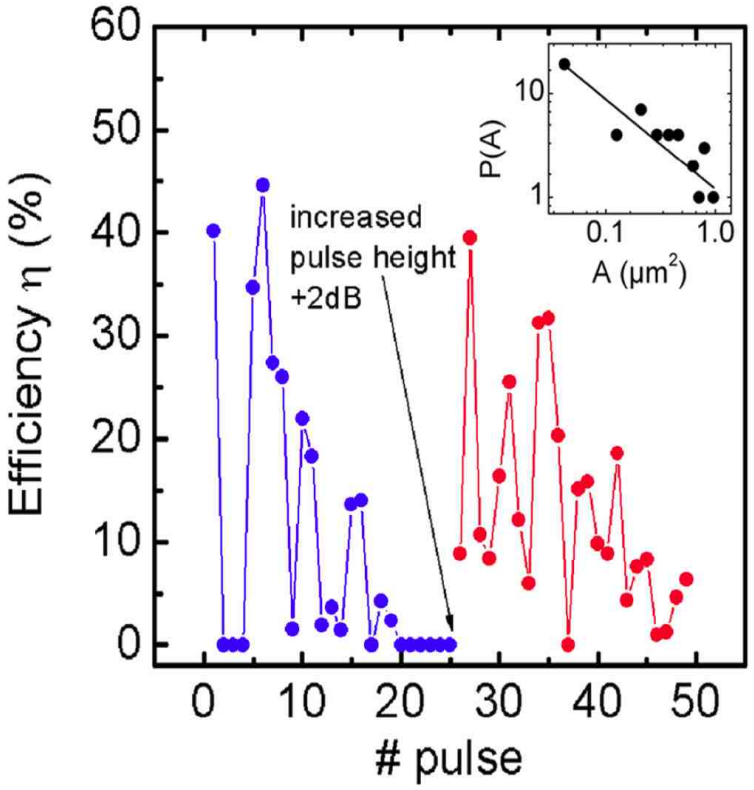

- creation of a domain wall and moving the DW by spin injection
- 1 ns pulses, current density $<10^{12}$ A/m^2
- v_{DW}= 110m/s in agreement with micromagnetic simulations
- strong indications for a stochastic character of the DW motion

G. Meier, PRL 98, 187202 (2007)

Differential interference contrast (DIC)

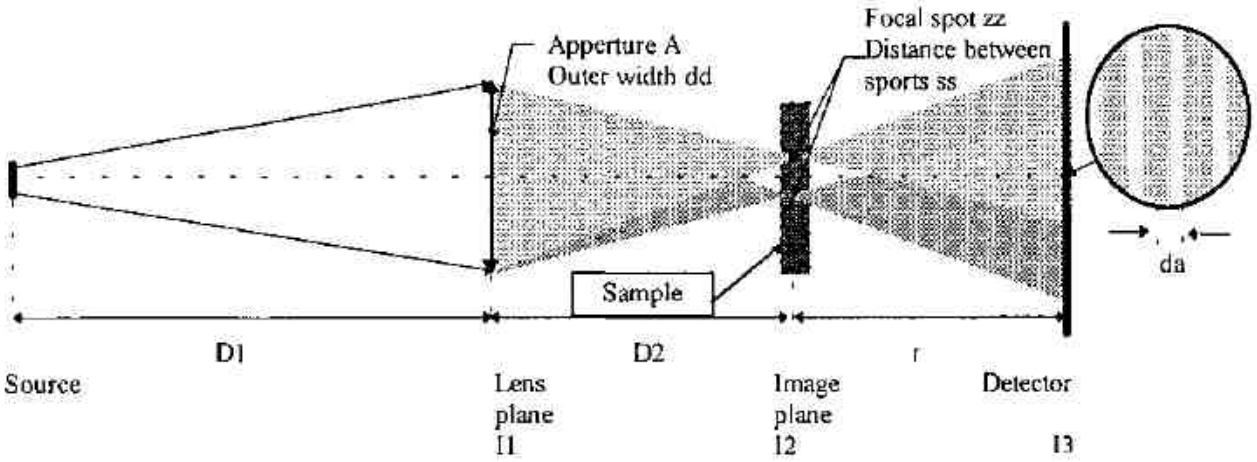

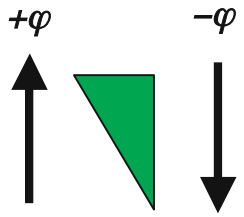

- Use double source or lens to make two focal spots on sample
- Absolute phase gradients converted to intensities at image plane
- Polarization not required, works with birefringent samples

V. Aristov, AIP Conf. Proc. CP507, 554 (2000)

"XOR" DIC

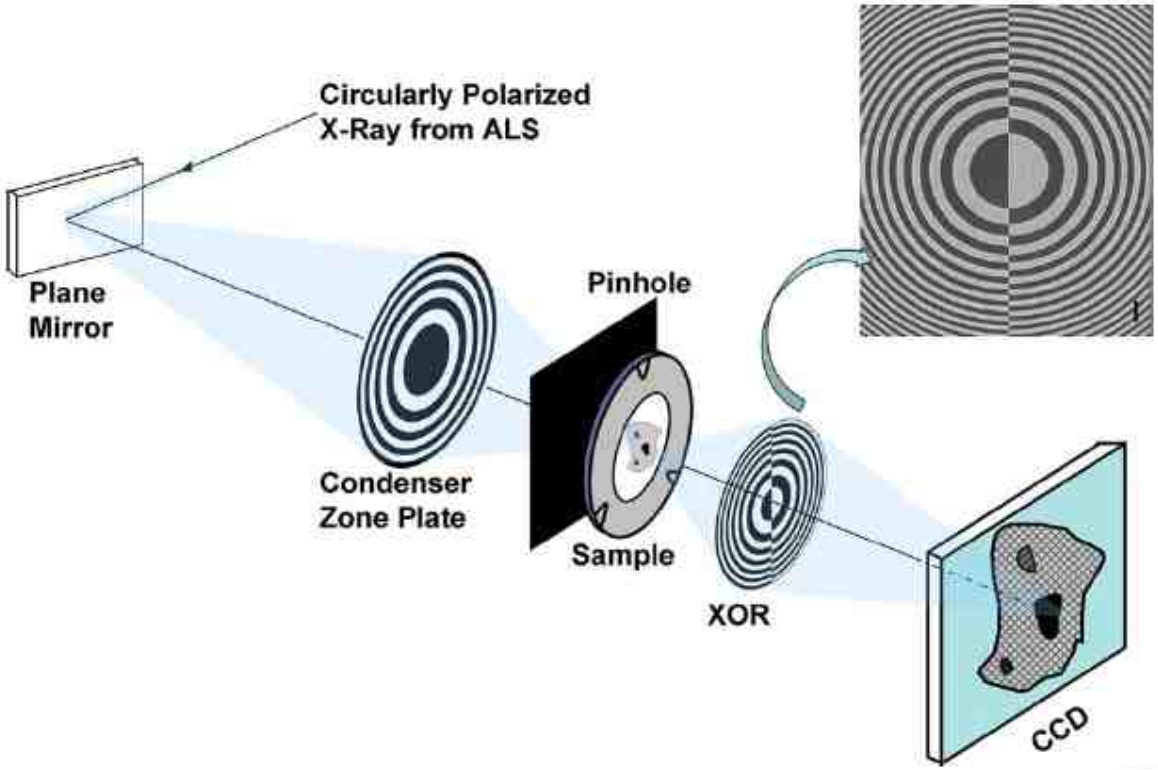

C. Chang et al., Opt. Lett. 31, 1564 (2006)

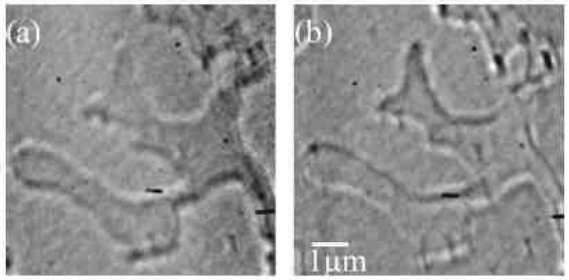

Fig. 3. DIC images of a 59 nm thick $Gd_{25}Fe_{75}$ sample obtained across the iron L_3 and L_2 edges at (a) 705 and (b) 711 eV.

3D imaging

$R \approx 0.61 \lambda / NA$ $\qquad$ $DOF \approx 1.22 \lambda / (NA)^2 = 2 R^2 / (0.61\lambda)$

$|n| \approx 1 \quad \Rightarrow \quad NA << 1 \quad \Rightarrow \quad DOF << R$

Synthesize larger NA with multiple views

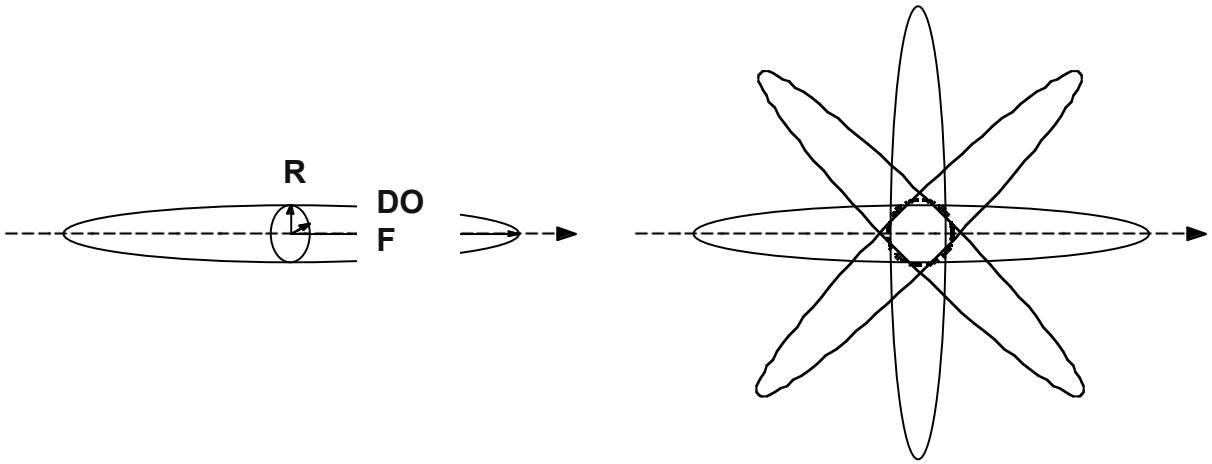

Cannot improve R, only DOF by tomography

Computed tomography

1 **Record many projections through sample over wide angular range. Projections at angles *q* contain:**

$$I(x,y,\theta) \;=\; I_0\, e^{-\int \mu_\theta(x',y',z')dz'}$$

2 **Reconstruct 3D sample density from suite *S* of projections**

$$\text{Invert}\;\; S\{I(x,y,\theta)\} \;\Rightarrow\; \mu(x,y,z)$$

A.C. Kak and M. Slaney, "Principles of Computerized Tomographic Imaging," (IEEE Press, New York, 1988), Chapter 3.

L. Grodzins, NIM 206, 541 (1983).

X-ray nanotomography of cryo-preserved yeast

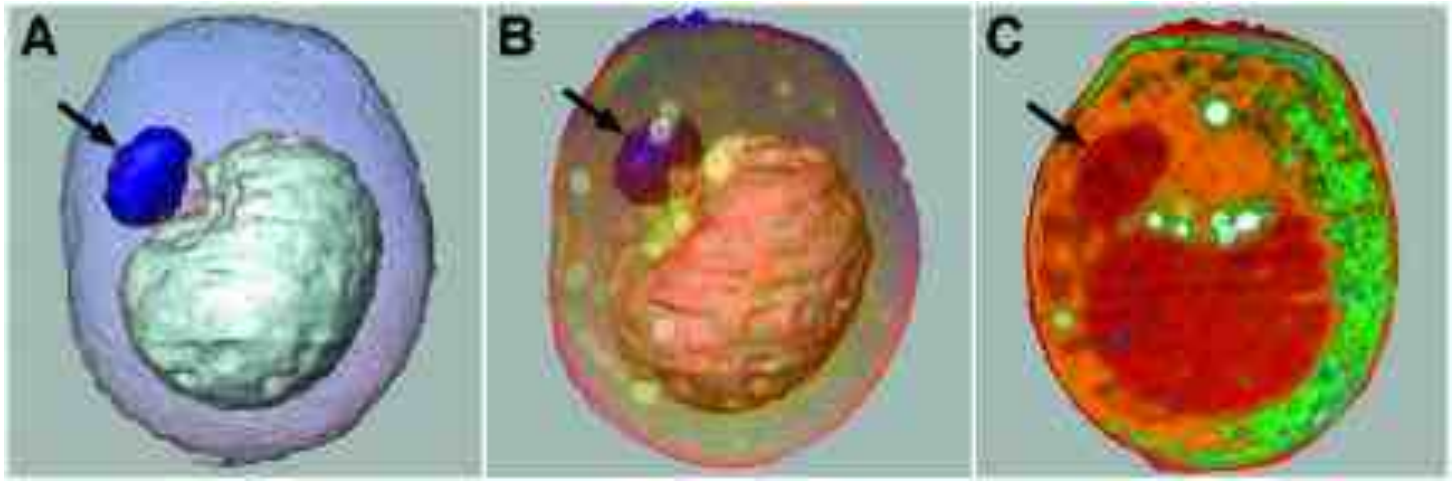

Frozen hydrated yeast Saccharomyces cerevisiae
C. Larabell, M. Le Gros, Mol. Biol. Cell 15, 957 (2004)

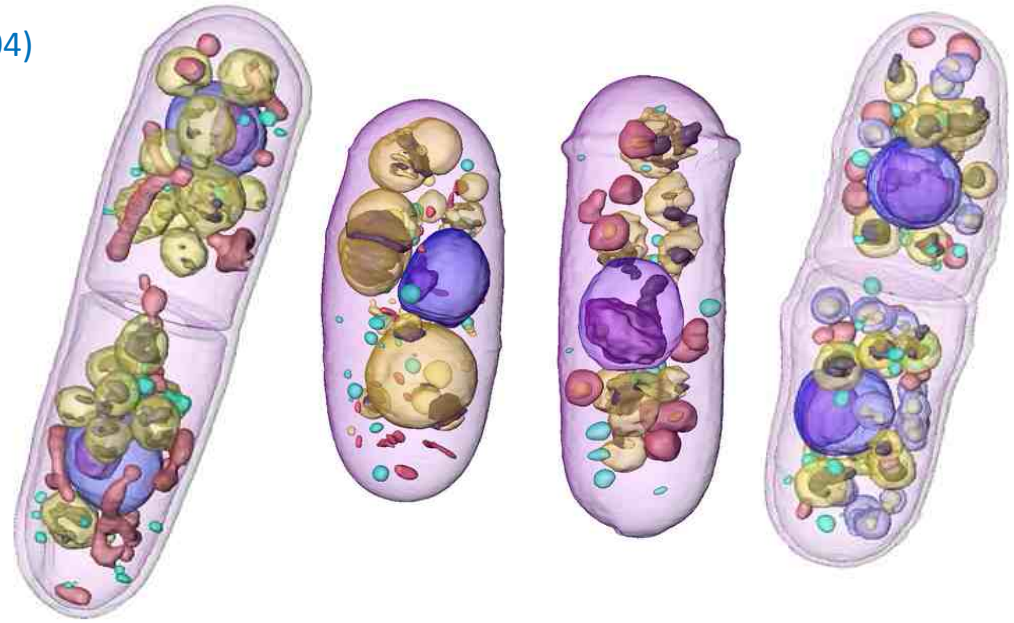

Schizosaccharomyces pombe

Parkinson, J. Struct. Biol. 162, 380 (2008)

G. McDermott, C. Larabell,
Ann. Rev. Phys. Chem. 63, 225 (2012)

Designing stable electodes for Li battery cells

- Multifunctional battery electrodes offer potential for increased energy density and stability during charge cycling. Cu_6Sn_5 has a volumetric energy density of 1800 mAh/cm^3, more than twice that of graphite.

- *We are learning how Cu-Sn electrode structures degrade during charge-cycling*

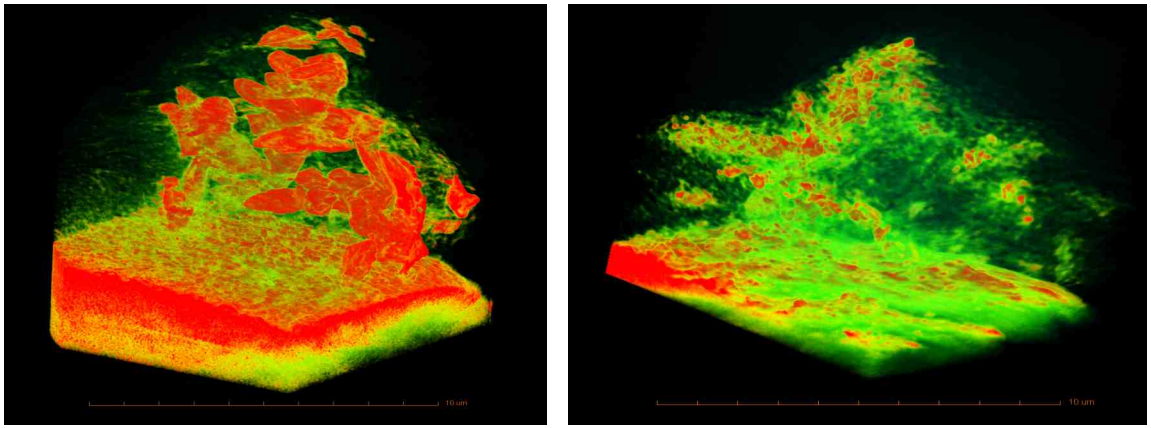

3D reconstructions of Sn-Cu coatings on stainless steel tips. Left: as-deposited (uncycled) electrode. Cu crystals (red) are formed during electrodeposition process. Right: electrode after cycling 5 times.

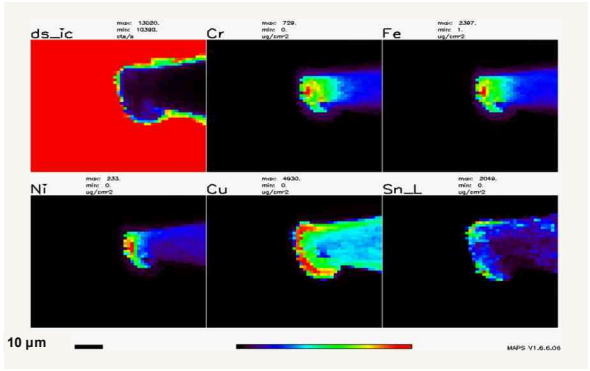

Elemental distribution at Sn-Cu/stainless steel tip

R. Winarski, V. Rose, B. Blaiszik, F. Brushett, L. Trahey, C. Johnson (ANL)

Quantitative phase tomography

- Defocus series (a, b, c) and phase (d) of a silicon AFM tip
- Quantitative 3D reconstructions of real part of refractive index from ±70° tomographic projections through tip
- Calculated $\delta = 5.1 \times 10^{-5}$

  Measured $\delta = 5.0 \pm 0.5 \times 10^{-5}$

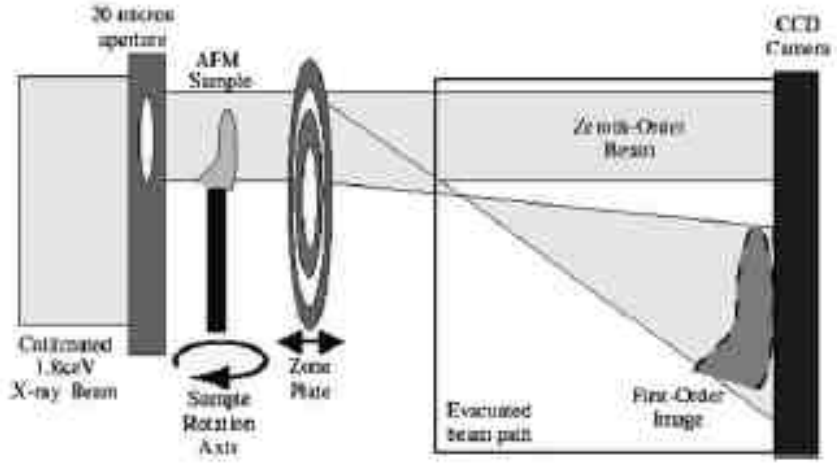

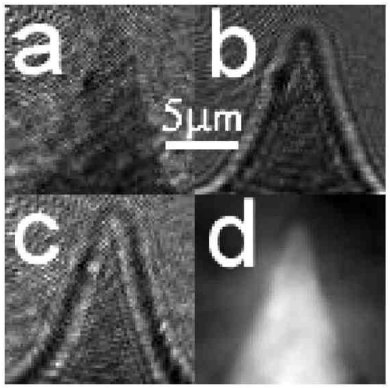

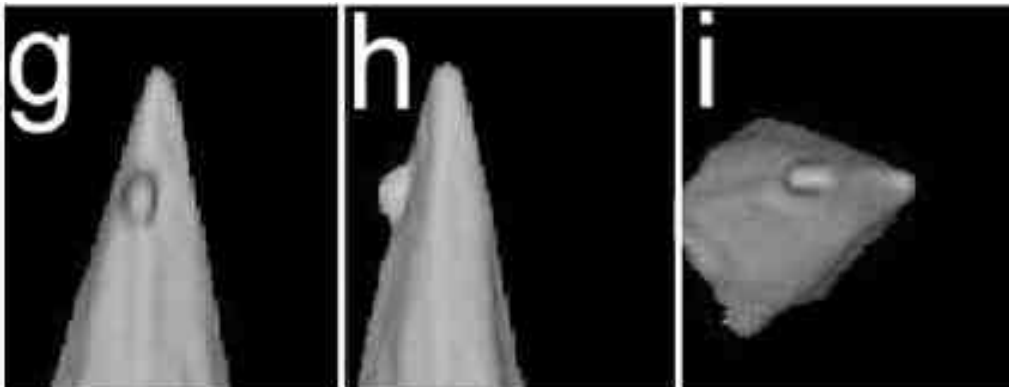

P. McMahon, Opt. Commun. 217, 53 (2003)

Full-field microscopy with hard x-rays

Scanning x-ray microscope

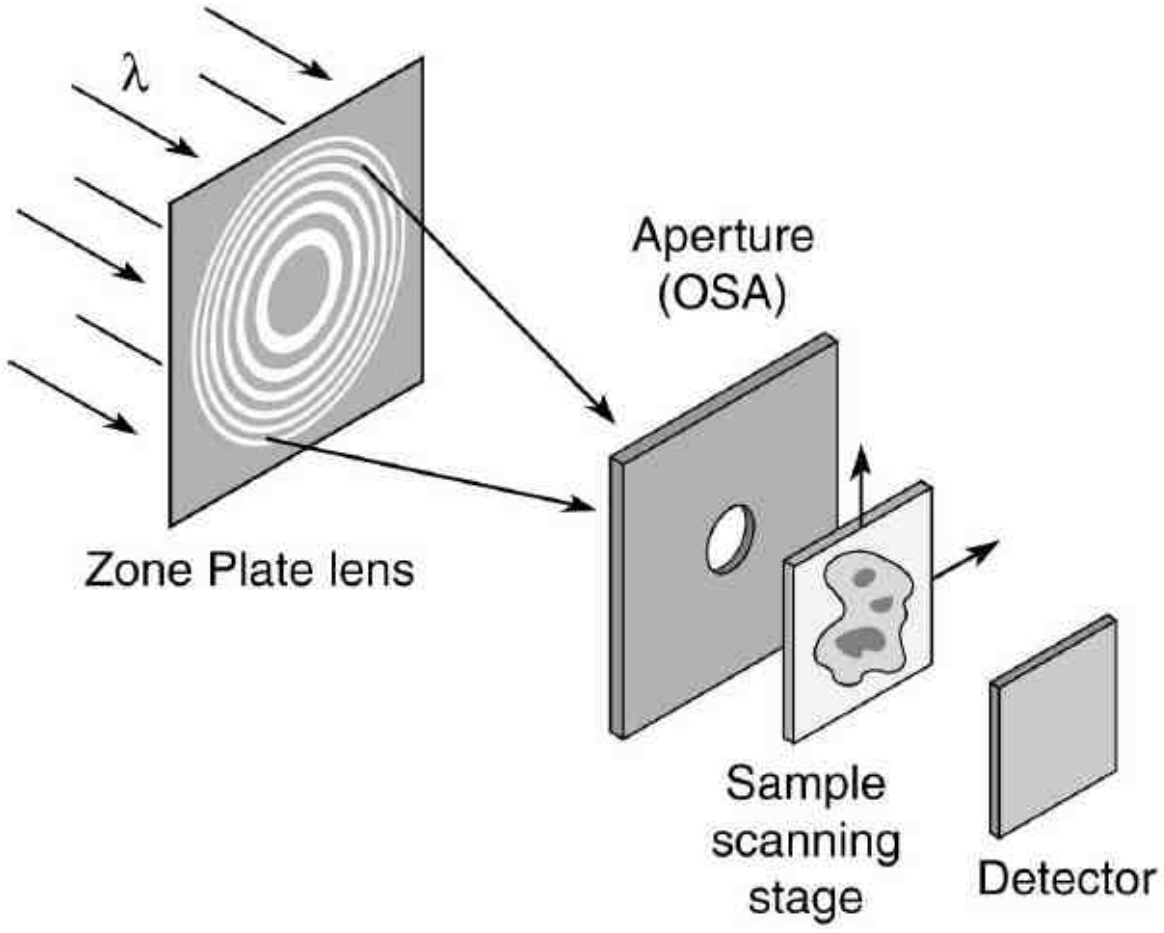

J. Kirz, Rev. Sci. Instrum. 56, 1 (1985)

Detect both fluorescence and transmitted signal in scanning mode

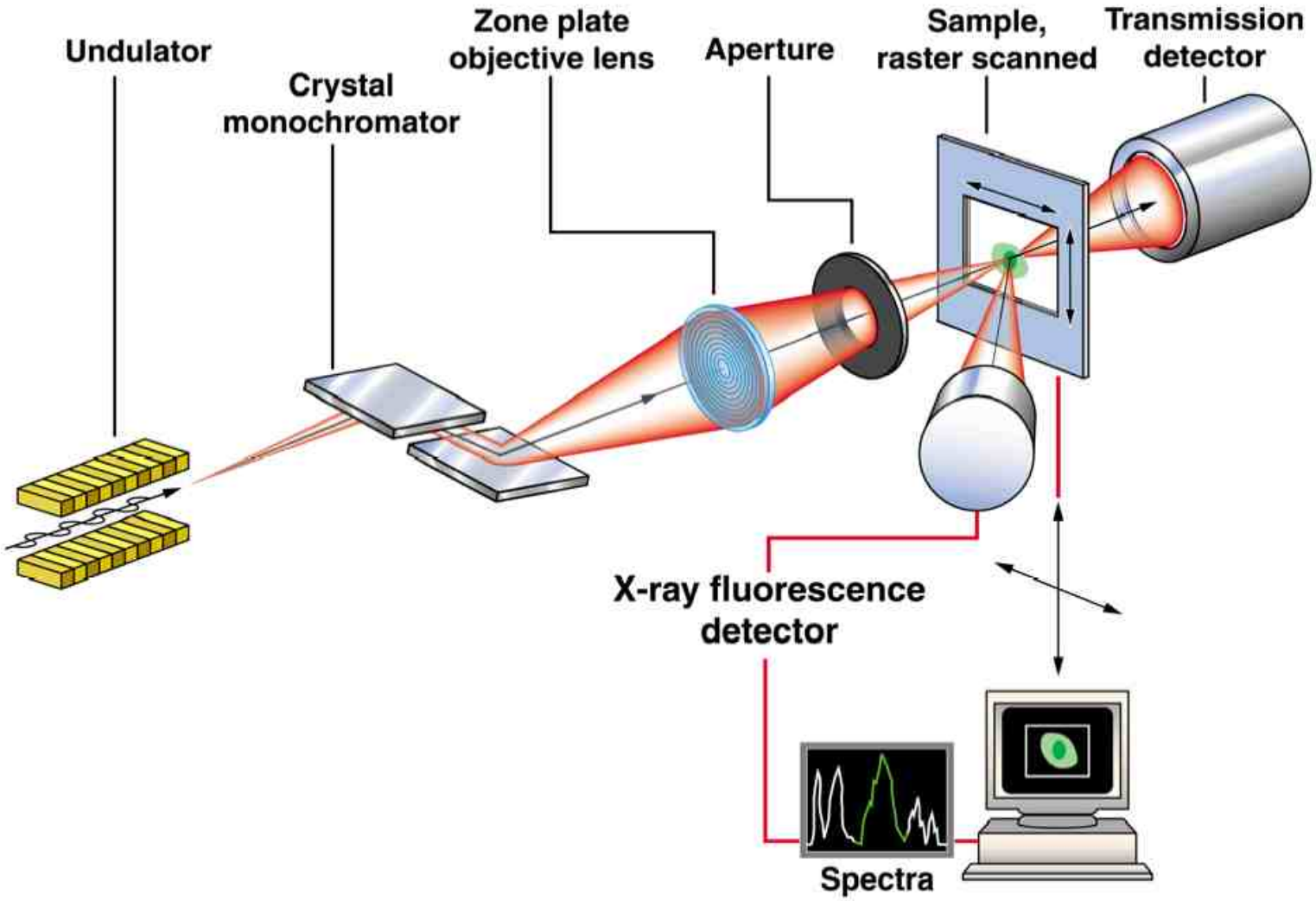

APS 2-ID-E scanning x-ray microscope

Use to probe buried defects in microelectronic devices

Example: Ta-lined Cu interconnect, W vias

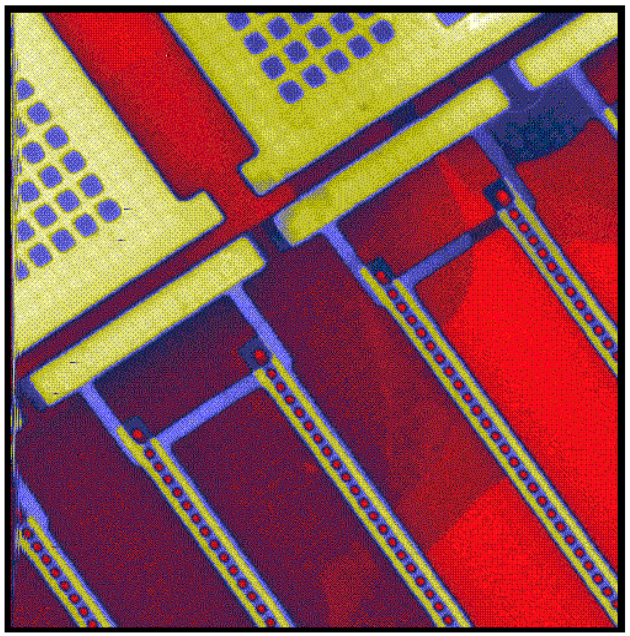

10 μm

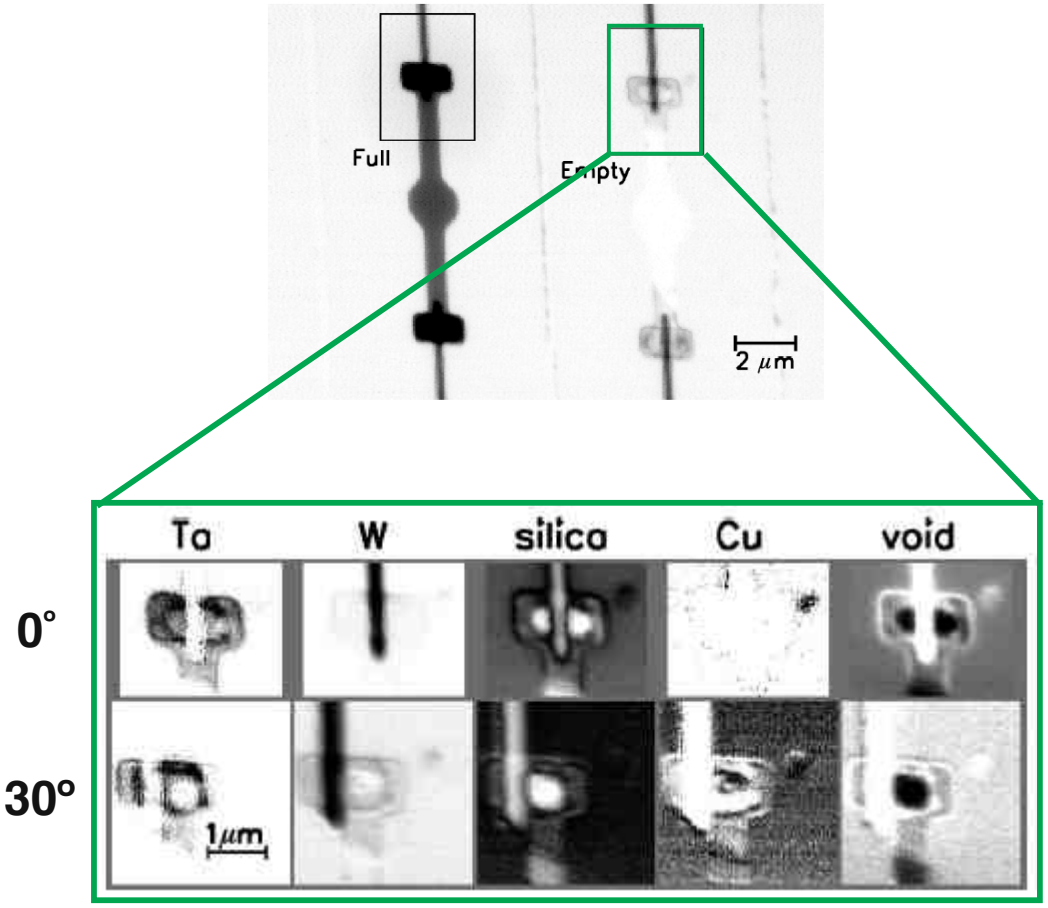

Z. Levine, JAP 95, 405 (2004)

Study light elements with 1-4 keV x-rays

Marine sediments contain complex, heterogeneous P chemistry.
P typically shows little covariance with most other elements.

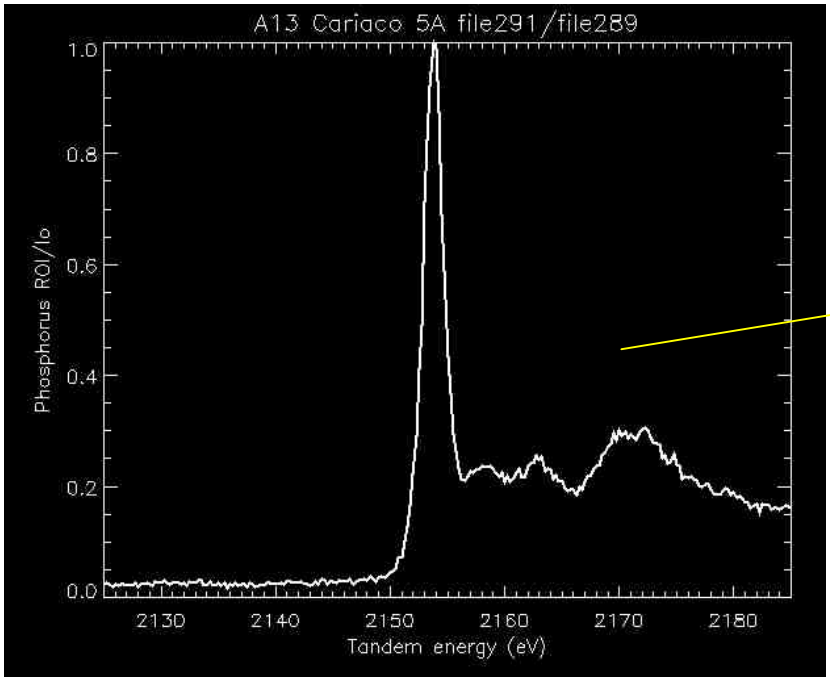

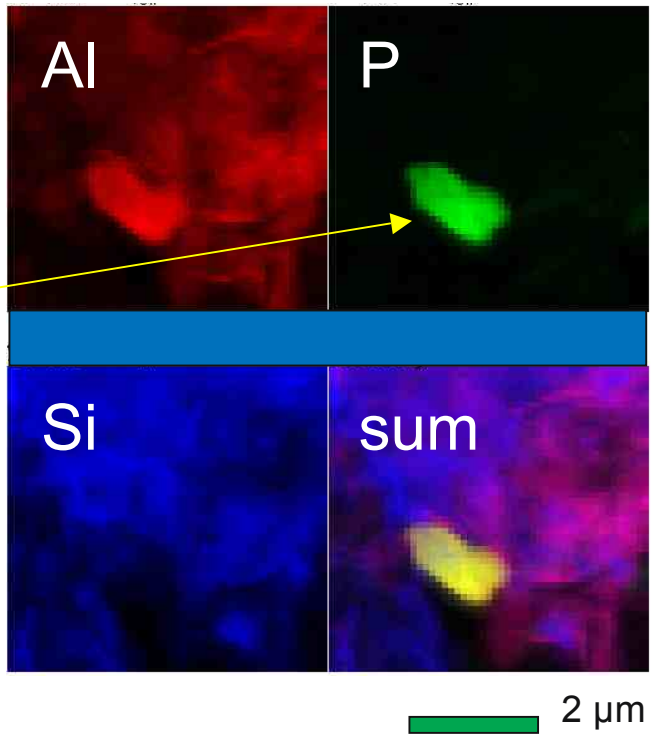

- Occasionally find odd P-containing minerals with distinctive P-XANES that do not match closely with any known Al-phosphate mineral
- Previously unknown in marine samples - Riverine or Aeolian source?

J. Brandes, Marine Chem. 103, 250 (2007)

X-ray spectra reveal chemical state with exquisite sensitivity

Marine polyphosphate formation influences geological P sequestion

In-situ formation of calcium phosphate in marine sediments is known to be a major sink for the vital nutrient phosphorus, but *how* it forms is a mystery. Sediment chemistry is not conducive to precipitation of these minerals.

Scanning x-ray spectro-microscopy shows diatom-derived polyphosphates play a critical role in P sequestration. This mechanism explains the puzzlingly broad distribution of these minerals observed worldwide.

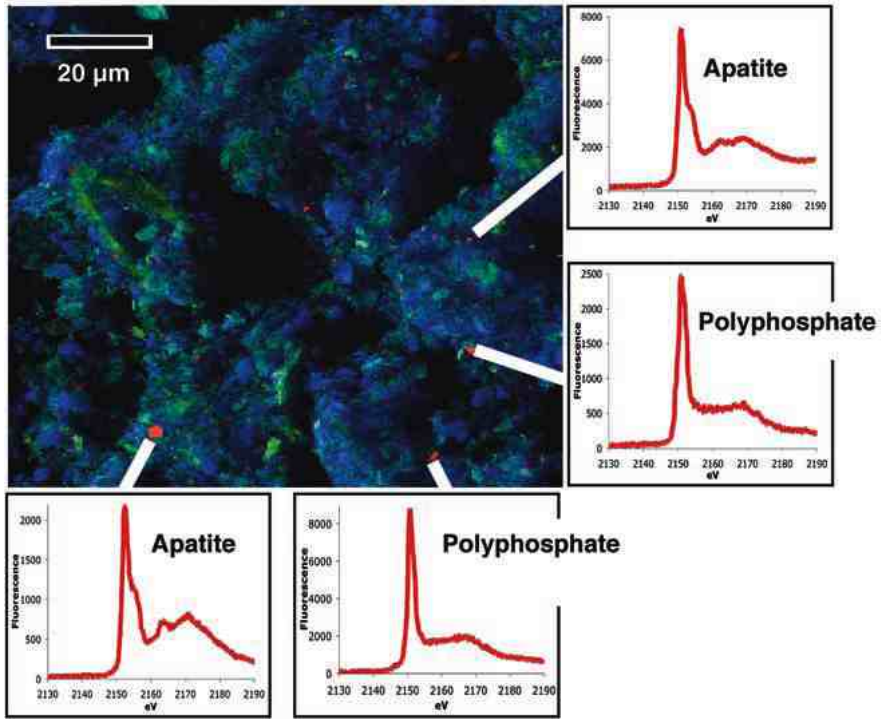

J. Diaz, Science 320, 652 (2008)

Bio-magnetism: magnetotactic bacteria

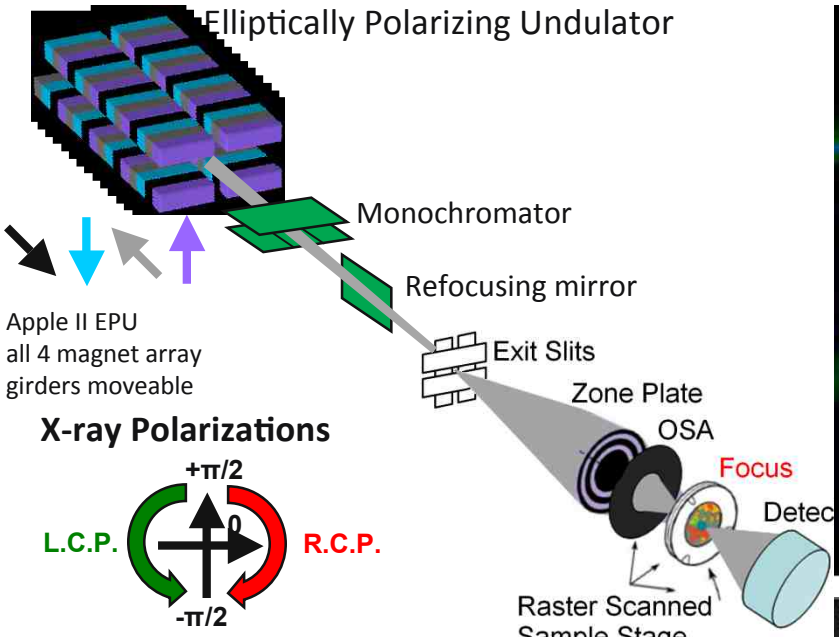

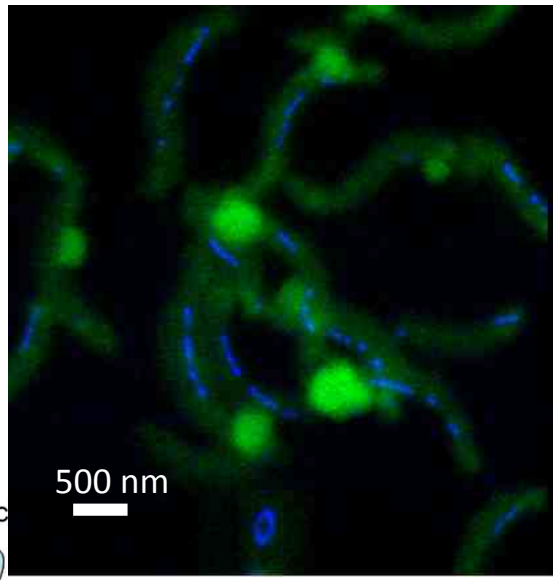

Magnetosomes are Fe(II)-rich relative to mineral magnetite

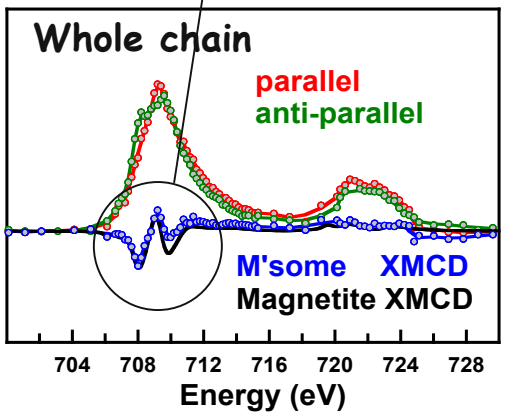

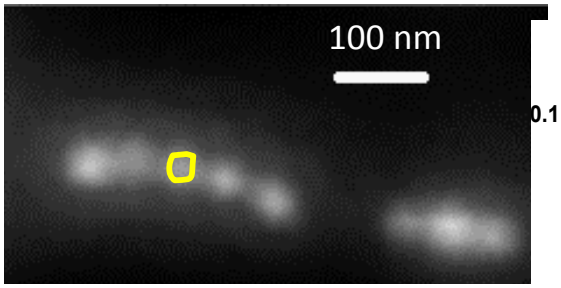

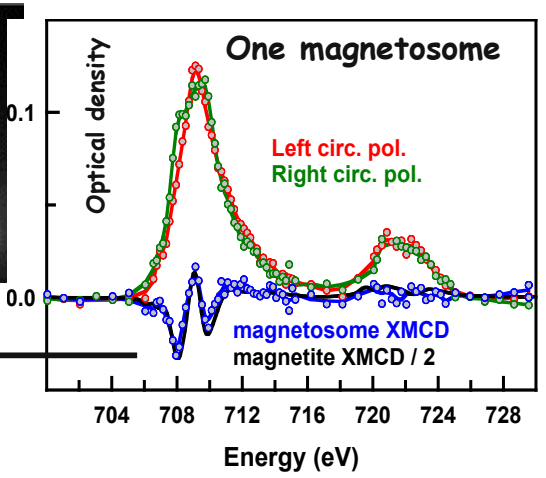

Magnetite Fe 2p spectra courtesy E.J. Goering - see J. Mag. & Mag. Mats 310 (2007) e2493

Each crystal site has a different XMCD signal

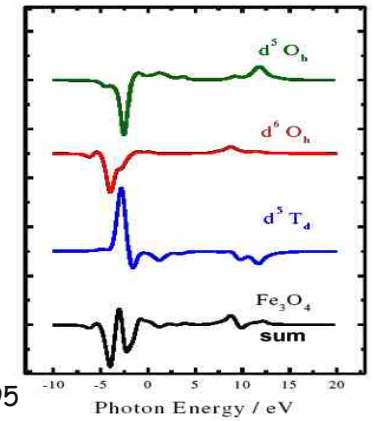

R.A.D. Pattrick, Eur. J. Mineral. 14 (2002) 1095

K. Lam, Chem. Geo. 270, 110 (2010)

Use differential phase contrast for biological specimens

Complex transmission function: $\exp(i\,\delta\,kt)\,\exp(-\,\beta\,kt)$

phase shift absorption

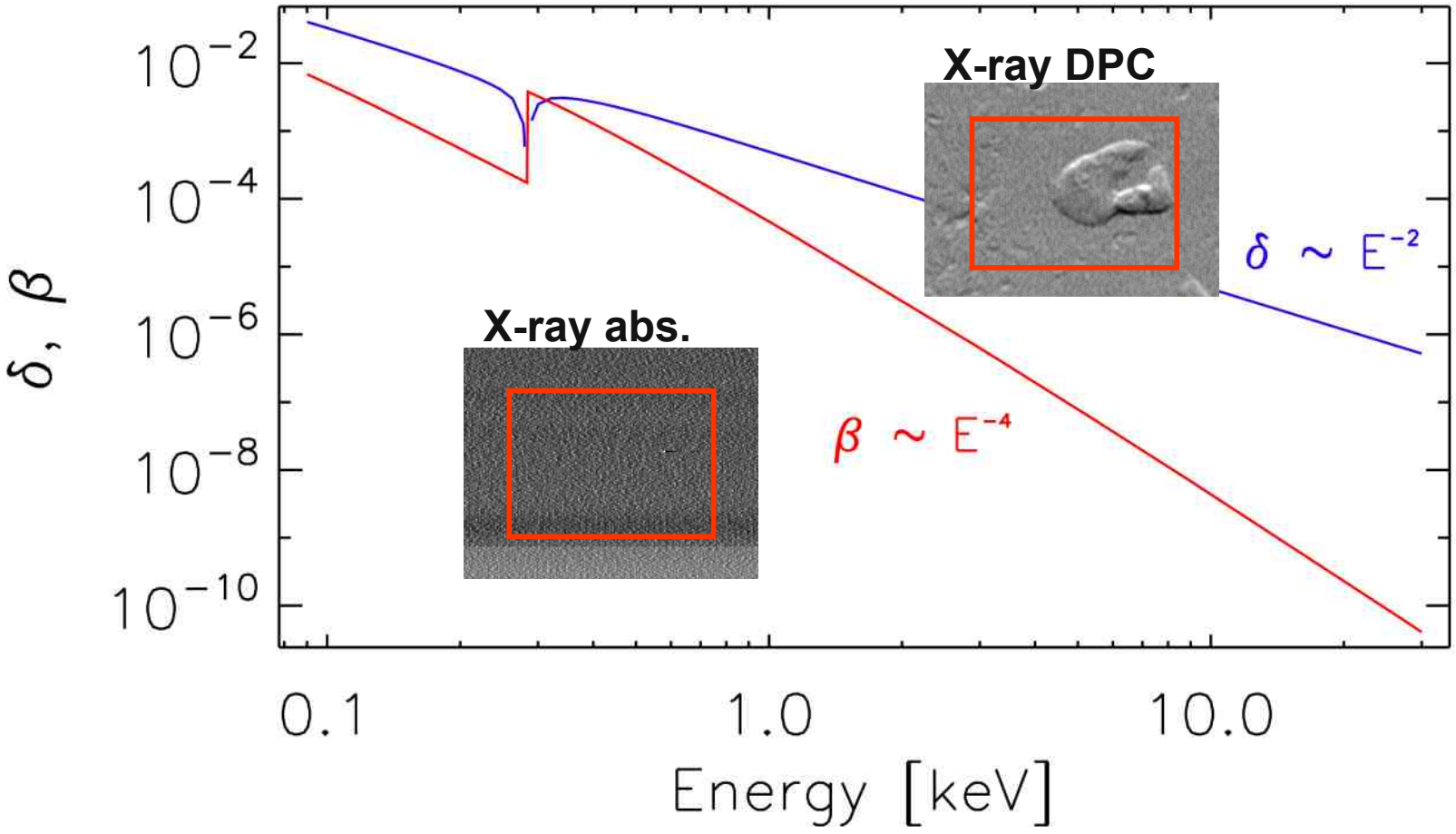

STXM: absorption contrast

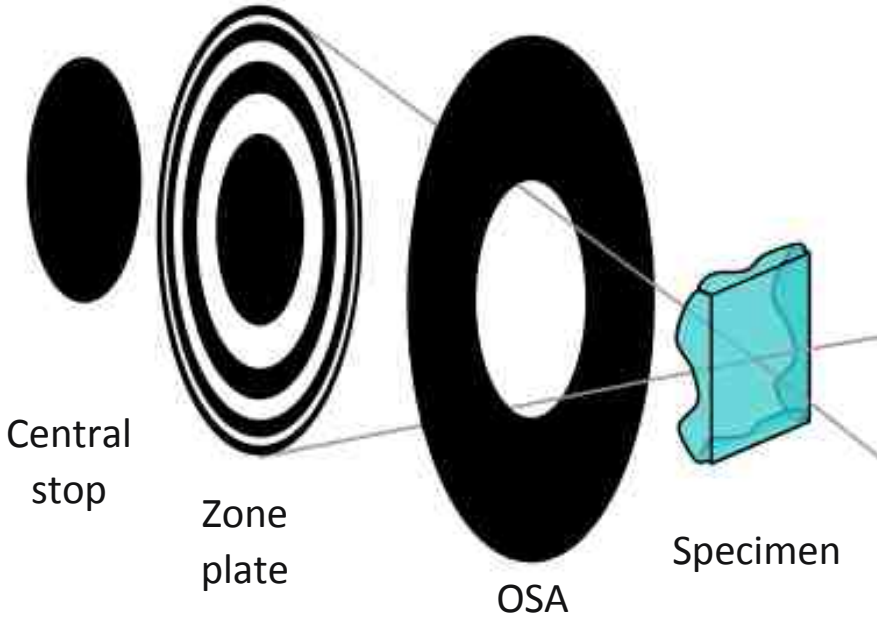

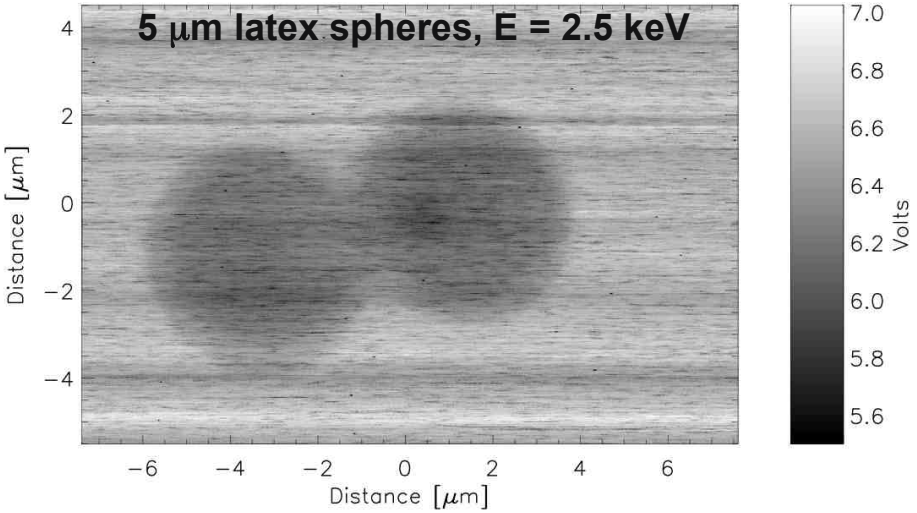

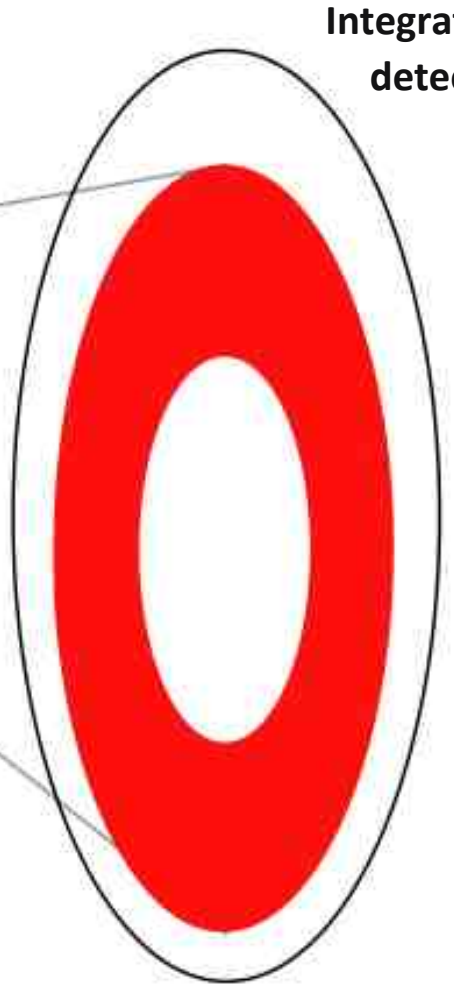

Signal = TOTAL

STXM: differential phase contrast

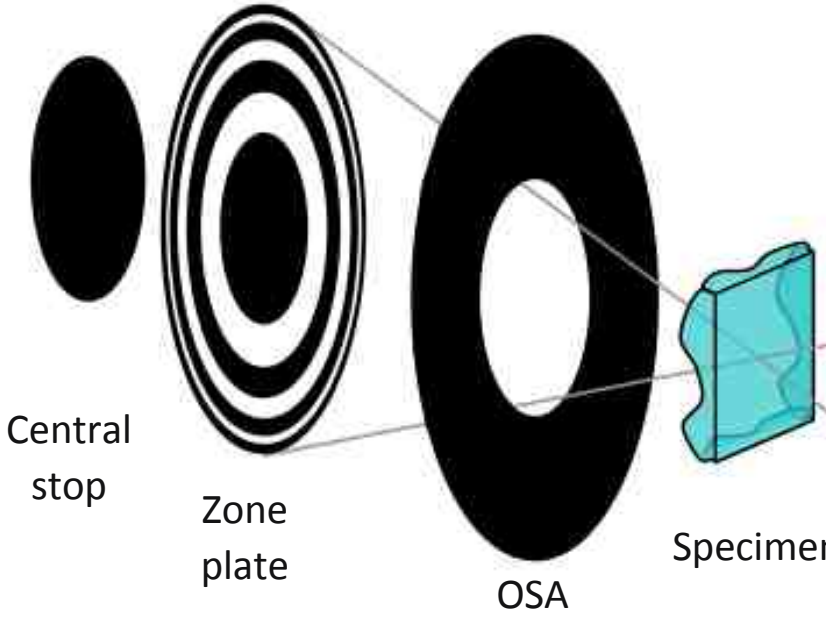

Configured detector

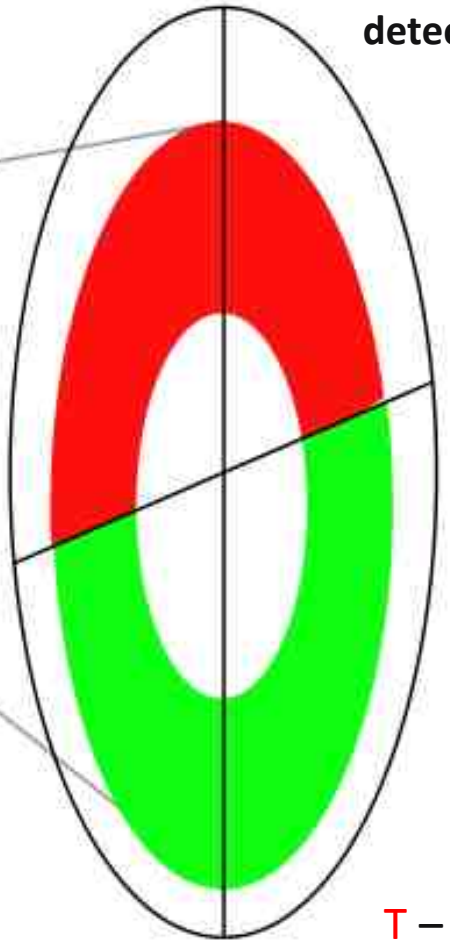

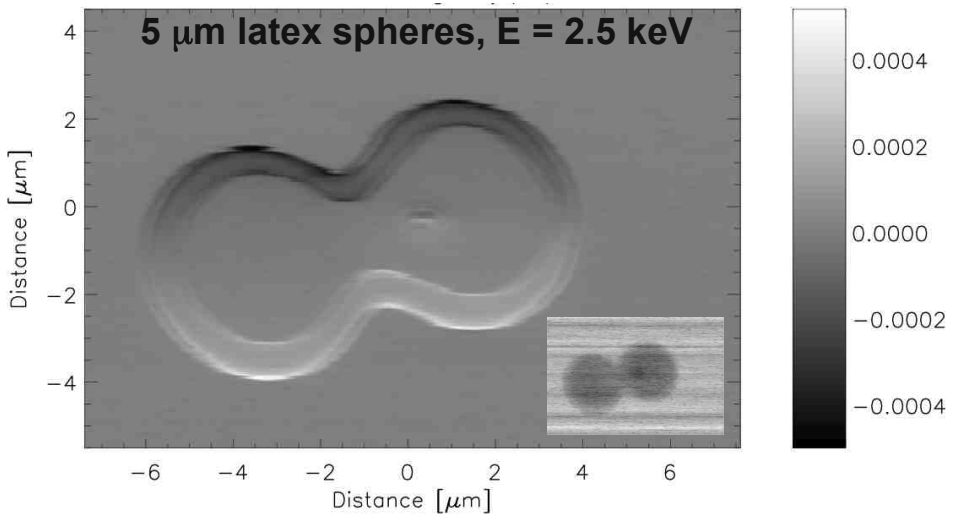

$$\text{DPC}_V \text{ signal} = \frac{T - B}{T + B}$$

M. de Jonge, PRL 100, 163902 (2008)

Charge integrating silicon DPC detector

B. Hornberger, C. Jacobsen (Stony Brook U.),
M. de Jonge, S. Vogt (ANL), D. Paterson (Australian Synchrotron)

Developed for NSLS STXM:
M. Feser, NIM A 565 (2006)

2nd generation optimized for APS

Charge integrating segmented Si detector:
- segmentation matched to experiment
- simultaneous recording of all segments
- read by multichannel V/F or ADC
- 1 msec dwell typ., sub-msec achievable

Dead time ~ 10 us

Repeat rate ~ 50 us

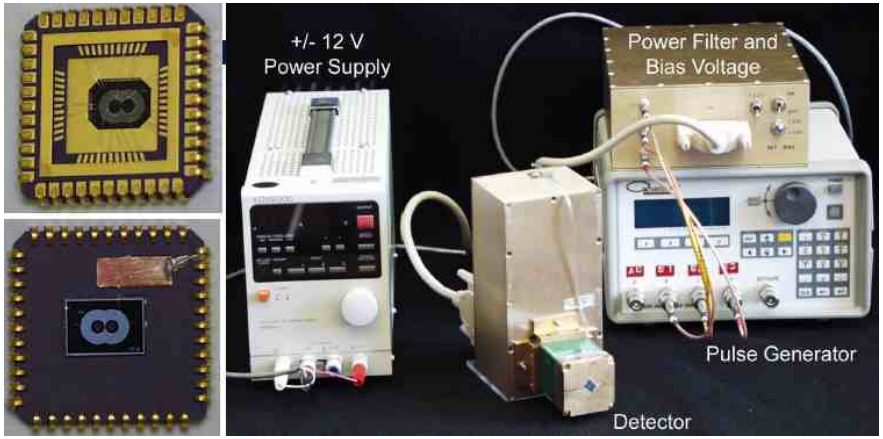

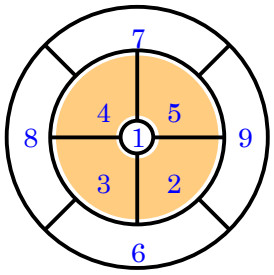

1200 μm diameter

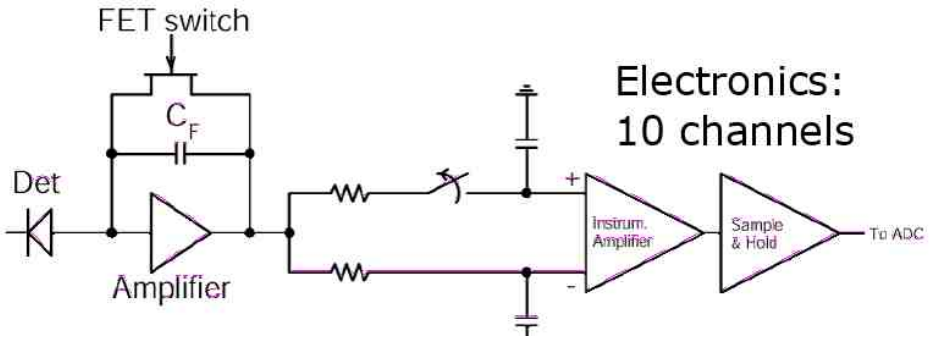

Chip fabrication: Max Planck Semiconductor Lab, Munich

B. Hornberger, Ph.D. Thesis (2007)

Pennate diatoms

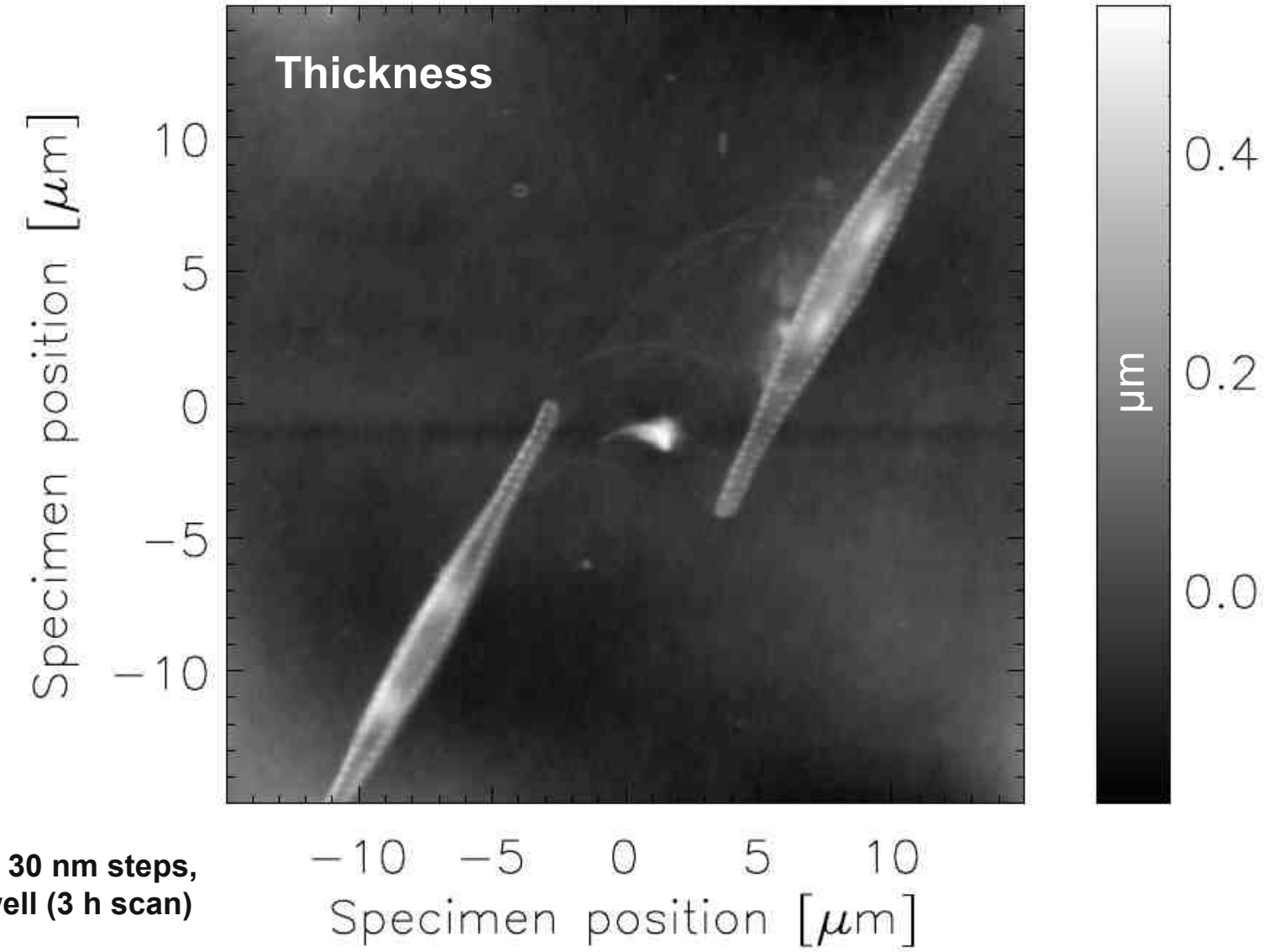

2535 eV, 30 nm steps,
5 ms dwell (3 h scan)

Copper is an essential trace element for all life forms

- **Catalyzes production of highly reactive oxygen species**

  ⇒ oxidative damage to lipids, proteins, DNA, etc

- **Defects in regulatory processes may led to:**
  - ✓ Menkes syndrome
  - ✓ Wilson's disease
  - ✓ Amyotropic lateral sclerosis (ALS)
  - ✓ Alzheimer's disease

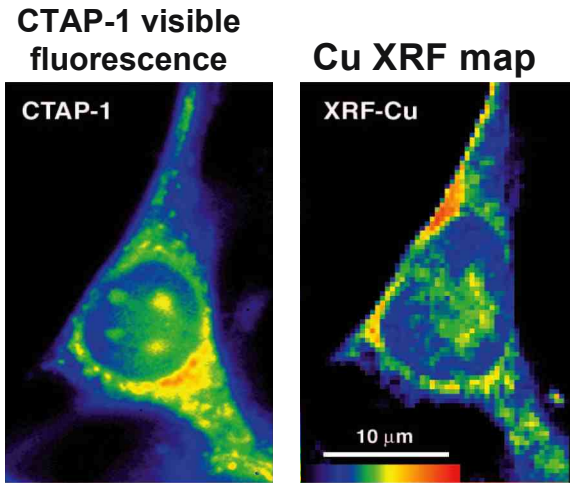

Mouse fibroblast cell + 150 μM $CuCl_2$

- **Need to understand cellular uptake, trafficking, storage of Cu**
- **Novel Cu(I) fluorescent sensor (CTAP-1) was recently developed**

⇒ ***Does it reflect the true cellular distribution?***

μ-XANES indicates Cu(I) is present (reducing environment)

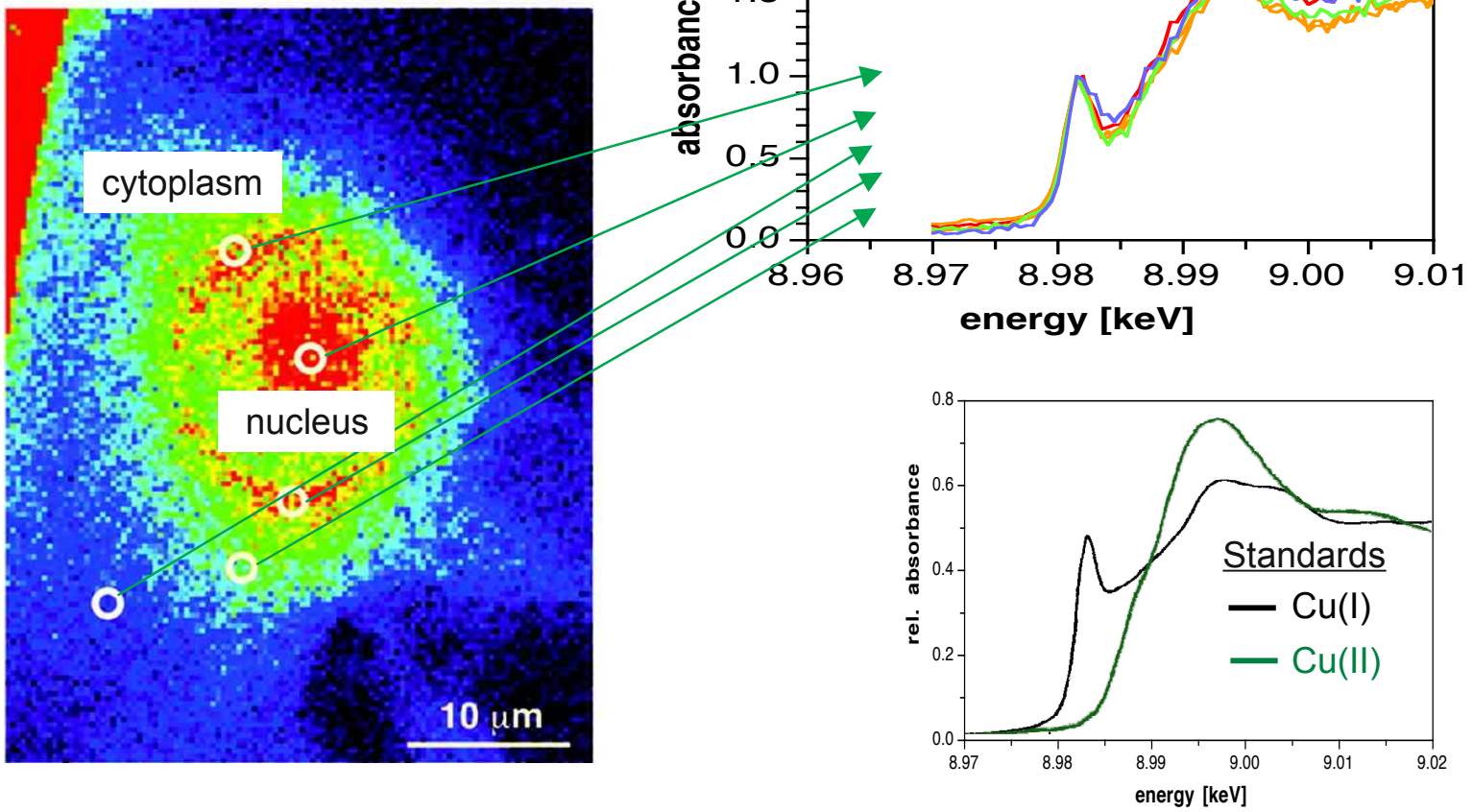

L. Yang, PNAS 102, 11179 (2005)

There is worldwide concern over elevated arsenic concentrations in contaminated rice paddies

- Rice production increasingly occurs in As and metal contaminated soils in Asia
- S-XRF was utilized to locate As in polished (white) and unpolished (brown) rice grains from the United States, China, and Bangladesh
- As dispersed in white rice but localized in the pericarp and aleurone layer of brown rice - Cu, Fe, Mn, and Zn localization followed that of As in brown rice
- μ-XANES and bulk extraction revealed the presence of mainly inorganic As and dimethylarsinic acid.

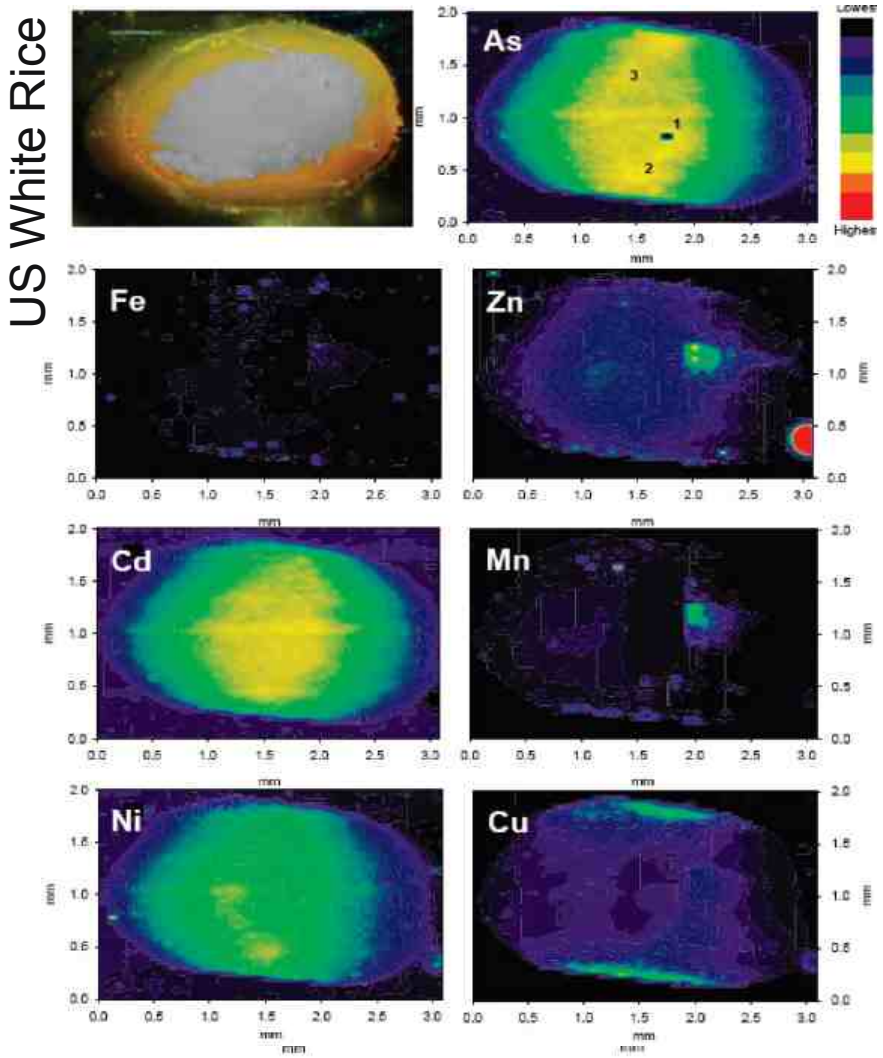

A. Meharg, Environ. Sci. Technol. 42, 1051 (2008)

Small defects mean big problems for solar cells

- Nanoscale clustering of metal impurities at intragranular dislocations is observed within industrial multi-crystalline Si solar cells
- Clusters directly correlate with local recombination activity within the solar cell, regulating its overall photo-conversion performance

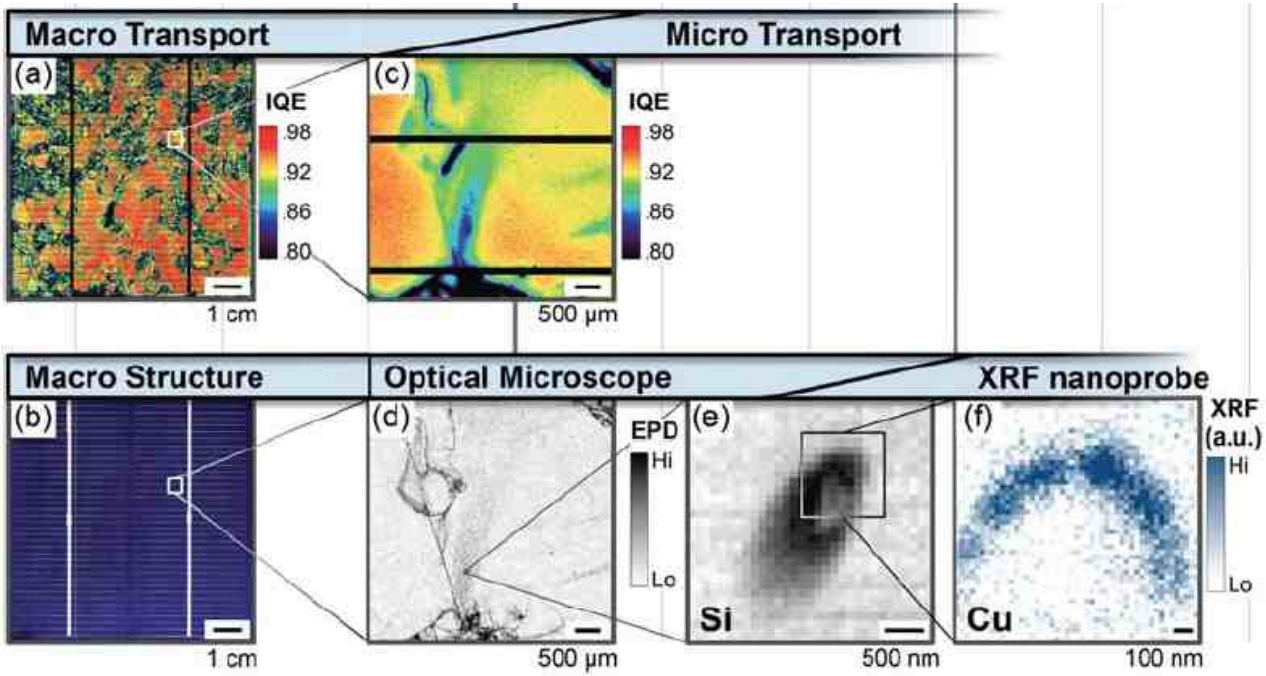

Recombination-active dislocations to contain a high degree of Fe and Cu decoration.

Recombination-inactive dislocations appear clean.

M. Bertoni, Energy & Environ. Sci. 4, 4252 (2011)

Portland cement and CO_2 emission

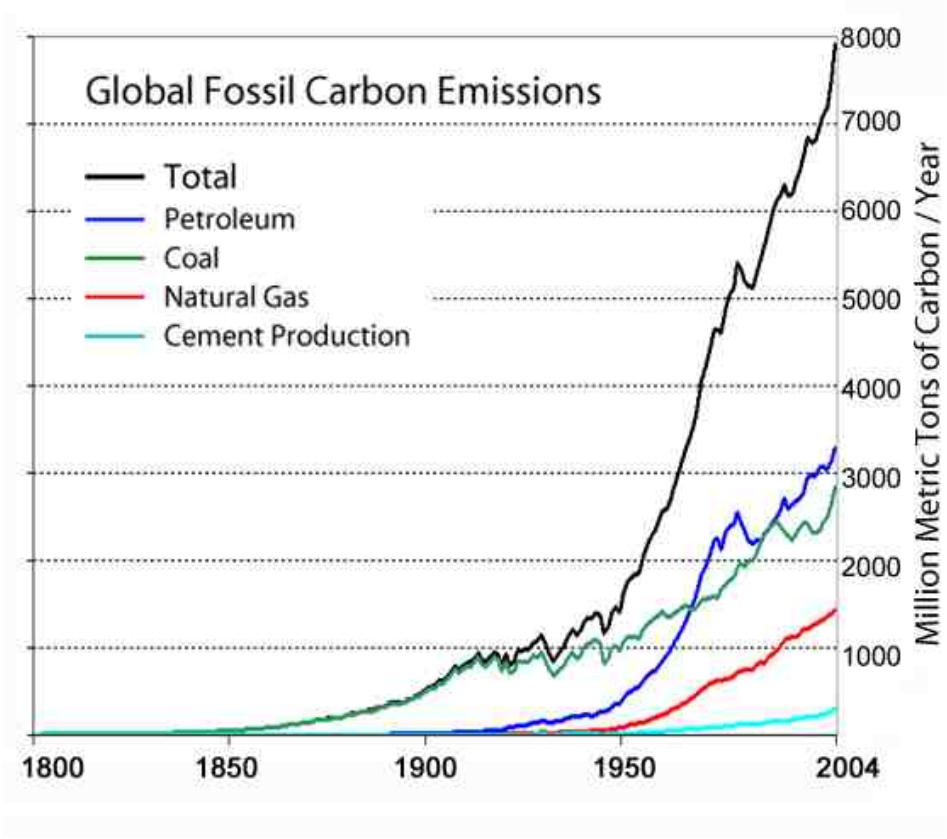

7% to 8% globally

CO_2

Mehta, P.K., in Sixth CANMET/ACI/JCI Conference: Fly Ash, Silica Fume, Slag & Natural Pozzolans in Concrete, 1998.

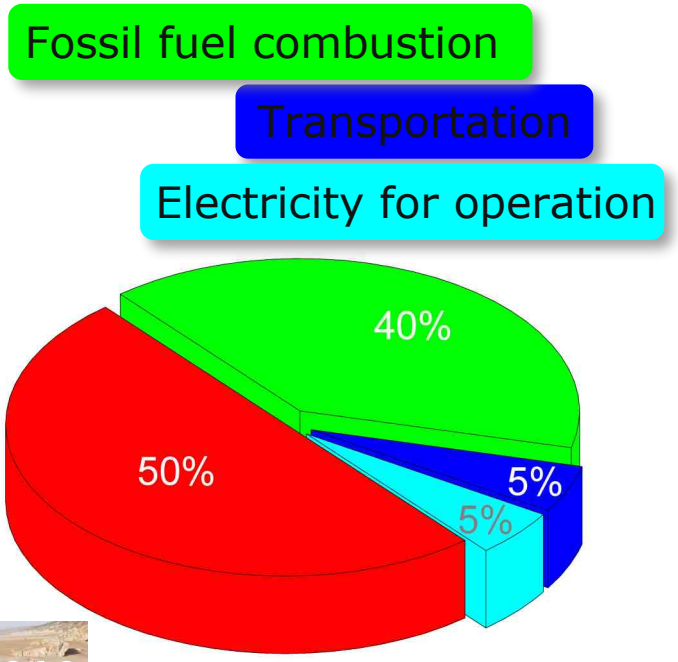

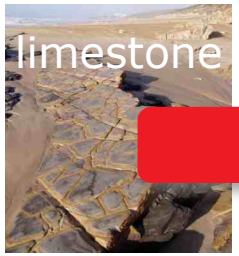

primary precursor

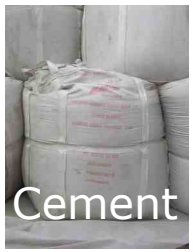

"Green" geopolymeric cement can reduce annual worldwide CO_2 emission by tens of mega-tons

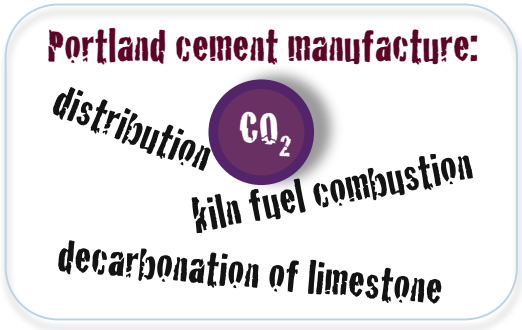

Geopolymers are being developed as an environmentally beneficial replacement to Portland cement for concrete production

Hard x-ray nanoprobe clarifies the poorly understood heterogeneity and complex chemistry of geopolymers

X-ray fluorescence maps of a hydroxide-activated geopolymer

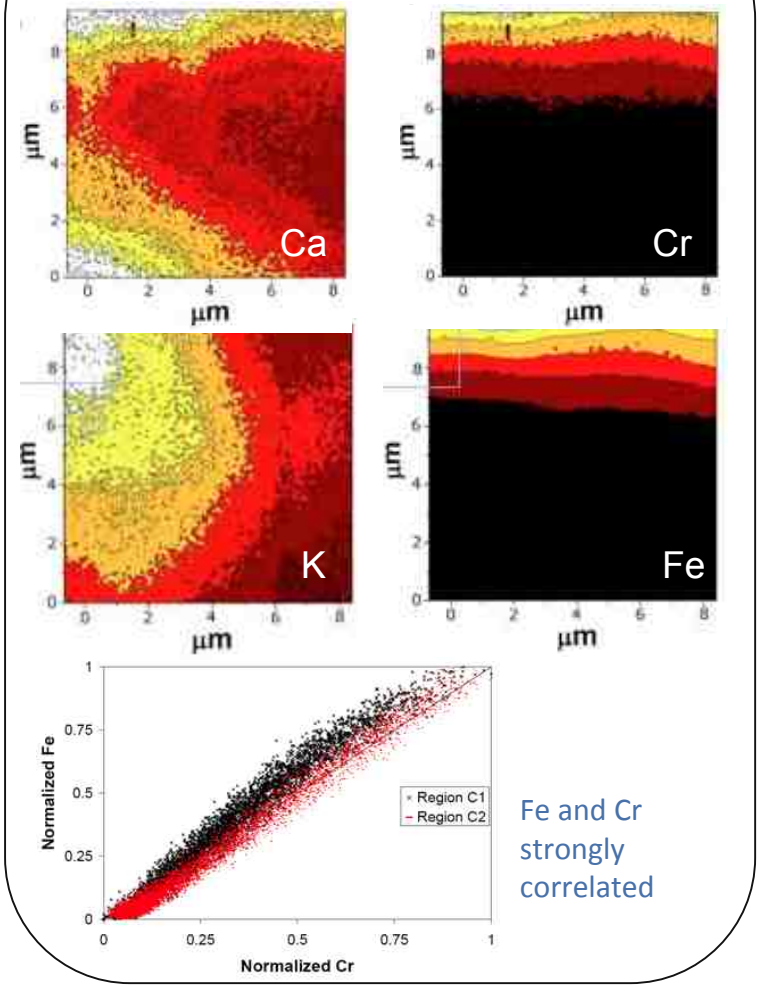

Fe and Cr strongly correlated

J.L. Provis, Langmuir 25, 11897 (2009)

Use fluorescence to see 3D elemental distribution

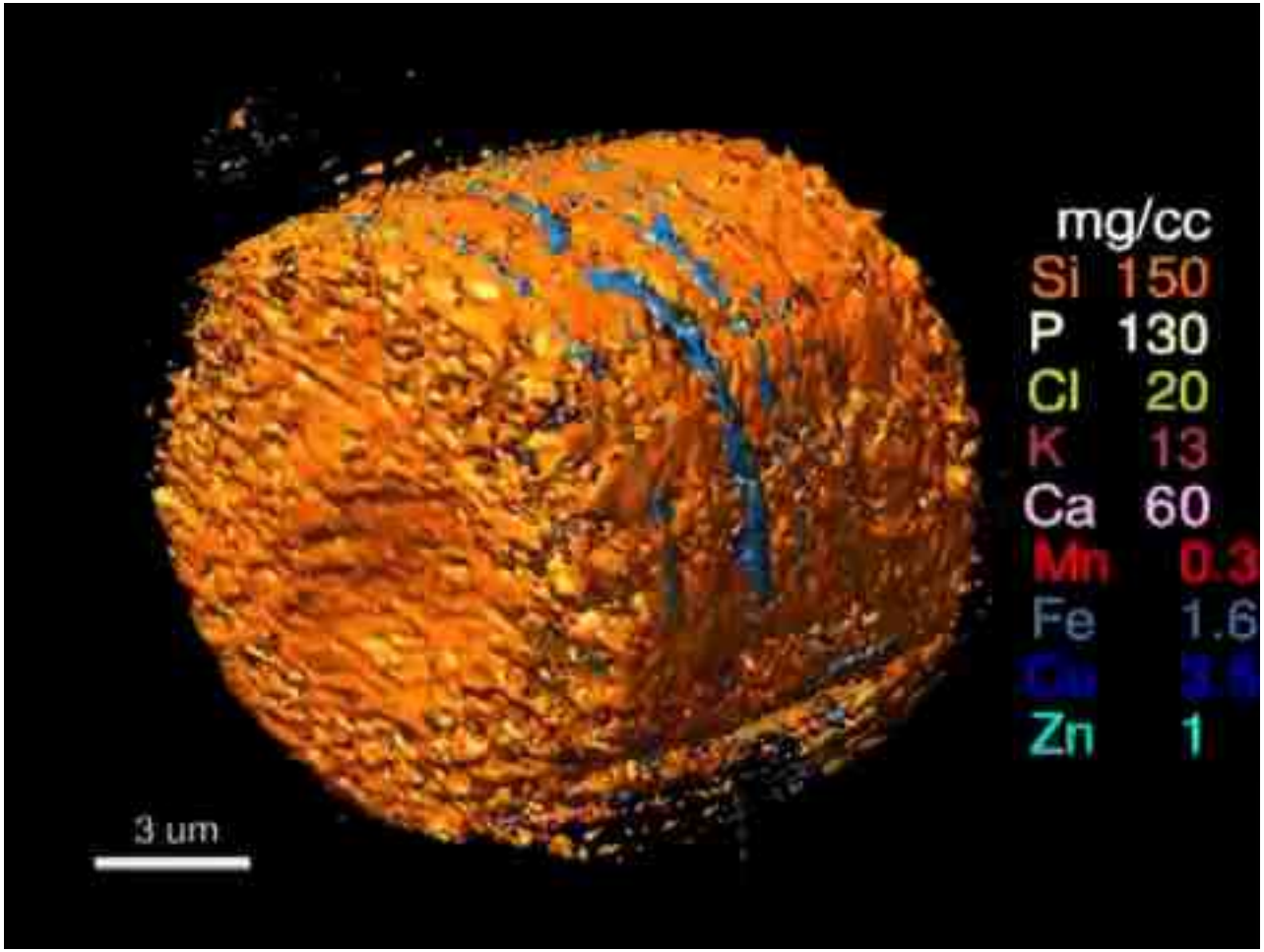

C. meneghiniana

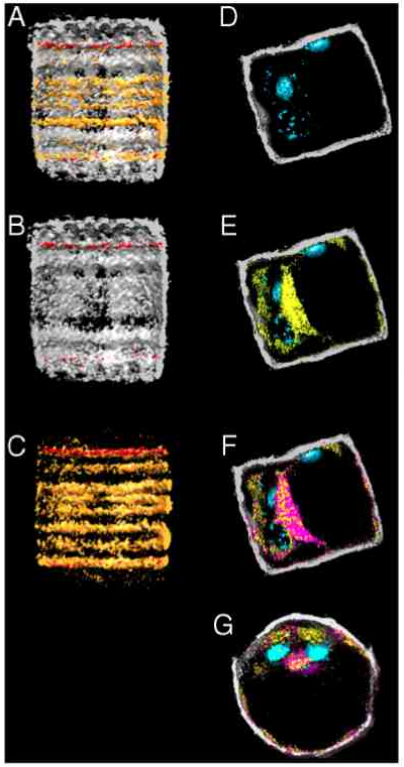

(A-F) Longitudinal slices showing Si (gray), Fe (orange), Mn (red). P (blue), S (yellow), Cl (yellow-green), and Zn (purple. (G) Transverse slice showing cytoplasmic pillar, vacuole, and association of two P-bodies with pillar.

M. De Jonge, PNAS 107, 15676 (2010)

Maia detector: a revolution in fluorescence imaging

384 x Si detector array

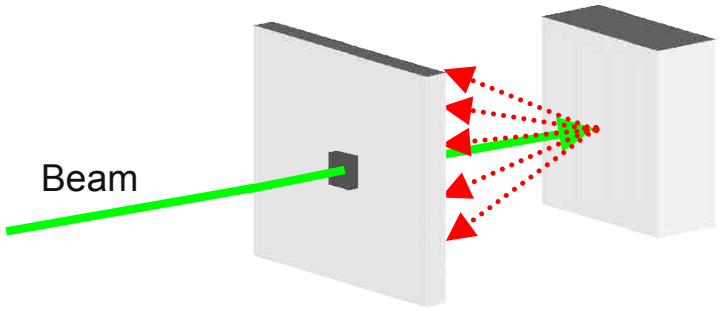

solid-angle ~1.5 steradians

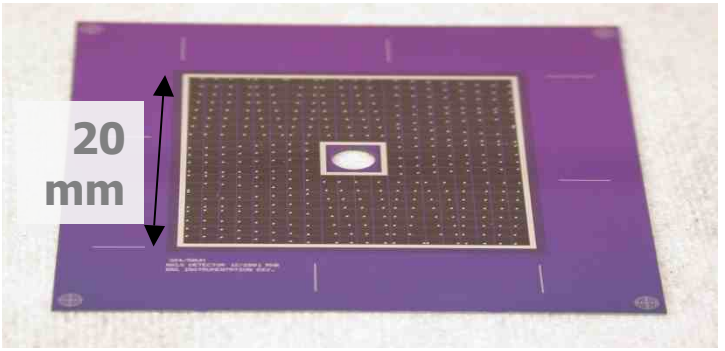

Maia detector removes all overheads, dramatically increasing detection efficiency

Collaboration between CSIRO, BNL, AS & NSLS

- solid-angle ~1.5 str (~10*previously!)
- on-board, event-mode processing reduces overheads to zero; GeoPIXE analysis supplies real-time analysis

Chris Ryan (CSIRO)

Where is the limit for x-ray focusing ?

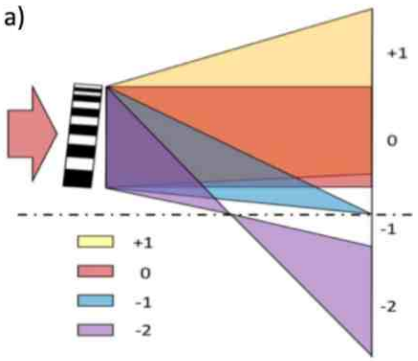

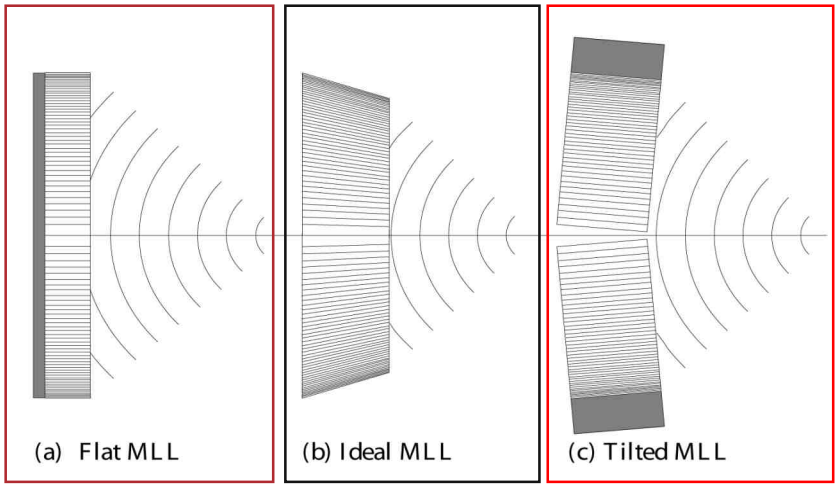

1D multilayer Laue lens

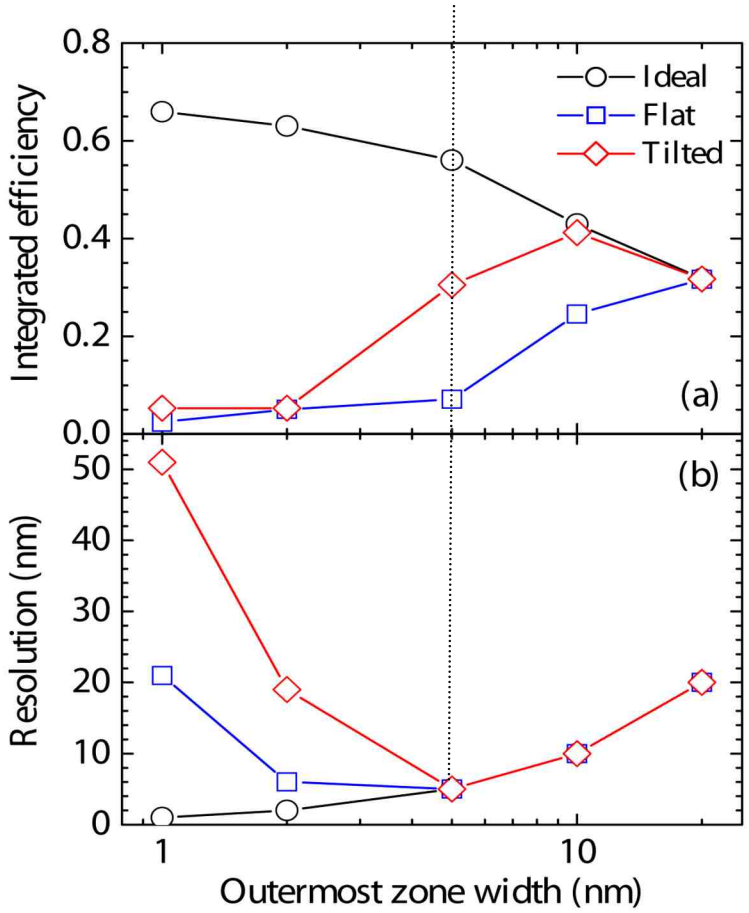

H.C. Kang, PRL 96, 127401 (2006)

2D focusing with a multilayer Laue lens

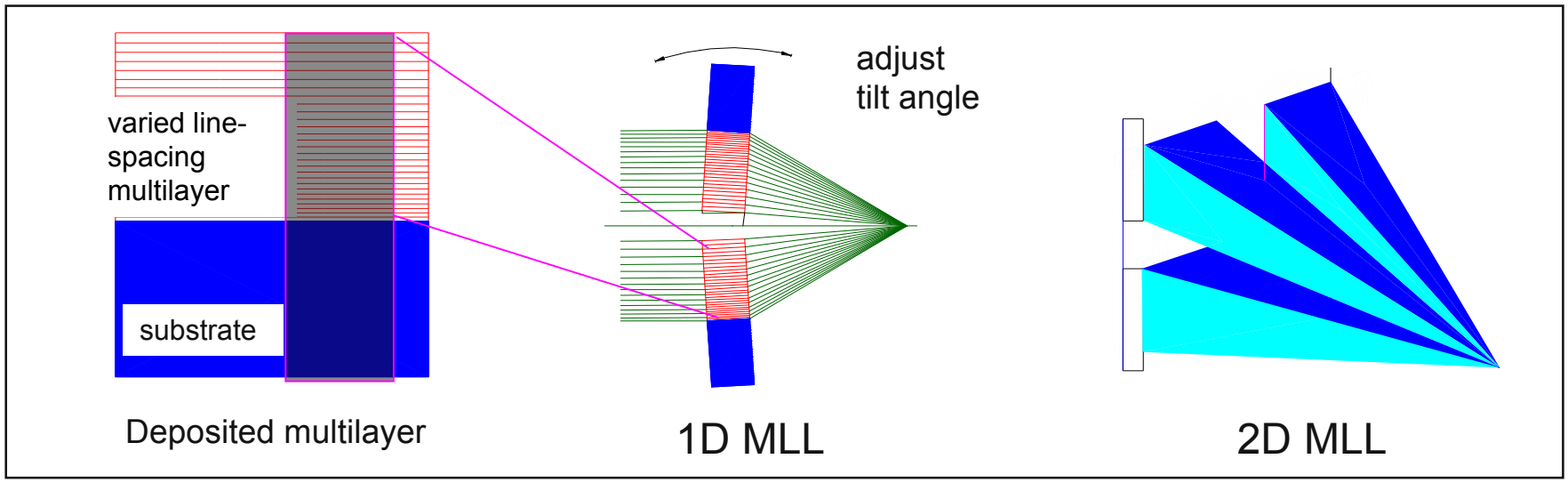

- Deposit varied depth-graded multilayer on flat substrate (thinnest structures first)
- Section to 5-20 μm depth
- Assemble into a linear MLL
- Assemble two linear MLL's into a 2D MLL.

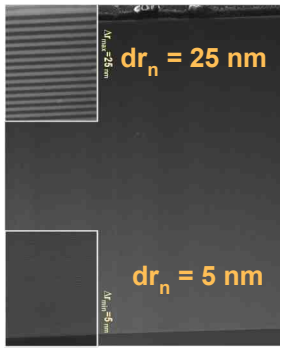

Material: WSi_2/Si

Total deposition thickness: 13.25 um

d-spacing: 5 – 25 nm

MLLs are approaching the 10 nm limit of "thin" lenses

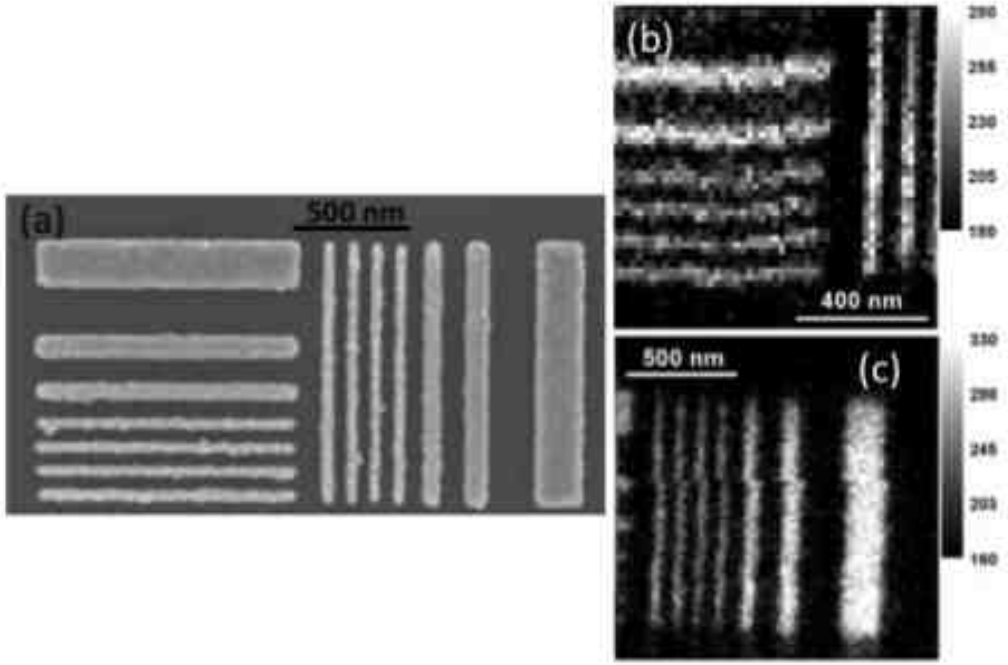

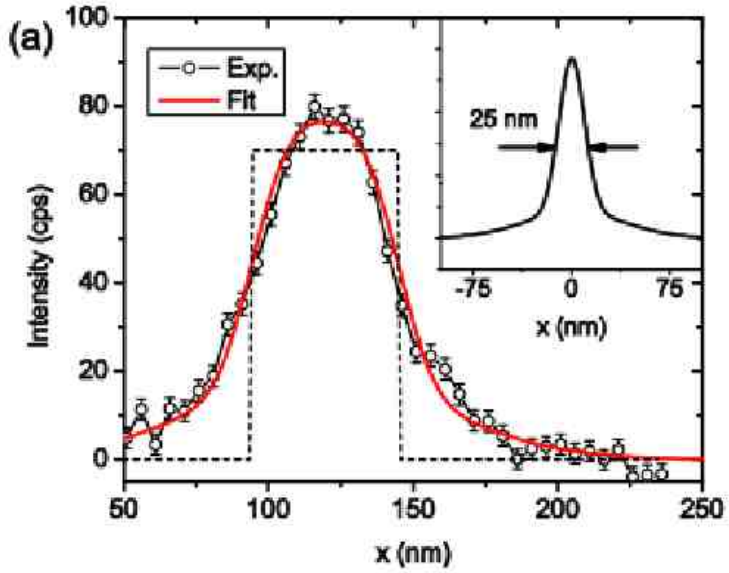

H. Yan, Opt. Expr. 19, 15069 (2011)

Photon Energy:	19.5 keV
Measured Resolution:	25 x 40 nm
Diffraction Efficiency:	17%

Summary

1. Fundamentals
   - resolution
   - contrast
   - x-ray sources
   - x-ray optics

2. Direct methods
   - projection
   - full-field
   - scanning

   (and lots of examples)

Problems

1 What is the longitudinal coherence length for a 14.4 keV x-ray beam and ΔE = 1 eV ?

2 What is the transverse coherence width for an x-ray source with an energy of 14.4 keV and size of 100 µm, measured at 60 m from the source?

3 A zone plate has a 20 nm finest zone width and 100 nm diameter. What is (a) the focal length for !0 keV x-rays? (b) What is it 5 keV x-rays?

4 Approximately what x-ray energy is best to perform microscopy with absorption contrast of organic material in an aqueous environment? What energy is best to optimize the phase contrast? Assume the organic material is 1 µm thick surrounded by 2 µm total thickness of water.

5 Reflective optics are achromatic (wavelenth-independent). How could these optics make high resolution x-ray microscopes more accurate and easier to use for spectro-microscopy applications?

6 Calculate the ideal phase contrast for a 5 µm diameter polystyrene sphere with 9.1 keV x-rays. Assume the sphere is on a completely x-ray transparent support and you have 10% noise on the detected signal.

7 You have a 6 nm GaAs nanodot, a 150 nm Au polycrystalline cluster, and a 2 µm rat pancreas cell. What type of x-ray microscope would be best to image each? Which would best be studied with electron microscopy if you had the choice?

8 Derive the basic expression describing the Zernike phase contrast x-ray microscope.